IMPROVING THE TOPICAL DELIVERY OF PHENOL-CONTAINING DRUGS: AN ALKYLCARBONYLOXYMETHYL AND ALKYLOXYCARBONYLOXYMETHYL PRODRUG APPROACH

By

JOSHUA DENVER THOMAS

A DISSERTATION PRESENTED TO THE GRADUATE SCHOOL
OF THE UNIVERSITY OF FLORIDA IN PARTIAL FULFILLMENT
OF THE REQUIREMENTS FOR THE DEGREE OF
DOCTOR OF PHILOSOPHY

UNIVERSITY OF FLORIDA

2006

Copyright 2006

by

Joshua Denver Thomas

This document is dedicated to my wife Amber, my daughter Miriam, and to my parents Richard and Delores.

ACKNOWLEDGMENTS

It is clear to me that every accomplishment in my life has been fueled by the love of my family and friends and by the wisdom and knowledge of my advisors. It is with this realization that I would like to thank my wife Amber for her unwavering love, support, and encouragement (especially during my first and last semesters of graduate school); and my daughter Miriam, whose smile is sometimes all I need. I would also like to thank my parents, Richard and Delores, who have taught me that there is no greater purpose in life than to know my Creator. I would be remiss if I did not also thank Christopher E. Dahm, James M. Gibson, and James W. Hall for the advice and early research opportunities they provided; my committee members Margaret O. James and William R. Dolbier for their help at critical junctures in my graduate career; and Raymond Booth for graciously accepting a position on my committee. Finally, I will always be indebted to Kenneth B. Sloan for his direction and immense patience and for giving me the opportunity to conduct graduate research. I am grateful to know him as my mentor.

Above all, I would like to thank my Savior Jesus Christ for his unconditional love and for the peace that comes from knowing that my life is in his hands.

TABLE OF CONTENTS

LIST OF TABLES

LIST OF FIGURES

Abstract of Dissertation Presented to the Graduate School
of the University of Florida in Partial Fulfillment of the
Requirements for the Degree of Doctor of Philosophy

IMPROVING THE TOPICAL DELIVERY OF PHENOL-CONTAINING DRUGS: AN ALKYLCARBONYLOXYMETHYL AND ALKYLOXYCARBONYLOXYMETHYL PRODRUG APPROACH

By

Joshua D. Thomas

August 2006

Chair: Kenneth B. Sloan
Major Department: Medicinal Chemistry

Although most drugs are administered orally, this route is not suitable for many compounds due to their extensive metabolism in the GI tract and liver. Topical delivery is an alternative route of administration for such drugs that avoids this "first-pass effect" and permits the drug to enter the systemic circulation following penetration of the skin—a much less metabolically active tissue than the liver. One of the most effective methods for improving topical delivery while minimizing side effects involves the use of prodrugs.

Most previous attempts to improve the topical delivery of phenols via a prodrug have involved some type of aryl ester, carbonate or carbamate. In the present work, alkylcarbonyloxymethyl (ACOM) and alkyloxycarbonyloxymethyl (AOCOM) prodrugs of 4-hydroxyacetanilide (acetaminophen) have been evaluated *in vitro* as novel permeation-enhancing derivatives of phenol-containing drugs. Alkylcarbonyloxymethyl iodides were synthesized by way of a new one-step route and were subsequently reacted

with various phenols to obtain the target ACOM derivatives. The coupling reaction between ACOM iodides and phenols was shown to favor the alkylated product regardless of the steric hindrance in the alkylating agent or the phenol. On the other hand, the coupling reaction of AOCOM iodides with phenols seemed to be more sensitive to steric effects, with the acylated product being favored when steric effects were minimal. However, under phase-transfer conditions, the influence of steric hindrance was minimized and yields of AOCOM phenol were increased.

More importantly, the ACOM and AOCOM prodrugs were able to improve the topical delivery of APAP up to 3.6 and 1.3-fold, respectively. The ACOM and AOCOM prodrugs were also added to the Roberts-Sloan database (n = 61) to obtain a new database of 71 compounds. A fit of this new database (n = 71 $r^2 = 0.92$) to the Roberts-Sloan (**RS**) equation resulted in a more robust model for predicting flux (J_M) through hairless mouse skin: $\log J_M = -0.562 + 0.501 \log S_{IPM} + 0.499 \log S_{4.0} - 0.00248$ MW where S_{IPM} and $S_{4.0}$ are the solubilities in isopropyl myristate and pH 4.0 buffer, and MW is molecular weight.

CHAPTER 1
BACKGROUND

Topical Delivery

Rationale

Although there are many available routes of drug administration, the oral route is by far the most popular. This is primarily due to a high incidence of patient compliance. While it is true that patients often find an oral drug regimen more palatable than the parenteral alternative (e.g., intravenous or intramuscular injection), oral drug absorption is a much more complicated problem[1, 2] for the drug discovery scientist to solve. If given orally, a drug molecule must surmount numerous chemical and enzymatic hurdles in order to reach the systemic circulation. For example, if the drug survives the acidic environment of the stomach, it still faces efflux transporters and various biotransformation enzymes in the gut wall. Following absorption in the gut, the drug enters the liver, where a host of biotransformation enzymes await. At each stage of absorption, there is the potential for the drug to be inactivated and excreted, thereby reducing the amount of the original dose that reaches the intended site of action in the body.

Given the extent to which a drug can be inactivated as it is absorbed into the systemic circulation, alternative methods that avoid first-pass metabolism yet retain the simplicity needed to achieve high patient compliance are desirable. Topical delivery is one such approach. In general, the levels of drug-metabolizing enzymes in the skin are much lower than those in the liver and intestine.[3-6] For example, transferase activity in

the skin (e.g., glucuronidation and sulfation) may approach 10% of the liver while cytochrome P-450 activity in the skin is typically 1-5% of the corresponding hepatic activity.[7] In fact, skin permeability rather than drug metabolism appears to be the major barrier to topical bioavailability.[8, 9]

Although it is an important consideration in drug delivery, minimal drug inactivation is not the only advantage to be gained from avoidance of first-pass metabolism. Potential side effects must also be taken into account. Topically applied drugs frequently exhibit fewer side effects than the corresponding oral dosage forms. One of the most studied medications in that respect is estrogen. Several recent studies have indicated that the detrimental effects of hormone replacement therapy in postmenopausal women may be due to the route of drug administration.[10-13] In a comparison between oral and transdermal estrogen therapies, both treatments were equally effective at increasing bone mineral density and decreasing luteinizing hormone levels.[10] However, patients treated with oral estrogen for six months experienced an increase in triglyceride levels and fat mass with an accompanying decrease in lean body mass. Triglyceride levels and body composition of patients treated with transdermal estrogen did not significantly change over the course of the six month treatment.[10]

Other studies indicate that oral estrogen may play a role in the elevated levels of C-reactive protein (CRP)[11, 13] and serum amyloid A (SAA)[12] detected in women undergoing hormone-replacement therapy. These studies found no such side effects in patients undergoing transdermal estrogen therapy. In both cases, the evidence suggests that the differences in side effects between the routes of administration are directly related to the action of oral estrogen in the liver.[11-13] Since both CRP and SAA have been identified as

important indicators of systemic inflammation and are predictive of future cardiovascular disease,[14] transdermal estrogen replacement therapy appears to offer a better safety profile than the more common oral route. In fact, in the case of SAA, transdermal estrogen may exert a protective effect compared to the oral route. Abbas and coworkers[12] found that the levels of SAA and the SAA-HDL complex (HDL-SAA) in postmenopausal women receiving transdermal estrogen were substantially lower than those in women receiving oral estrogen.

While the examples given above for estrogen support the case for transdermal delivery (to the systemic circulation), it is perhaps more obvious that topical delivery is an important route for treating skin diseases (dermal delivery). The main advantage of topical over oral administration for the treatment of skin diseases is that high levels of the drug can be delivered to the skin with minimal exposure to the rest of the body. One example of the benefits of topical delivery for the treatment of a skin condition is the topical application of dapsone (4,4'-sulfonyldianiline).[15, 16] Although dapsone is normally given orally for the treatment of leprosy,[17] oral dapsone has also proven effective in treating moderate cases of acne.[15] However, the effectiveness of orally administered dapsone is limited due to its hemotoxic side effects. In a recent study, topically applied dapsone was successfully used to treat moderate acne with side effects no different than those of the vehicle (a gel) itself.[16]

Anatomy and Physiology of Skin

Although topical delivery presents fewer complications than the oral route, this does not mean that overcoming the barrier properties of the skin is a small task. Unlike the gastrointestinal tract, the primary purpose of skin is to restrict the passage of endogenous and exogenous substances into and out of the body. As a consequence,

topical delivery is a viable option for a relatively small percentage of drugs. For example, all the drugs currently approved for use by the FDA as transdermals have molecular weights less than 400 Da, exhibit relatively high lipid solubility, and are therapeutically effective at low doses (0.04-10 ng/ml).[3, 9] Furthermore, since most transdermal drug candidates were originally designed for oral administration,[18] they typically do not possess the particular physiochemical properties required for adequate diffusion through skin.[19] Although the relationship between flux and the physicochemical properties of the permeant is still a matter of debate,[20] a knowledge of skin anatomy and physiology is helpful in understanding why some compounds permeate the skin better than others.

The skin is composed of three main layers of varying thickness: the hypodermis (1-2 mm), dermis (1-5 mm), and epidermis (60-120 μm).[3, 5] The actual composition of each layer varies with age, disease state, and anatomical location. Though one might expect the thickest of these layers to be the primary barrier to percutaneous absorption, this is not the case. In fact, the most impervious layer of the skin is actually the thinnest—the outermost layer of the epidermis which is referred to as the stratum corneum (10-20 μm). Although diffusion through the stratum corneum is generally recognized as the rate-limiting step to percutaneous absorption, disruptions in the integrity of the other layers can also affect skin permeability. Thus, the structure and function of each layer will be reviewed in the following sections.

Hypodermis

The deepest layer of the skin, the hypodermis, is primarily composed of adipose tissue. As such, it functions as an energy depot, a layer of insulation, and as a shock absorber. As with the other layers of the skin, the thickness of the hypodermis varies

from one part of the body to another. For instance, the eyelids are altogether missing a hypodermal layer. Variations in diet can affect the thickness of this layer as well.

The hypodermis serves as the entry point for the major blood vessels and nerves that service the skin. Although adipose tissue may sometimes function as a depot for highly lipophilic xenobiotics, this is generally not the case with the hypodermis. Compounds that reach this layer by diffusion are usually taken up by the network of blood vessels that run throughout the subcutaneous fat. Because the loose connective tissue of the hypodermis is interwoven with that of the dermis, there is no distinct boundary between these two layers. In addition, although most hair follicles originate in the dermis, course hair can often extend deep (3 mm) within the hypodermis.[3, 5, 21]

Dermis

Directly above the hypodermis is the dermis—the thickest layer of the skin. In sharp contrast to the underlying layer of adipose tissue, the dermis is a much more aqueous-like environment. For instance, the gelatinous substance in which the various structures of the dermis are imbedded consists of proteoglycans and glycosaminoglycans—compounds that are capable of binding up to 1000 times their weight in water. Running throughout this gel-like "ground substance" is a dense, irregular network of collagen fibers. These fibers make up the bulk of the dermal connective tissue and act as a supporting framework for blood vessels, hair follicles and various other structures. Microfibrils composed of elastin, fibrillin, and vitronectin make up the elastic connective tissue (the second most abundant tissue in the dermis), and provide a certain amount of elasticity to the skin.[3, 5]

Most of the appendages of the skin originate in the dermis. These include the hair follicles, sebaceous glands, and sweat glands. As with other features of the skin, the

density and presence of these structures vary with anatomical location. For example, of these three appendages, only the sweat glands are found in the palms and soles. Hair follicles are sheath-like structures that enclose each hair and extend from the surface of the skin into the dermis. Although the follicle consists of living epidermal cells, the hair shaft inside the follicle is mainly composed of dead, keratinized cells. Attached to the follicle is a band of smooth muscle fibers that are collectively known as an arrector pili muscle. Under conditions of emotional stress or cold temperatures, these muscles contract, causing the hair to stand erect and the skin to take on the familiar "goose bump" appearance. In most regions of the skin, sebaceous glands merge with hair follicles and secrete their contents (sebum) directly into the follicle. However, in various sites throughout the body the sebaceous glands extend to the outermost layers of the skin and deposit their contents directly at the surface. In a similar fashion, sweat glands either connect to the hair follicle (as in apocrine glands) or open up at the skin surface (as in eccrine glands). Sebum (a mixture of fatty acids, triglycerides, and wax secreted by the sebaceous glands) and sweat (a mixture of salts and various waste products (e.g., urea and uric acid)) help keep the surface of the skin slightly acidic (pH 5). With regard to topical delivery, skin appendages may offer an alternative pathway to permeating compounds that avoids the stratum corneum. However, since the appendages make up a such a small percentage of the total surface area of the skin (approximately 0.1%), these "shunt routes" are not expected to significantly affect the observed flux of most permeants.[3, 5, 21]

The dermal-epidermal border resembles a transverse wave running parallel to the skin surface. As a result of these undulations (referred to as dermal papillae), sections of

the dermis come within 200 μm of the skin surface. Capillaries also extend into the dermal papillae and help maintain "sink" conditions within the skin by efficiently transporting permeated compounds to the systemic circulation. In addition, the vascular network of the dermis is responsible for supplying nutrients and oxygen to the skin and also plays a role in regulating body temperature. A system of lymphatic vessels comprises an additional dermal circulatory system. These vessels are involved in removing cellular waste and help regulate the volume of the interstitial fluid in the dermis. During times of wound healing and inflammation, the lymphatic system also delivers macrophages, lymphocytes, and leucocytes to the affected areas of the dermis. These cells facilitate the healing process by destroying invading bacteria via phagocytosis or via the secretion of certain cytotoxic agents. In general, the lymphatic circulatory system plays only a minor role in the clearance of permeated compounds from the dermis.[3, 5]

Epidermis

Directly above the dermis lies the epidermis. The epidermis is composed of four distinct regions, each representing a different phase of kertinocyte differentiation. From the dermal-epidermal border to the skin surface they are the stratum basale, stratum spinosum, stratum granulosum, and stratum corneum. Since there are no blood vessels in this layer of the skin, nutrients reach epidermal cells by way of passive diffusion across the basement membrane at the dermal-epidermal border. The passage of nutrients and other materials across the basement membrane is facilitated by the relatively high surface area provided by the dermal papillae. The final stage of keratinocyte differentiation is represented by the stratum corneum—the outermost layer of skin. Although it is

essentially dead tissue, the stratum corneum is the rate-limiting barrier to percutaneous absorption.[3, 5, 21]

Stratum basale. Keratinocytes of the stratum basale are unique in that they are the only epidermal cells that undergo mitosis. Following mitotic division, one cell remains in the stratum basale while the other daughter cell detaches from the basement membrane and migrates outward through the remaining epidermal layers. Basal keratinocytes are attached to the basement membrane by structures known as hemidesmosomes. Similar desmosome plaques are found throughout the epidermis and function as proteinaceous rivets linking adjacent cells. Other cell types found in the stratum basale include melaninocytes, Langerhans cells, and Merkel cells. Melaninocytes are responsible for producing the pigment melanin. Though melanin is produced by the melaninocytes, it is also transferred to neighboring cells through dendritic connections. Langerhans cells play an important role in the immune response by binding to foreign antigens in the epidermis and presenting them to T-lymphocytes in the lymph nodes. Merkel cells are involved in sensory reception and are found at sites along the basement membrane where dermal nerve endings extend into the papillae.[5]

Stratum spinosum. Upon migration from the stratum basale to the stratum spinosum, keratinocytes undergo several morphological changes including the formation of desmosomal plaques between adjacent cells. These intercellular linkages make substantial contributions to the overall cohesiveness and organization of the epidermis. Besides forming desmosomes, the keratinocytes of this layer also lose their columnar shape and begin to take on a more flattened appearance. Both the volume and diameter of the keratinocyte continue to increase as the cell makes its way through the remaining

strata. In addition to changes in structure, keratinocytes also begin to synthesize keratins 1 and 10 and develop special organelles called lamellar granules that play an important role in maintaining the barrier properties of the stratum corneum.[5, 22]

Stratum granulosum. At this stage of keratinocyte differentiation, the cell begins to die and the nucleus and organelles are enzymatically degraded. As the name suggests, the cells of the stratum granulosum (SG) are filled with keratohyalin granules (KHGs) and lamellar bodies (LB, also known as lamellar granules). Keratohyalin granules are enriched in the precursors of intracellular corneocyte proteins and of the cornified envelope. Included among these precursors are profillaggrin, loricrin, and keratins 1 and 10. Lamellar bodies are ovoid organelles containing stacks of lipid membranes composed of phospholipids, cholesterol, and glucosylceramides. In addition, LB contain high levels of various catabolic enzymes including acid hydrolases, sphingomelinase, and phospholipase A_2.[3] The accordion-like appearance of these lipoidal structures likely results from the compression and subsequent stacking of Golgi-derived lipid vesicles—a process thought to be mediated by acylglucosylceramide (Figure 1-1).[23] The incorporation of the glucose and linoleic acid moieties into a ω-hydroxyceramide backbone allows acylglucosylceramide to be anchored in the polar phase of one vesicle, span the lipid interior, and insert itself into the polar surface of an adjacent vesicle thereby functioning as a "molecular rivet."[8] At the stratum corneum-stratum granulosum interface, lamellar bodies are excreted from the cell and their contents made ready for incorporation into the stratum corneum (SC).

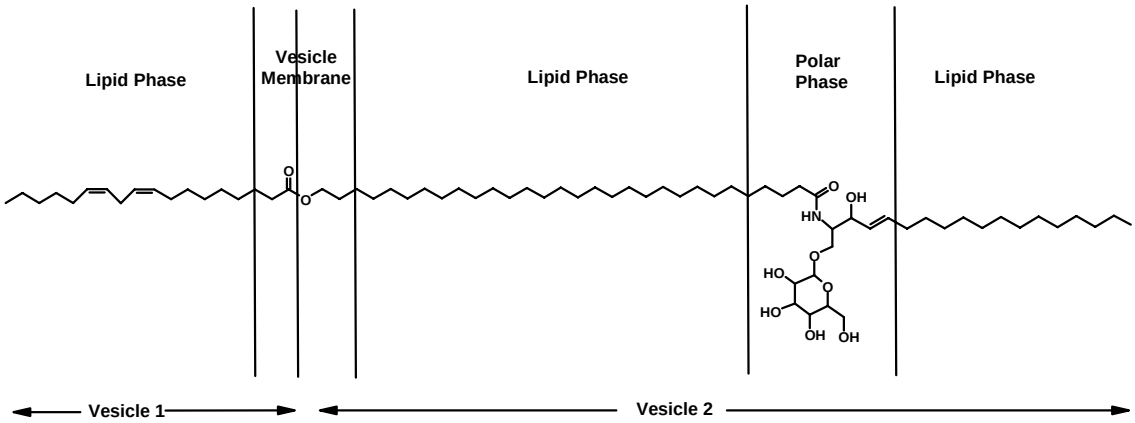

Figure 1-1: Structure of Acylglucosylceramide and General Orientation in Lamellar Bodies

Stratum corneum. Although the stratum corneum (SC) is the last major layer of the epidermis, it can be further divided into inner (stratum compactum) and outer (stratum disjunctum) layers. As the name implies, the cells of the stratum compactum are packed together more tightly than those of the stratum disjunctum. This difference in packing and cell cohesion between the two layers is primarily due to the loss of linkages (corneodesmosomes) between cells in the outer layer in a process known as desquamation. At the SG-stratum compactum interface, LB fuse with one another[24] to form the intercellular lipid lamellae of the stratum corneum.

The cells of the SC are known as corneocytes. They are nonliving and are generally considered to be impermeable to most compounds. Compared to the other layers of the skin, the overall water content of the SC is quite low (approximately 15% by weight versus 70% for viable epidermis)—the majority of which is associated with the proteinaceous material (mainly keratins 1 and 10 and various degradation products of filaggrin) that comprises the inner compartment of the corneocytes.[3] An impermeable membrane (the cornified envelope) composed of highly cross-linked protein encloses the core protein of the corneocytes. This membrane not only functions as a barrier to

permeation, but it also plays an important role in the organization of the intercellular lipid lamellae via the interaction of ω-hydroxyceramides that are covalently bound to the exterior surface of the cornified evelope.[3, 8] These particular lipids are derived from ceramides 1, 4 and 9 (Figure 1-2) by a deesterification reaction that removes the linoleic acid group. The primary constituent of the exterior lipids is a ω-hydroxyceramide derived from ceramide 1 which itself is derived from another important LB lipid (i.e. acylglucosylceramide, Figure 1-1). These very long chain lipids are likely attached by an ester linkage at the ω-hydroxyl end to a surface protein (possibly involucrin) on the envelope.[8]

The intercelluar lamellae of the SC consist of the following three lipids in their approximate order of abundance: ceramides (50% by weight), cholesterol (30% by weight) and free fatty acids (10% by weight).[22] To date, nine different ceramides (Figure 1-2) have been isolated from human SC. They have traditionally been labeled in a way that reflects their relative polarities on thin layer chromatography (TLC). In that regard, it should be noted that the recently discovered ceramide 9 exhibits a retardation factor (R_f) on TLC that is between ceramides 2 and 3. Interestingly, ceramide 1 may also serve the same molecular rivet role in the lipid lamellae as its precursor, acylglucosylceramide, does in LB.[8] Although it is evident from the brief overview presented here that the composition of the SC is much different from the plasma membranes found in most tissues of the body, this point is further emphasized by the absence of phospholipids in the SC.[5]

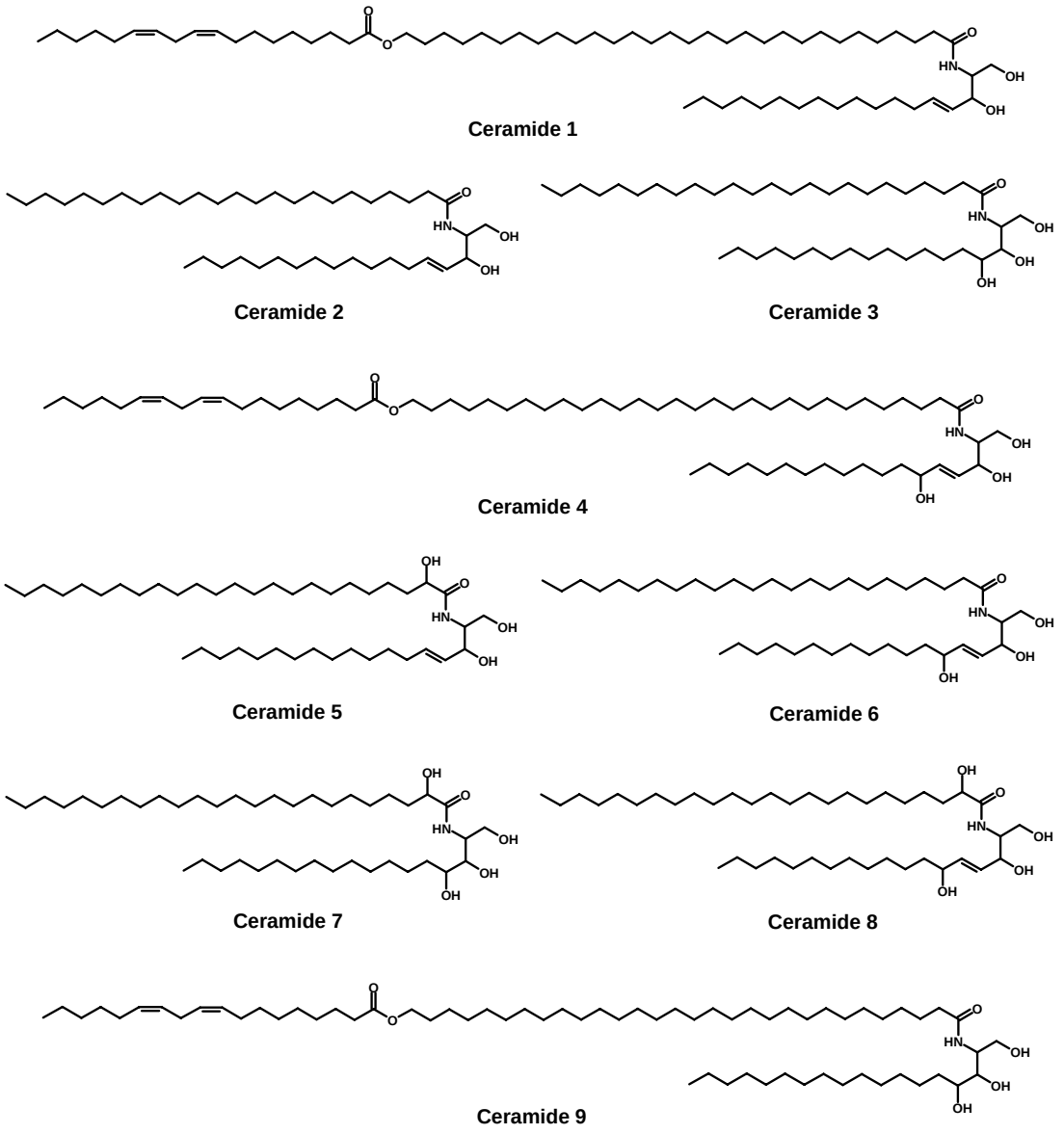

Figure 1-2: Structure of Ceramides found in Human Stratum Corneum

Barrier Properties of the Skin

Physicochemical barrier

The primary barrier to percutaneous absorption is presented by the SC.[3, 5] Given that the enzymatic activity of the SC is much lower than that of the viable epidermis and dermis,[3] the barrier properties of the SC are mainly physicochemical rather than

biochemical in nature. One of the key features of this barrier is the organization of the corneocytes within the intercellular matrix. As the corneocytes are practically impermeable to most compounds, they act as "road blocks" in the path of diffusion. In fact, Potts and Francoeur[25] have shown that the diffusion of water through the SC is 1000-times lower than its diffusion through a comparable homogeneous lipid phase. They also found that the diffusion pathlength was 50-times greater than the thickness of the membrane. From these results, it was concluded that the diffusion of permeants through the SC occurs by way of a meandering path around the corneocytes and through the intercellular lamellae (Figure 1-3).[25]

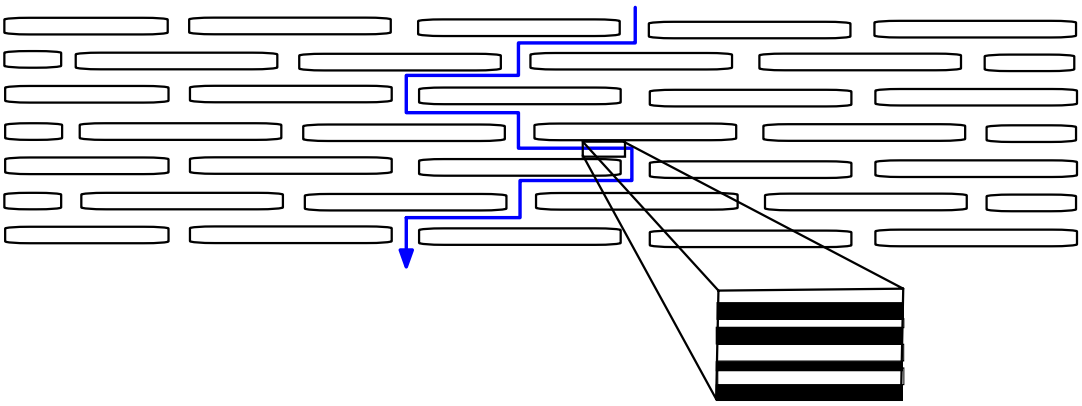

Figure 1-3: Tortuous Path of Permeant Through the Stratum Corneum and Expanded View of Alternating Nonpolar (White Bands, Electron Lucent) and Polar (Dark Bands, Electron Dense) Phases Found Within the Intercellular Matrix (Phases Presented as they Generally Appear in Ruthenium Tetroxide Fixation of Normal Skin)[24]

As the intercellular lamellae represent the only continuous pathway in the SC, the composition and organization of the lipids in this matrix are of primary importance to percutaneous penetration. Due to the edge-to-edge fusion of the LB at the SG-SC interface, the intercellular domain is composed of continuous lipid sheets consisting of repeating units of polar and nonpolar phases (Figure 1-3).[24, 26] Despite the high degree of

order within the lipid lamellae, the lipid phases are often interrupted by hydrophilic bridges that link two neighboring polar phases. As a consequence of the structure of the intercellular matrix, a permeant must pass through alternating lipid-poor and lipid-rich layers. The implication for drug design is that in order to maximize flux, the solubilities of the drug in both lipid and aqueous solvents must be increased.[19, 20]

Biochemical barrier

Although the skin is primarily a physical barrier, the enzymatic activity of the skin is significant and should not be ignored. Of the three main skin layers, the epidermis exhibits the highest enzymatic activity per unit tissue mass and is considered the major region of drug metabolism in the skin.[27] Many of the major types of phase I and phase II reactions are known to occur in the skin including oxidation, reduction, ester hydrolysis, epoxide hydrolysis (microsomal and cytosolic), methylation, glucuronidation, sulphation, glycine conjugation, and glutathione conjugation.[6, 27, 28] It is particularly important to note that many of the cytochrome P450 enzymes responsible for metabolizing a wide variety of pharmaceutical compounds in the liver and gut are also found in the skin.[4]

One of the major obstacles to the oral absorption of drugs is the presence of efflux transporters such as multidrug resistance-associated proteins (MRP) and P-glycoprotein (P-gp) in the gut wall.[1] Early attempts to determine the tissue distribution of P-gp found evidence of this protein in the liver, pancreas, intestine, and kidney but were unable to detect P-gp in the skin.[29] However, recent work in this area has shown that the skin contains several constitutively expressed MRPs (1 and 3-6). P-gp was also found but only after induction with dexamethasone.[30] Current knowledge about the function of MRP in the skin is limited.[31] In contrast to its infamous role as a contributor to multidrug resistance, Randolph and coworkers have demonstrated that P-gp plays an important role

in the migration of Langerhans cells out of the skin by way of the lymphatic vessels.[32] Thus P-gp helps maintain a healthy immune response in the skin. Li and coworkers have also found evidence to suggest that MRP-1 acts as an efflux transporter in the skin.[33] Specifically, they found that the tissue-to-plasma concentration ratio of grepafloxacin in the skin of MRP-1 knockout mice was higher than the corresponding ratio in the skin of wild type mice following an i.v. injection of grepafloxacin. Other experiments demonstrated that the uptake of another MRP-1 substrate ("fluo 3") into the keratinocytes was significantly increased in the presence of an MRP-1 inhibitor.[33] Though these results provide evidence of active transport of xenobiotics out of kerainocytes via MRP-1, it is unclear whether such transport would ultimately result in the expulsion of the xenobiotics to the skin surface (though this does not seem likely given the nature of the SC barrier). Yet if an active xenobiotic efflux system exists in the skin, it would probably have a greater effect on delivery into the skin (dermal delivery) rather than through it (transdermal delivery). In short, the presence of efflux transporters in the skin raises the possibility of an additional biochemical barrier (efflux transport out of the skin) to skin permeability, but the current evidence for such a barrier is not definitive.

Overcoming the Skin Barrier

Strategies

Much research has gone into developing effective methods for overcoming the barrier properties of the skin.[5, 9, 34] Typical examples of such strategies include the use of electricity[35] to either create temporary holes in the skin (electroporation) or to electrostaticly push charged drug molecules into the skin (iontophoresis); penetration enhancers,[36] chemicals designed to temporarily decrease the barrier properties of the skin; microneedles[37] which physically create micron-sized holes in the skin through which

drug molecules bypass the stratum corneum altogether; and prodrugs[19, 20] which are transient derivatives of active drugs that temporarily improve the solubility of the drugs in the skin (thereby increasing their flux through the skin) and then rapidly convert to the parent drugs in the skin or in the systemic circulation.

Of the methods listed above, penetration enhancers have received the most attention in industry. However, despite this predilection for chemical enhancers, the improvement in drug flux is often only modest at best.[9] Moreover, the enhancing effects are often directly proportional to the concentration of the enhancer—a situation which often results in toxic side effects.[36] In order to reduce or avoid the adverse side effects associated with penetration enhancers, it has been suggested[19, 38, 39] that a prodrug/formulation combination might be a better way to approach the problem. In many cases, a drug molecule exhibits poor solubility in the skin due to one or more polar functional groups in the molecule that are either highly charged at physiological pH or that promote hydrogen bonding and high crystal lattice energies. A prodrug approach attempts to overcome this problem by temporarily masking the offending functional group. Since the prodrug is already more soluble in the skin than the parent drug, a much lower concentration of the chemical enhancer would be needed to experience great improvement in drug permeability.

Predictive models for optimizing topical delivery

As mentioned in previous sections of this chapter, the intercellular lipid matrix of the SC is the rate-limiting barrier to the passive diffusion of drugs through skin. Due to the particular arrangement of the intercellular lipid lamellae (Figure 1-3), permeating compounds must pass through alternating polar and nonpolar layers within the SC. On this knowledge alone one might expect percutaneous absorption to be positively

dependent on lipid and aqueous solubilities. Though such dependency is most clearly seen in homologous series of prodrugs in which the homolog exhibiting the highest flux also exhibited the best balance of high lipid and high aqueous solubilities.[20, 38] Although such qualitative relationships can serve as a general guide for optimizing topical delivery, a mathematical model for accurately predicting permeation through skin based on easily-determined physicochemical properties would be of even greater value as a tool for quickly identifying lead compounds (i.e. those compounds expected to exhibit the highest flux).

Mathematical modeling of diffusion through a complex heterogeneous membrane like the skin can be a formidable challenge. However, the problem can be simplified by assuming that the skin behaves like a homogeneous membrane. Once this assumption is made, most quantitative treatments of skin permeability data begin by considering Fick's first and second laws of diffusion expressed by equations 1 and 2, respectively:

$$J = -D(\partial C/\partial x) \quad (1)$$

$$\partial C/\partial t = D(\partial^2 C/\partial x^2) \quad (2)$$

Fick's first law (equation 1) states that the amount of material passing through a given area of a homogeneous membrane over time (flux, J) is directly proportional to the concentration gradient across the membrane where D (the diffusion coefficient) functions as the proportionality coefficient. Fick's second law (equation 2) states that the rate at which the concentration changes ($\partial C/\partial t$) at any point within the membrane is proportional (again, D is the proportionality coefficient) to the rate of fluctuation in the concentration gradient at that point ($\partial^2 C/\partial x^2$).[40] If the concentration of the permeant in the first layer of skin does not change with time, equations 1 and 2 simplify to equation 3:

$$J = (D/L)(C_{MEM} - C_0) \quad (3)$$

where L is the distance traveled by the permeant on passage through the skin (note: this is not the same as the thickness of the skin; see "Physicochemical Barrier" section above) and C_{MEM} and C_0 are the concentrations of the permeant in the first and last layers of the skin. For all practical purposes, the body functions as a limitless reservoir on one side of the skin where the concentration of the permeant is essentially zero (i.e. sink conditions). In this case, $C_{MEM} >> C_0$ and equation 3 reduces to

$$J = (D/L)(C_{MEM}) = (D/L)(K_{MEM:V})C_V \quad (4)$$

where $K_{MEM:V}$ is the partition coefficient between the membrane and the vehicle (solvent) in which the permeant has been applied, and C_V is the concentration of the permeant in the vehicle.[41]

In the development of the Kasting-Smith-Cooper (KSC) model,[41] the authors noted that in order to make reliable comparisons of flux the experimental conditions under which flux was measured should ensure that each permeant exhibited the same thermodynamic activity. To meet this requirement, Kastings and coworkers decided to only consider those cases in which the permeant is applied as a saturated solution ($C_V = S_V$, where S_V is the solubility in the vehicle). This approach ensures that each permeant experiences the same thermodynamic driving force since each permeant is at its respective maximum concentration (i.e. saturation) in the first layer of the skin. Under these conditions, equation 4 becomes

$$J_M = (D/L)(S_{MEM}) = (D/L)(K_{MEM:V})\ S_V \quad (5)$$

where J_M is the maximum flux, and S_{MEM} is the solubility in the skin. In order to arrive at the diffusion coefficient D, Kasting et al assumed[41] that diffusion through the

intercellular lipids of the SC can be approximated from similar models that describe diffusion through polymer membranes. By this approach, D becomes

$$D = D_o \exp(-\beta MV) \quad (6)$$

where D_o is the diffusivity of a hypothetical molecule having zero molecular volume,[42] β is a constant that is specific to the skin,[43] and MV is molecular volume. The value for S_{MEM} in equation 5 was either calculated from ideal solution theory or was assumed to be approximately equal to the solubility in a model lipid (S_{LIPID}) such as octanol (S_{OCT}).[41] The general form of the KSC model is shown below in logarithmic form:

$$\log J_M = \log (D_o/L) + \log S_{MEM} - (\beta/2.303)\, MV \quad (7)$$

As noted by Potts and Guy,[42] one of the weaknesses of the KSC model is the assumption that S_{OCT} can approximate the solubilizing capacity of the intercellular lipids of the SC (S_{MEM}). To account for the differences between S_{MEM} and S_{OCT}, Potts and Guy proposed that when the vehicle is water ($S_V = S_{AQ}$), $K_{MEM:AQ}$ and $K_{OCT:AQ}$ are related by equation 8

$$K_{MEM:AQ} = (K_{OCT:AQ})^y \quad (8)$$

in which the coefficient y is a measure of the similarities between the two partitioning domains. Since

$$S_{MEM} = (K_{MEM:AQ})(S_{AQ}) \quad (9)$$

substitution of equation 9 into equation 7 gives the following equation for flux

$$\log J_M = \log (D_o/L) + y \log K_{OCT:AQ} + \log S_{AQ} - \beta' MW \quad (10)$$

where molecular weight (MW) has been substituted for molecular volume and $\beta' = \beta/2.303$ but also includes a conversion factor for using MW in place of MV.[42] Whereas

the Potts-Guy model (PG)[42] is an expression of the permeability coefficient (log P = log J – log S_V) equation 10 is a modified version of PG that describes flux.

Though equation 10 is an improvement over KCS, it suffers from the fact that it only applies to aqueous vehicles. Furthermore, it offers little insight into the relative impact of aqueous and lipid solubilites on flux since the S_{OCT} term is "hidden" within $K_{OCT:AQ}$. In order to address these issues, Roberts and Sloan[43] were able to extend the applicability of equation 10 to vehicles other than water in a model which clearly shows the dependency of flux on aqueous and lipid solubilities. Using isopropyl myristate (IPM) as example of when a lipophilic vehicle is applied, the following identity may be used:[43]

$$K_{MEM:IPM} = K_{MEM:AQ}/K_{IPM:AQ} \quad (11)$$

Modification of equation 8 to include IPM gave equation 12

$$K_{MEM:AQ} = (K_{IPM:AQ})^y \quad (12)$$

Substitution of equation 12 into equation 11 gave equation 13

$$K_{MEM:IPM} = (K_{IPM:AQ})^y/K_{IPM:AQ} \quad (13)$$

The general form of the Roberts-Sloan (RS) equation[43] (equation 14) followed from the assumption that solubility ratios could be substituted for partition coefficients and that equation 13 could be substituted into equation 10 to give (after collecting terms):

$$\log J_M = x + y \log S_{IPM} + (1-y) \log S_{AQ} - z\,MW \quad (14)$$

where $x = \log (D_o/L)$ and $z = \beta'$.

It is important to note that all three models predict a negative dependence of flux on the size of the permeant (expressed as either molecular volume MV or molecular weight MW). However, in contrast to KSC (equation 7 where $S_{MEM} = S_{OCT}$)[41] and PG (equation

10 where $S_{MEM} = (K_{OCT:AQ})^{y}(S_{AQ})$,[42] RS (equation 14 where $S_{MEM} = (S_{IPM})^{y}(S_{AQ})^{1-y}$) indicates that the intercellular matrix of the SC is a biphasic material consisting of aqueous and lipid phases—a description which is consistent with electron micrographs of normal[24, 26] and hydrated[44] human skin. A fit of the flux, molecular weight, and solubility data from 61 prodrugs (*in vitro* mouse) to RS suggested that water solubility was nearly as important as lipid solubility (0.52 S_{IPM}, 0.48 S_{AQ}, $r^2 = 0.91$).[45] When a similar analysis was performed on a smaller dataset (n = 10) from the delivery of nonsteroidal anti-inflammatory drugs from mineral oil (MO) through human skin *in vivo*, flux was again positively dependent on solubilities in water (0.28 S_{AQ}) and in a lipid (0.28 S_{AQ}, 0.72 S_{MO}, $r^2 = 0.93$). A recent analysis of a much larger database (n = 103) of *in vitro* human skin data gave similar values for octanol and water solubilities (0.56 S_{OCT}, 0.44 S_{AQ}, $r^2 = 0.90$).[46]

Prodrugs

By definition, an inactive derivative of an active drug that does not revert to the parent compound *in vivo* can not be considered a prodrug, and more importantly, is not therapeutically useful. For example, Billich and coworkers recently reported that certain trimethylammonio-alkyl carbonyl derivatives of cyclosporin A (CsA) exhibited fluxes that were 180-times greater than CsA.[47] However, the authors were unable to detect any CsA in the skin and only trace amounts (< 5% total CsA species as CsA) were found in the receptor phases of the diffusion cells. In this case, since the derivative was inactive,[47] the improvement in flux was therapeutically useless except as a demonstration of the potential permeation-enhancing effect of a trimethylammonio-alkyl carbonyl group.

Most prodrugs are designed to be enzymatically labile in order to avoid chemical stability problems that might arise during formulation. One major benefit of enzymatic

activation is the potentially greater tissue-specific delivery of the active drug.[48] An example for purely enzymatic activation is the conversion of minoxidil (6-(1-piperidinyl)-2,4-pyrimidinediamine-3-oxide) to minoxidil sulfate following topical application of minoxidil to the scalp (Figure 1-4).[49] At least four different sulfotransferase enzymes are believed to be responsible for the bioactivation of minoxidil.[49, 50] Although it was originally given orally as an antihypertensive agent, it was later found to stimulate hair growth and is now used as a treatment for alopecia.[50] While the benefits of enzymatic activation are clear, it is important to recognize that enzyme-mediated reactions are subject to interspecies and inter-individual variation, whereas chemical activation is largely under the control of the researcher—a situation that results in more predictable rates of delivery of active drug. In the case of minoxidil, there is evidence to suggest that the inefficacy of topical minoxidil in some individuals is due to relatively low sulfotransferase activity in those patients.[51]

The rationale for using prodrugs to overcome the skin barrier was briefly mentioned in Section A-4. Although the most well-known and profitable prodrugs have been developed for oral administration,[2, 48, 52] many of the same types of prodrugs have been evaluated as topical delivery agents as well.[19, 20] A comprehensive review of all the major classes of prodrugs evaluated to date in topical delivery investigations is beyond the scope of this thesis. However, the interested reader may find such information in several detailed reviews of the subject.[19, 20, 38] In this section, only two of the major classes of prodrugs, acyl and soft alkyl, will be discussed.

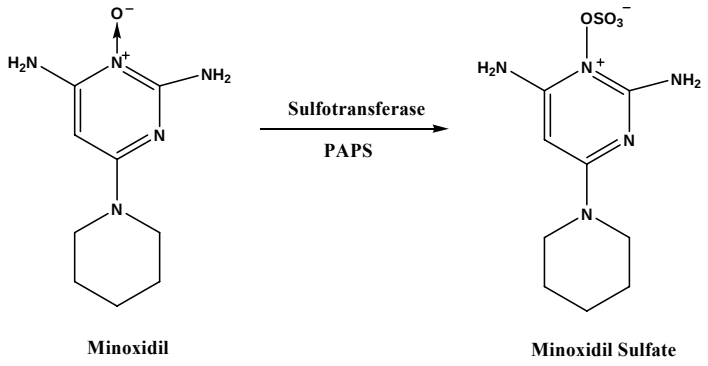

Figure 1-4: Bioconversion of Minoxidil to Minoxidil Sulfate by Scalp Sulfotransferase in the Presence of 3′-Phosphoadenosine-5′-phosphosulfate (PAPS)

Acyl Prodrugs

The most common type of prodrug found on the market today is one in which a heteroatom on the drug has been acylated to give the corresponding ester, carbonate, amide, or carbamate.[2] Most of these promoieties contain simple aliphatic groups in the acyl chain such as the esters of captopril ((2S)-1-(3-mercapto-2-methylpropionyl)-L-proline) recently evaluated by Moss et al (Figure 1-5).[53] Six esters of captopril were synthesized in which only the length of the alkyl chain was varied from the methyl to the hexyl ester. As expected, all of the prodrugs were less soluble in water (S_{AQ}) than captopril (range of S_{AQ} = 0.03-0.58 times the S_{AQ} value for captopril). However, all were much more soluble in octanol (S_{OCT}) than the parent. Although solubilities in octanol (S_{OCT}) were not measured, they may be estimated from the calculated partition coefficients ($K_{OCT:AQ}$) reported by the authors. By this approach, all of the ester prodrugs were approximately 4- to 89-times more soluble in octanol. As a result of their higher lipophilicity, five of the derivatives permeated porcine skin more effectively than captopril. Within this series of more lipophilic homologs, the member that exhibited the greatest increase in flux (40-fold) was also the second-most water soluble member of the

series. Thus these results agree with literature precedent[19, 20] and the RS model (equation 14),[43] and they demonstrate the dependence of flux on biphasic solubility.

While most acyl-type prodrugs contain simple aliphatic groups in the acyl chain, there are many reports[19, 20] of the benefits of incorporating other functional groups into the acyl chain. Milosovich and coworkers[54] have shown that in lieu of the aliphatic ester approach that is typically used to deliver steroids,[19] introduction of a tertiary amine into the promoiety can lead to dramatic improvements in flux. To prove the usefulness of such an approach, the authors reported that a 10% solution of the hydrochloride salt of testosteronyl-4-dimethylaminobutyrate (TSBH) exhibited a 60-fold greater flux through human skin *in vitro* than a 10% suspension of testosterone (TS) (Figure 1-5). The free base of TSBH also exhibited a flux that was 35-times greater than TS.[54] As noted by Milosovich et al.,[54] the relatively high fluxes of the prodrugs are likely the result of increasing aqueous solubility without compromising lipophilicity. For instance, TSBH is at least 340-times more soluble in pH 7 phosphate buffer than TS, yet the decrease in partition coefficient ($K_{OCT:AQ}$) on going from TS (log $K_{OCT:AQ}$ = 3.3) to TSBH (log $K_{OCT:AQ}$ = 2.7) is minimal. Similar results were reported by Wasdo and Sloan[45] in a study of alkylcarbonyloxy (AOC) derivatives of acetaminophen (4-hydroxyacetanilde, APAP) (Figure 1-5). In this case, the goal was to improve the biphasic solubility of the parent by replacing a methylene group in the acyl chain with oxygen to give an ether. Thus, the difference between this and the previous example is the absence of an ionizable group in the acyl chain of the AOC promoiety. The effect of heteroatom substitution on the physicochemical properties of the prodrugs is most apparent in a comparison of 4-butyloxycarbonyl-APAP (4-BuOC-APAP) with 4-(2′-methoxyethyloxycarbonyl)-APAP

(4-MOC2-APAP). Although 4-MOC2-APAP was 0.74-times less soluble in isopropyl myristate (IPM) than 4-BuOC-APAP, it was 81-times more soluble in water than 4-BuOC-APAP and consequently exhibited 8-times the flux of 4-BuOC-APAP. Both prodrugs were more soluble in IPM (5- to 7-fold) than APAP, but neither was more soluble in water than the parent. However, since 4-MOC2-APAP exhibited better biphasic solubility than APAP, its flux was 1.5-times higher than the flux of APAP.

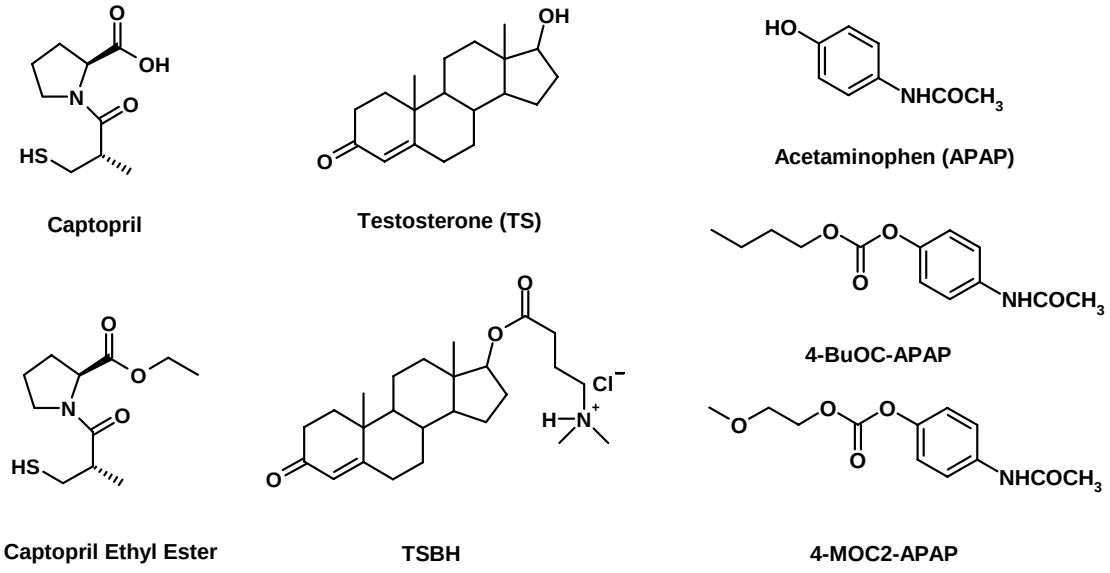

Figure 1-5: Structures of Acyl Prodrugs for the Topical Delivery of Captopril Testosterone, and Acetaminophen

A variety of mechanisms have been identified for the conversion of acyl prodrugs to their respective parent compounds.[19, 20] However, simple aliphatic acyl prodrugs are typically hydrolyzed by one of the mechanisms shown in Figure 1-6.[2, 55] Although both reactions are theoretically reversible, the base-catalyzed hydrolysis is usually driven to completion by the formation of the carboxylate anion[55] and is shown in Figure 1-6 as an irreversible process.

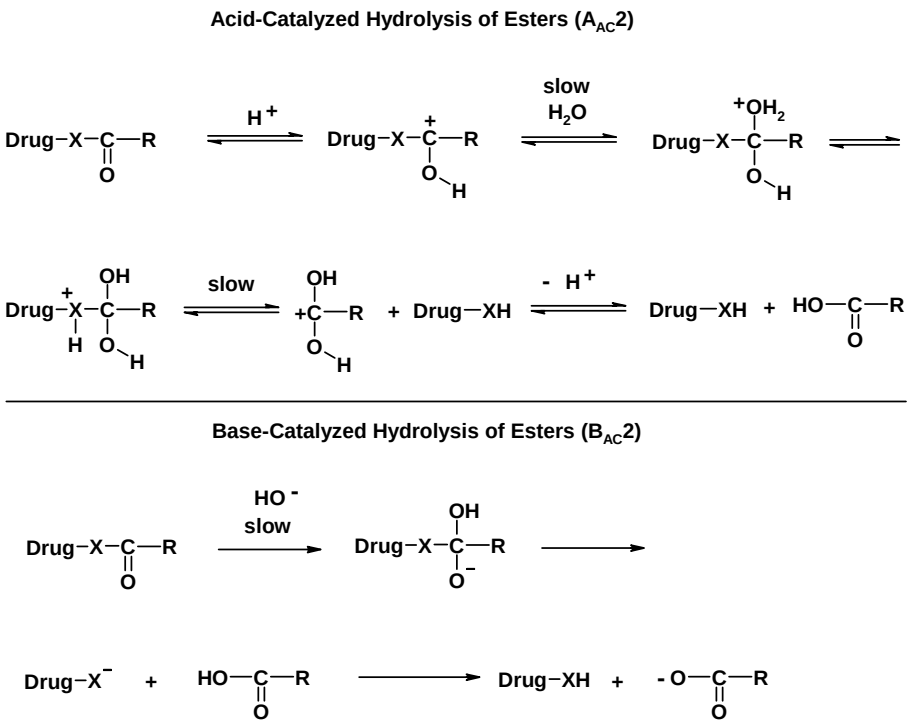

Figure 1-6: Most Common Mechanisms by which Acyl Prodrugs are Hydrolyzed Chemically

Soft Alkyl Prodrugs

The term "soft alkyl" was first given[56] to the alkylcarbonyloxymethyl (ACOM) derivative of the amide-type compound shown in Figure 1-7 because it is an ester derivative of the corresponding hydroxymethyl compound which is an alkyl derivative of the parent drug. Whereas the hydroxymethyl prodrug requires chemical activation to give the parent, the corresponding ACOM derivative generally undergoes a two-step process involving an initial enzymatic (or chemical) hydrolysis followed by chemical activation to give the parent.[19] This is in contrast to the "hard alkyl" prodrug shown in Figure 1-7 for which bioconversion is restricted to enzymatic oxidation.[56] Although soft alkyl derivatives cover a wide range of promoieties,[19] only ACOM and

alkyloxycarbonyloxymethyl (AOCOM) derivatives will be considered since they are the focus of this thesis.

Much of the work on soft alkyl approaches to improve topical delivery[19, 20, 38] has focused on polar heterocycles such as theophylline (Th) and 6-mercaptopurine (6-MP). Three of these examples are shown in Figure 1-8. In their report on the synthesis and *in vitro* evaluation of a homologous series of 7-ACOM-Th derivatives, Kerr and coworkers[57] noted that all of the homologs (R = CH_3 to C_5H_{11} and $(CH_3)_3C$) were substantially more soluble in IPM (8- to 229-times) than Th. However, the maximum flux exhibited by any of the prodrugs was only 2.2-times higher (for R = C_3H_7) than the flux of Th. Such a modest increase in flux is probably due to the loss of water solubility (S_{AQ} = 0.04 to 0.27-times the S_{AQ} of Th) on going from the parent to the prodrug. This situation is much different for the ACOM prodrugs of 6-MP (R = CH_3 to C_5H_{11} and C_7H_{15}). The first three members of the 6-ACOM-6-MP series were 2 to 6-times more soluble in water than the parent. As with the Th series, all of the 6-ACOM-6-MP prodrugs were much more soluble (50 to 200-times) in IPM than the parent. In contrast to the Th series, the 6-MP prodrugs permeated the skin much more effectively than 6-MP (53 to 69-fold improvement in flux for the first four members of the series). The relative ineffectiveness of the ACOM approach in the case of Th may be rationalized by considering the fact that Th itself is 41-times more soluble in water and 15-times more soluble in IPM than 6-MP. Consequently, Th is much more effective (126-times higher flux) at penetrating the skin than 6-MP. These results demonstrate that it is easier to improve the flux of a poorly soluble compound such as 6-MP with a prodrug approach.

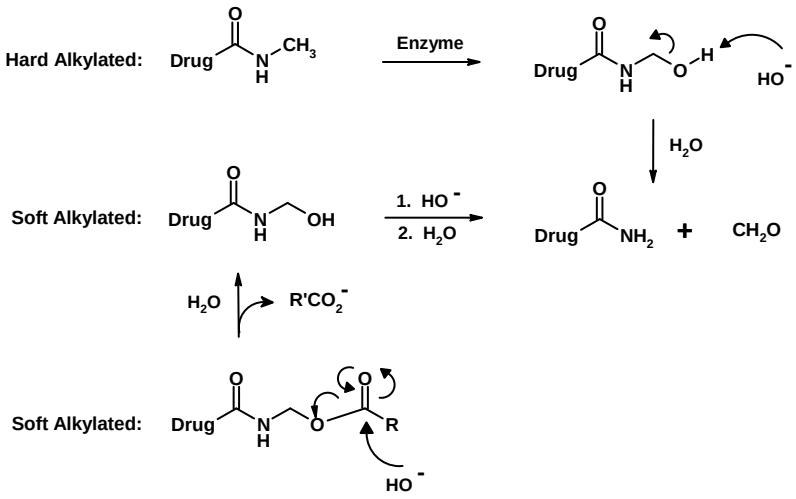

Figure 1-7: Mechanism of Hydrolysis of Soft Alkyl Prodrugs (Alkylcarbonyloxymethyl and Hydroxymethyl Derivatives are shown) and Comparison to Metabolism of "Hard Alkyl" Derivatives (General Mechanism for an Enzymatic N-Demethylation Reaction is given as an Example)

In spite of their proven effectiveness in oral drug delivery,[2] AOCOM prodrugs have received little attention in topical delivery. In fact, the 7-AOCOM derivative of Th shown in Figure 1-8 appears[19, 20] to be the only example of the use AOCOM prodrugs to improve percutaneous absorption.[58] However, the authors of the study for which it was synthesized were more interested in the hydrolytically more labile 7-ACOM-Th prodrugs and chose not to evaluate this particular derivative in diffusion cells.[58] The example of bacampicillin, an orally administered prodrug of ampicillin, has been included in Figure 1-8 as a reminder of the potential usefulness of the AOCOM promoiety. In a comparative study of the pharmacokinetics of orally administered pivampicillin (an ACOM prodrug of ampicillin), bacampicillin and ampicillin, bacampicillin exhibited the highest rate of absorption and shortest absorption lag time. Both prodrugs were equally effective at improving the oral bioavailability of ampicillin.[59]

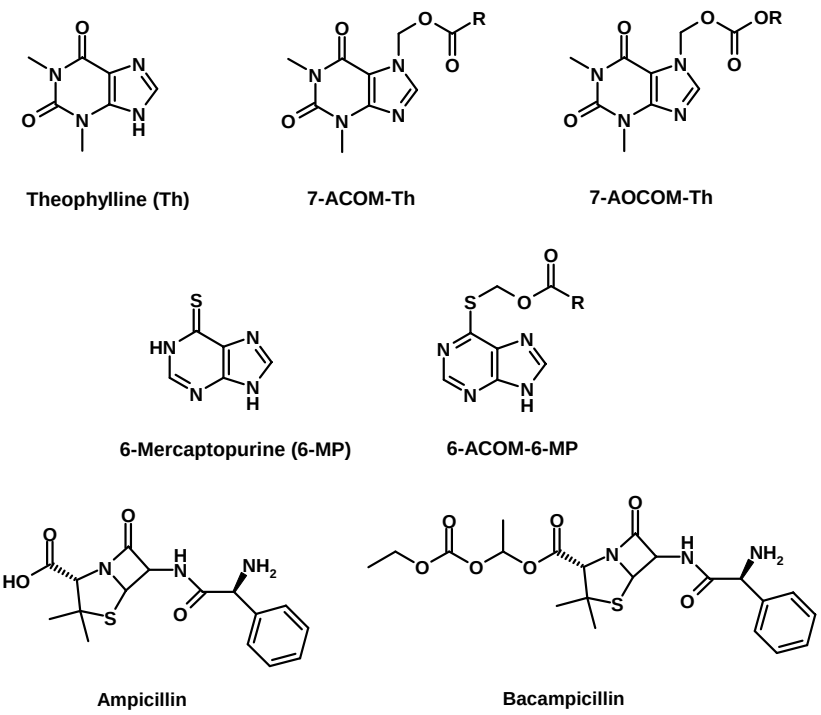

Figure 1-8: Examples of Alkylcarbonyloxymethyl (ACOM) and Alkyloxycarbonyloxymethyl (AOCOM) Prodrugs

Conclusions

Although oral drug delivery will likely remain the method of choice for drug administration, it is not a suitable route for many different medications due to the substantial biochemical barrier presented by the GI tract and liver. One of the main advantages of transdermal delivery is the avoidance of first-pass metabolism that stems from the relatively low enzymatic activity of the skin compared to the liver. As illustrated in the case of transdermal versus oral estrogen, topical delivery is often a safer alternative to the oral route. In addition, topical delivery provides a means for treating local conditions without exposing the systemic circulation to high levels of the therapeutic agent.

In contrast to the GI tract and liver, the skin functions mainly as a physical barrier to drug absorption with the outermost layer, the stratum corneum, providing most of the

resistance to permeation. Electron micrographs of the stratum corneum have shown that intercellular matrix through which a permeant must pass is composed of alternating layers of polar and nonpolar material. Such evidence supports *in vivo* and *in vitro* skin penetration experiments in which flux through skin was positively dependent on the aqueous as well as lipid solubility. These qualitative observations were subsequently used to develop a mathematical model (i.e. the Roberts-Sloan model, RS) for accurately predicting flux through skin based on the solubility properties and molecular weight of the permeant.

Among the many methods used to overcome the skin barrier, a prodrug/formulation approach is one of the most attractive as it would likely increase permeation while minimizing side effects. Two of the most successful promoieties used in topical delivery are the acyl and soft alkyl-type. Of these two types, the acyl promoiety is the most common perhaps by virtue of its relatively facile synthesis and generally low toxicity of its hydrolysis byproducts. Though they are not as common, soft alkyl prodrugs have a long history of improving oral bioavailability as well as topical delivery. AOCOM derivatives are a sub-type of soft alkyl prodrugs that are underrepresented in topical delivery and should be further investigated using skin permeation experiments. Regardless of the promoiety, flux was shown to depend directly on the lipid and aqueous solubilities of the prodrug.

CHAPTER 2
SPECIFIC OBJECTIVES

First Objective

The first objective of the present investigation was to synthesize a homologous series of alkylcarbonyloxymethyl (ACOM) and alkyloxycarbonyloxymethyl (AOCOM) derivatives of a model phenol. There are currently no examples of the topical delivery of ACOM and AOCOM derivatives of phenols. This is in spite of their well-documented effectiveness at improving the oral bioavailability[2] of phosphates and carboxylic acids, and the topical delivery[19] of amides, imides, thioamide, and carboxylic acids. Most of the previous work on the topical delivery of phenols via a prodrug approach has focused on the corresponding acyl derivatives.[19, 45, 60-65] One of the most studied classes of drug in that respect is the narcotic analgesics (see Figure 2-1 for examples). Narcotic analgesics are usually given intravenously, sublingually, or intramuscularly in order to avoid extensive first-pass metabolism on oral administration, but the parenteral routes are also associated with high peak plasma levels and require frequent dosing. In addition to its avoidance of first-pass metabolism, transdermal administration is typically associated with constant rates of delivery into the systemic circulation and has a relatively high degree of patient compliance.[5] Thus, topical delivery is an attractive alternative to the current methods by which these compounds are administered.

Most reports on the use of ester (alkylcarbonyl AC)[60, 62-64] and carbonate (alkyloxycarbonyl AOC)[45, 61, 65] prodrugs to increase the percutaneous absorption of narcotic analgesics indicate that the improvement in flux is only modest (2-7 fold).

However, Sung et al.[63] found that the decanoate ester of nalbuphine was 40-times more permeable than the parent when delivered from pH 4 buffer, and Drustrup et al.[60] found that the 3-hexanoate ester of morphine was approximate 3500-times more permeable than morphine when delivered from IPM. Although it is impossible to know whether ACOM and AOCOM prodrugs of phenols will work better than the corresponding acyl derivatives,[19] there does not appear to be great differences in permeation enhancement when an acyl promoiety is used in place of an ACOM in the same parent drug (compare 1-AC[66] to 1-ACOM-5-fluorouracil[67] and 3-AC[68] to 3-ACOM-5-fluorouracil[69]). On the other hand, since the carbonyl moiety of the prodrug is separated from the parent compound by a methylene spacer, the physicochemical properties of soft alkyl derivatives are governed less by the parent drug and more by the promoiety. The result is that soft alkyl prodrugs such as ACOM and AOCOM are more easily customized to meet the particular objectives (drug solubility, stability, etc.) of the investigator.[38]

One example where a soft alkyl prodrug may be more effective than the corresponding AC derivative is α-tocopherol (Vitamin E). Vitamin E is one of several key compounds responsible for maintaining an effective barrier against free-radical damage in cellular membranes.[70] In fact, it is the primary antioxidant for membranes and lipids. Since the body does not synthesize vitamin E, it must be taken in through diet or given as a supplement. However, there is currently no efficient way to administer supplemental Vitamin E.[70] Oral administration of Vitamin E suffers from slow absorption rates[71] and generally provides inferior photoprotection compared to topically applied Vitamin E.[71, 72] Intravenous formulations of Vitamin E have also been administered, but in some cases,[73] life-threatening side effects have ensued. Part of the

difficulty in delivering Vitamin E is that it is practically insoluble in water[74] and readily oxidizes in air. The problem of instability has traditionally been solved by converting Vitamin E to its acetate or succinate esters. However, this approach introduces a new problem: the acetate and succinate esters do not readily revert to the active compound in vivo.[75] A similar problem has been addressed before in the case of β-lactam antibiotics.[76] Alkyl derivatives of the carboxylic acid group of these drugs exhibit poor bioavailability in vivo, but often see dramatic improvements in prodrug-to-drug conversion when a ACOM or AOCOM approach is used.[2] In the case of Vitamin E, nucleophilic attack at the carbonyl carbon is limited due to the flanking methyl groups on the aromatic ring. One potential solution to this problem is to move the site of hydrolysis away from the sterically hindered chromanol head of Vitamin E by way of a soft alkyl (ACOM or AOCOM) derivative.

Before applying the soft alkyl approach to the narcotic analgesics and Vitamin E, it seemed prudent to first validate the strategy using a simple phenol. Acetaminophen (4-hydroxyacetanilide, APAP) was selected as a model because its ACOM and AOCOM derivatives were expected to be solids (APAP mp = 167-170) and hence more easily characterized. Since a series of AOC derivatives of APAP had been previously evaluated in diffusion cell experiments,[45] it would also be possible to compare the effects of using an acyl versus a soft alkyl promoiety.

Second Objective

The second objective of this project was to determine whether the ACOM and AOCOM prodrugs could improve the topical delivery of APAP. Hairless mouse skin *in vitro* was selected as a model for human skin due to its relatively low cost and in order to

be consistent with all previous work by our lab. Mouse skin also has the advantage of exhibiting less variation than human skin.

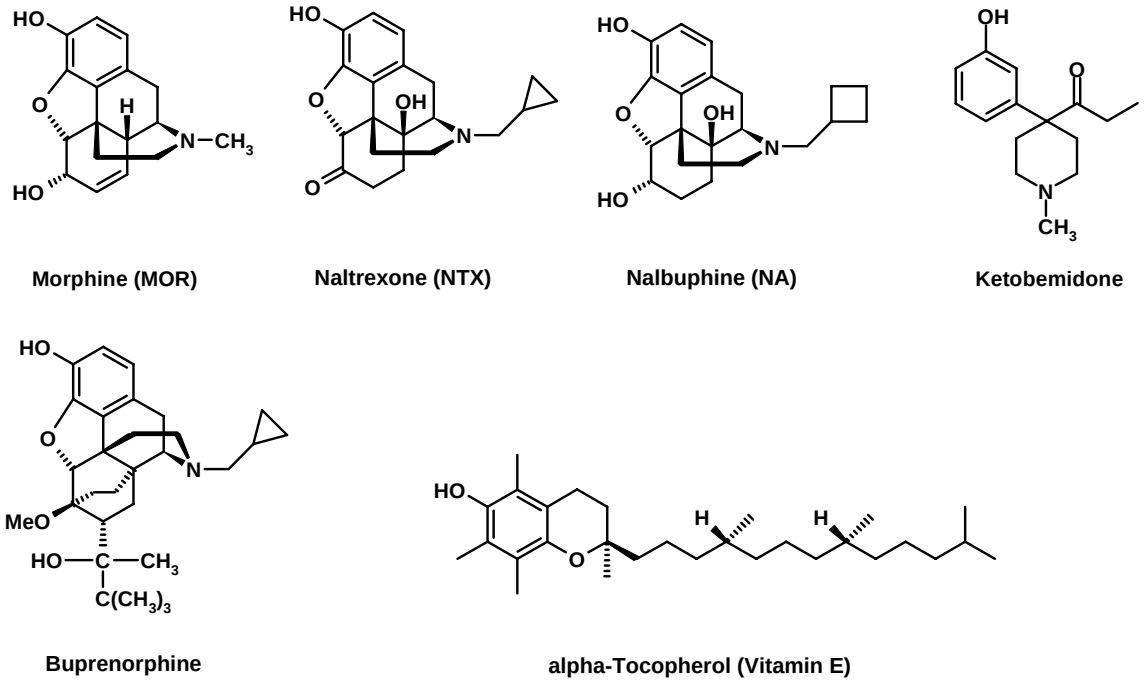

Figure 2-1: Phenol-Containing Therapeutic Agents that may benefit from Topical Delivery via Alkylcarbonyloxymethyl (ACOM) or Alkyloxycarbonyloxymethyl (AOCOM) Derivatization

Third Objective

The third objective of the present investigation was to improve the accuracy of the Roberts-Sloan equation (RS)[43] for predicting flux through hairless mouse skin. At present, the database (n = 61) upon which the RS equation is based is heavily dependant on data from heterocyclic compounds: 59% 5-fluorouracil related entries, 18% 6-mercaptopurine related entries, and 10% Theophilline related entries in the database. Only 8 of the 61 entries (13%) are of a phenolic compound (i.e. APAP). An earlier study found that in general, the error in predicting flux using RS was greater for a phenolic

prodrug (4-AOC-APAP) than for a heterocyclic prodrug.[45] In order to extend the applicability of RS to a wider range of drugs, the structural diversity of the database must be expanded. Incorporation of the ACOM and AOCOM prodrugs into the database would likely result in a more robust RS model.

CHAPTER 3
ALKYLCARBONYLOXYMETHYL PRODRUGS OF ACETAMINOPHEN (APAP)

Synthesis of Alkylcarbonyloxymethyl (ACOM) Iodides

A key feature of the Roberts-Sloan database (Chapter 1)[20] is that it is almost entirely comprised of homologous series. Such homogeneity was intentional as it is easier to determine the impact of physicochemical properties on flux when structural differences are minimal. In keeping with that theme, synthetic routes to **3** that allowed R' to be simple aliphatic groups was desired. Currently, there are three reported methods for synthesizing such alkylating agents. In two of these procedures, ACOM chloride **4** functions as the intermediate from which the corresponding iodide is subsequently generated via a Finkelstein-type halide exchange. Chloromethyl chlorosulfate has proven to be a useful reagent for obtaining ACOM chloride from carboxylic acids under phase-transfer conditions.[77, 78] However, since this method fails for carboxylic acids with fewer than 6 carbon atoms,[77] it was not suitable for the present study. Compound **4** may also be generated via the condensation of acid chlorides with aldehydes in the presence of a Lewis acid.[79, 80] However, this route to ACOM iodide frequently provides low yields of the desired compound.[81] A different approach was taken by Fleischmann and coworkers: they synthesized pivaloyloxyethyl iodide directly from acetaldehyde and pivaloyl chloride in the presence of NaI.[82] In an effort to extend the applicability of this reaction to **3** where R = H, it was found that trioxane **1a** reacts with acid chlorides in the presence of NaI to give predominately compounds **3a-f** in one step (Figure 3-1). Paraldehyde **1b** exhibited a similar reactivity with acid chlorides under the same conditions to give **3**

where R = CH_3. The structure of **3** was arrived at by comparison of its ^{1}H NMR spectra with ^{1}H NMR spectra reported for **3** in the literature.[81]

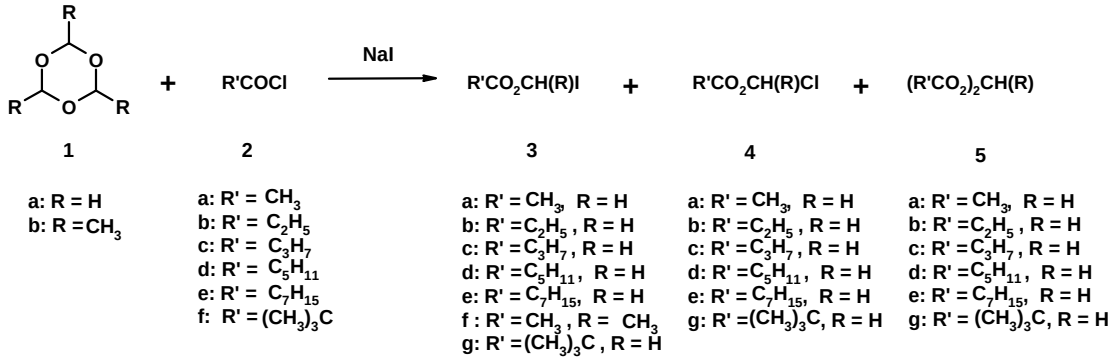

Figure 3-1: Reaction of Trioxane 1a and Paraldehyde 1b with Acid Chlorides in the Presence of NaI

Unfortunately, various amounts of **4** and **5** formed along with **3** as well. Byproduct **4** was identified as the chloride analogue of **3** based on the ^{1}H NMR spectra reported for this compound in the literature,[81] and by comparison to an authentic sample of **4** prepared via a previously reported method.[83] Compound **5** was assigned the structure shown in Figure 3-1 by comparison of its ^{1}H NMR spectra with the product of the reaction of acetic acid with **3a** by a modification of the method of Folkmann and Lund.[84] ^{1}H NMR analysis of the product mixture revealed an upfield shift in the diagnostic methylene singlet from 5.99 ppm in RCO_2CH_2I to 5.73 ppm in the product. Furthermore, the product gave a spectrum that was consistent with bis(acetyloxy)methane. It should be noted that others have observed the formation of bis(acetyloxy)methane in the reaction of trioxane with acetyl mesylate.[85] Thus, it is not surprising that **5** is also formed in the present case. However, in reactions involving paraldehyde (R = CH_3), **4** and **5** could not be detected in the ^{1}H NMR spectrum of the reaction mixture.

In an effort to optimize the reaction, various reaction conditions were employed; the results from some of these experiments are listed in Table 3-1. Given that ACOM

iodides are relatively unstable above room temperature,[81] 25 °C was set as the upper temperature limit for all ACOM iodide syntheses. No reaction occurs in the absence of NaI, and a slight excess of NaI is necessary to achieve good conversion of the starting materials, regardless of solvent. Similarly, pyridine was unable to catalyze the reaction (entry 5) and only carboxylic acid, acid anhydride, and starting material was detected in the product mixture. This result is interesting since French and Adams[86] had previously found that mixtures of pyridine and aromatic acid halides react with aromatic aldehydes to yield the corresponding ACOM halides. Thus, in the present case depolymerization of **1** may be rate-determining. Yields of the desired compound **3** appear to be unaffected by variations in temperature below 25 °C. For example, the yield of **3** does not change substantially if the reactants are allowed to stir for 1 hour at 0 °C after initial mixing, versus allowing the mixture to stir at room temperature immediately after all reactants have been added (data not shown). Likewise, the yield of **3** is substantially unaffected by the length of time over which **2** is added (entry 7 versus entry 9) and by the degree to which **2** is converted to the acyl iodide before **1** is added (entry 8). On the other hand, the formation of **3** appears to be more sensitive to the form of the aldehyde undergoing conversion. This relationship is most apparent in entries 6 and 10. As shown in the Table 3-1, trioxane reacts with octanoyl chloride to give octanoyloxymethyl iodide in 86 % yield (entry 6). In contrast, paraformaldehyde reacts under the same conditions to give only 45% yield of the desired ACOM iodide (entry 10). Though the reaction was run only once, byproduct **4** seems to be more favored when paraformaldehyde is used instead of trioxane (entry 10 versus entry 6). As shown in entries 3 and 11, the reaction is also

able to accommodate a certain amount of steric hindrance in **1** and **2**; however, the reaction of **1b** with **2f** was not attempted.

Table 3-1: Variation in Reaction Conditions, Crude Yield[a] of **3**, **4**, and **5**, and Percentage of **1** Remaining at the End of the End of the Experiment[b]

Entry	R	R'	Molecular Ratio[c] 1 : 2 : NaI	Solvent	% Yield			% of 1 Remaining
					3	4	5	
1[d, e]	H	C_2H_5	1 : 1 : 1	CD_3CN	46	11	11	18
2[d, e]	H	C_2H_5	1 : 1 : 1.2	CD_3CN	54	7	11	7
3[d, e]	CH_3	CH_3	1 : 1 : 1.2	$CDCl_3$	83	[f]	[f]	17[g]
4[d, e]	H	C_2H_5	1 : 1 : 0	$CDCl_3$	--	0	0	100
5[h]	H	C_7H_{15}	1 : 1 : 0	CH_2Cl_2	--	0	0	100
6[e]	H	C_7H_{15}	1 : 1 : 1.2	CH_2Cl_2	86	10	4	0
7[e]	H	C_7H_{15}	1 : 1 : 1	CH_2Cl_2	74	11	6	6
8[d, i]	H	C_3H_7	1 : 1 : 1	CH_3CN	33	[f]	[f]	[f]
9[j]	H	C_7H_{15}	1 : 1 : 1	CH_2Cl_2	70	16	8	8
10[e, k]	--	C_7H_{15}	1 : 1 : 1.2	CH_2Cl_2	45	40	15	0
11[e]	H	$(CH_3)_3C$	1 : 1 : 1.2	CH_2Cl_2	70	24	6	0
12[e, l]	H	C_7H_{15}	1 : 1 : 1.2	CH_2Cl_2	87 ± 2	6 ± 1	3 ± 0.6	6 ± 3
13[e]	H	C_5H_{11}	1 : 1 : 1.2	CH_2Cl_2	89	7	4	2
14[e, l]	H	C_3H_7	1 : 1 : 1.2	CH_2Cl_2	82 ± 4	14 ± 4	4 ± 1	0
15[e, l]	H	C_2H_5	1 : 1 : 1.2	CH_2Cl_2	80 ± 6	16 ± 4	5 ± 2	0
16[e, l]	H	CH_3	1 : 1 : 1.2	CH_2Cl_2	72 ± 2	19 ± 3	11 ± 2	0

[a] Unless otherwise noted, entries represent a single experiment (n = 1). [b] Reaction time was usually 20-24 hours. [c] Molecular ratio shown is based on equivalents of formaldehyde or in the case of paraldehyde, equivalents of acetaldehyde. [d] Crude yield determined using benzene as an internal standard. [e] **2** is added to a mixture of **1** and NaI within 1-20 min. [f] Could not determine from ^{1}H NMR spectrum. [g] Present as the monomer, acetaldehyde. [h] 0.3 mol % pyridine added as a catalyst. [i] **2** is allowed to react with NaI for 1 h at 25 °C. After 1 h, a solution of **1** is added over 40-60 min at 0 °C. [j] **2** is added over 2 h to a mixture of **1** and NaI. [k] Paraformaldehyde used instead of trioxane. [l] Average ± SD, n = 3.

As this study progressed, it became apparent that the product distribution was dependent on the type of NaI being used. Practically all of the ACOM iodides used in this study (including those represented in Table 3-1) were prepared using NaI from three different lots and purity grades purchased from Aldrich during the 1980s (see Experimental). These particular batches of NaI were eventually consumed and additional NaI of the same purity and catalog number was ordered from Aldrich. However, when this new (purchased 2005) NaI was used as shown in Figure3-1, the reaction failed to

reach completion even after 48 hours. Moreover, the mixtures resulting from such reactions were always contaminated with a large amount of unwanted byproducts. In other experiments, this "new" NaI was still able to convert alkyl chlorides to the corresponding iodides as expected for a Finkelstien reaction. These divergent results were rationalized by assuming that the older batches of NaI were contaminated with traces of an unidentified catalyst. Subsequent experiments in which various transition metals and Lewis acids were added to the reaction mixture indicated that this was indeed the case. For example, zinc dust[87] (23 mol %) was found to catalyze the reaction by fully converting **1** to products, but unfortunately compound **5** was the major product. Other transition metal catalysts such as iron also failed to improve the yield of **3**. Aluminum metal, as well as $AlCl_3$ (≤ 23 mol %), suppressed the formation of **4** and **5**, but failed to fully convert **1** to products. However, if a combination of $AlCl_3$ (≤ 10 mol %) and I_2 (≤ 5 mol %) was used, total **4** and **5** were minimized (< 14% and < 15% of product mixture, respectively) and **1** was completely consumed. It was further noted that aluminum metal is completely consumed during the reaction and that $AlCl_3$ gives the same results as aluminum metal under identical reaction conditions. These results suggest a reaction mechanism that involves Lewis acid (formed by traces of HCl in the acid chloride reacting with traces of metal in the NaI) catalysis. Interestingly, in the one case where AlI_3 and $AlCl_3$ were allowed to react separately under identical conditions, the resulting product mixtures differed considerably. Conversion rates in those experiments differed by 50% (though in neither case was **1** completely consumed), and in the AlI_3 reaction, several unidentifiable byproducts were formed as well. These results suggest that $AlCl_3$, and not AlI_3 is the principle catalyst in this reaction.

Though a Lewis acid such as $AlCl_3$ is (apparently) important for successful formation of **3**, other experiments indicate that iodide ion and I_2 are needed for the depolymerization of **1**. If $AlCl_3$ is replaced with an equivalent amount of I_2, **1** is completely converted to products: molar ratio **3**:**4**:**5** = 1:1:1.5 plus an unidentifiable byproduct. Also, in the absence of NaI, **1** reacts slowly with **2** and $AlCl_3$ to give a mixture of unidentifiable byproducts and only minor amounts of **4** (approximately 50% conversion of **1** to these products after 24 hours). Thus, iodide ion likely aids in opening compound **1**, perhaps through an S_N2 process similar to that proposed by Balme and Gore[88] for the cleavage of acetals by $TiCl_4$/LiI. Since I_2 also increases the rate at which compound **1** is converted to products, it may facilitate the cleavage of **1** by coordinating with the oxygen atoms in the ring thereby polarizing the CH_2O--CH_2 bond in the formal moiety. Unfortunately, a catalyst system that consistently matched the reactivity of the older batches of NaI could not be identified. However, it should be noted that when crude reaction mixtures of **3** generated via the modified procedure (5 mol % $AlCl_3$ and 2 mol % I_2 included in reaction mixture) were allowed to react with 4-hydroxyacetanilide, the product mixtures were no different than those obtained using **3** generated from the older batches of NaI.

Coupling Reaction of ACOM Iodides with 4-Hydroxyacetanilide

It has long been known that ACOM halides **3** display ambident reactivity—sometimes nucleophiles react at the carbonyl to give acylated products while at other times the alkyl halide carbon is attacked to give alkylated products (Figure 3-2). Such reactivity has been observed in reactions of ACOM halides with a variety of nucleophiles including amines,[89] phenols,[90] and alcohols.[90] In the initial report on the reactions of ACOM halides with phenols,[90] it was noted that the nucleophilicity of the phenol and the

nucleofugicity of the halide are key determinants of the product distribution. More nucleophilic phenols tend to give acylated products, while better leaving groups and less nucleophilic phenols shift the product distribution in favor of the alkylated phenol. It was also suggested[90] that **7** is favored by functional groups at the methylene spacer that are capable of stabilizing a positive charge.

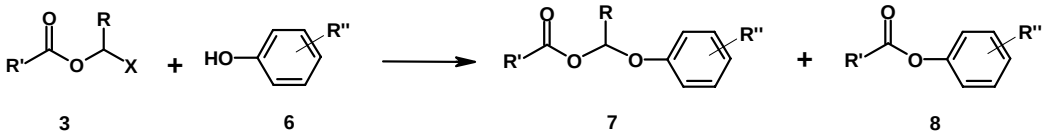

Figure 3-2: General Reaction of Alkylcarbonyloxymethyl (ACOM) Halide **3** with Phenol **6** to Give Aryl Acylal **7** and Aryl Ester **8**

Recently, Ouyang and coworkers have suggested that the percentage of **7** in the product mixture is also directly proportional to the degree of steric hindrance in **3** and in **6**.[91] According to Ouyang, compound **8** is the major product if **3** and **6** are relatively free from steric hindrance, but as the degree of steric hindrance in **3** and **6** increase so does the percentage of **7**. Ouyang's conclusions were based on reactions between various phenols and compounds **9** in which the size of the amino-protecting group was varied from the relatively small allyloxycarbonyl to the bulky 9-fluorenylmethoxy carbonyl (Figure 3-3). As shown in Table 3-2, the product distribution was shifted almost entirely toward acylated phenol **8** when the protecting group was small (entry 13). As the steric bulk of the protecting group increased, so did the percentage of alkylated product **7**, reaching as high as 15% of the product mixture (entry 15). Although higher yields of **7** were realized if both **3** and **6** were sterically hindered (entry 16), **8** remained the major product in all cases. Compound **7** became the major product (58%) only when the base was changed from K_2CO_3 to Cs_2CO_3, and both **3** and **6** were sterically hindered (R' = Boc-D-Leu, R =

H, Y = H, Z = $CCCO_2Pac$). Based on these results, it was concluded[91] that both **3** and **6** must be sterically hindered in order to shift the product distribution in favor of **7**.

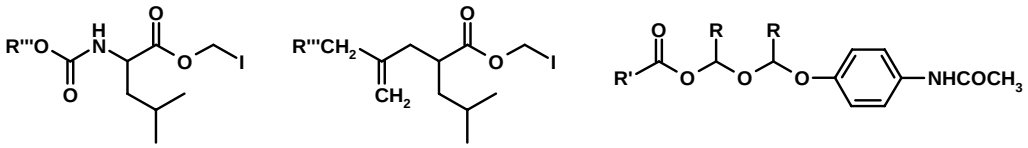

9 **10** **11**

Figure 3-3: Structures of ACOM Derivative of a Protected Amino Acid **9** (R‴ = Protecting Group) and its Corresponding Aliphatic Derivative **10**, and Structure of Byproduct **11**

Table 3-2: Product Distribution of the Reaction[a] of ACOM Halides **3** with Phenols **6**: Data Taken from the Literature

Entry	R'	R	X	Y	Z	Distribution (%)[b]		ν[c]	Ref
						7	8		
1	$(CH_3)_3C$	H	Cl	H	H	0	100	1.24[d]	90
2	$(CH_3)_3C$	H	Cl	OCH_3	H	0	100		90
3	$(CH_3)_3C$	H	Cl	NO_2	H	50	50		90
4	$(CH_3)_3C$	H	I	H	H	100	0		90,91[e]
5	$(CH_3)_3C$	H	I	OCH_3	H	100	0		90
6	$(CH_3)_3C$	H	I	NO_2	H	100	0		90
7	CH_3	H	I	H	$CONH_2$	(25)[f]	[g]	0.52[d]	93
8	C_3H_7	H	I	H	$CONH_2$	(47)[f]	[g]	0.68[d]	93
9	$(CH_3)_3C$	H	I	H	$CONH_2$	(29)[f]	[g]		93
10	CH_3	H	Br	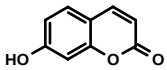		(25)[f]	[g]		92
11	C_2H_5	H	Br	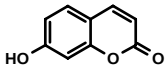		(24)[f]	[g]		92
12	$(CH_3)_2CH$	H	I	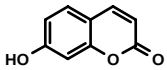		(30)[f]	[g]	0.76[d]	92
13	Alloc-D-Leu	H	I	H	H	5	95	1.75[h] (0.69)[i]	91
14	F-moc-D-Leu	H	I	H	H	10	90	1.75 (1.41)[j]	91
15	Boc-D-Leu	H	I	H	H	15	85	1.75 (1.24)[k]	91
16	Boc-D-Leu	H	I	H	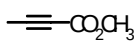	38	62		91

[a] For entries 1-9 and 13-16, base = K_2CO_3, solvent = acetone or acetonitrile. For entries 10-12, base = NaH, solvent = THF. [b] Determined from ^1H NMR spectrum of the crude reaction mixture. [c] Charton's steric parameter for R'. [d] Reference 94. [e] In this case, Cs_2CO_3 was used as a base in lieu of K_2CO_3. [f] Isolated yield. [g] Reference makes no mention of any products other than **7**. [h] Calculated as described in the text. [i] Steric parameter ν of the allyl group (reference 95). [j] Steric parameter ν of the 9-Methyl-9-fluorenyl group (reference 95). [k] Steric parameter of the *t*-butyl group (reference 94).

On the other hand, Bensel and coworkers[92] have demonstrated that good yields of **7** may be obtained when neither **3** nor **6** is sterically hindered (entries 10-12). Bundgaard and coworkers[93] have also shown that if **6** is sterically hindered but **3** is not, **7** may still be obtained in good yield (entries 7-9). Yet, it was unclear whether sterically unhindered ACOM derivatives of 4-hydroxyacetanilide (APAP) could be synthesized given the prior assertions of Ouyang on the importance of steric hindrance.[91] The results from the reactions of **3a-3f** with APAP **6a**, phenol **6b**, and 2,2,5,7,8-pentamethyl-chroman-6-ol **6c** (Figure 3-4) are shown in Table 3-3.

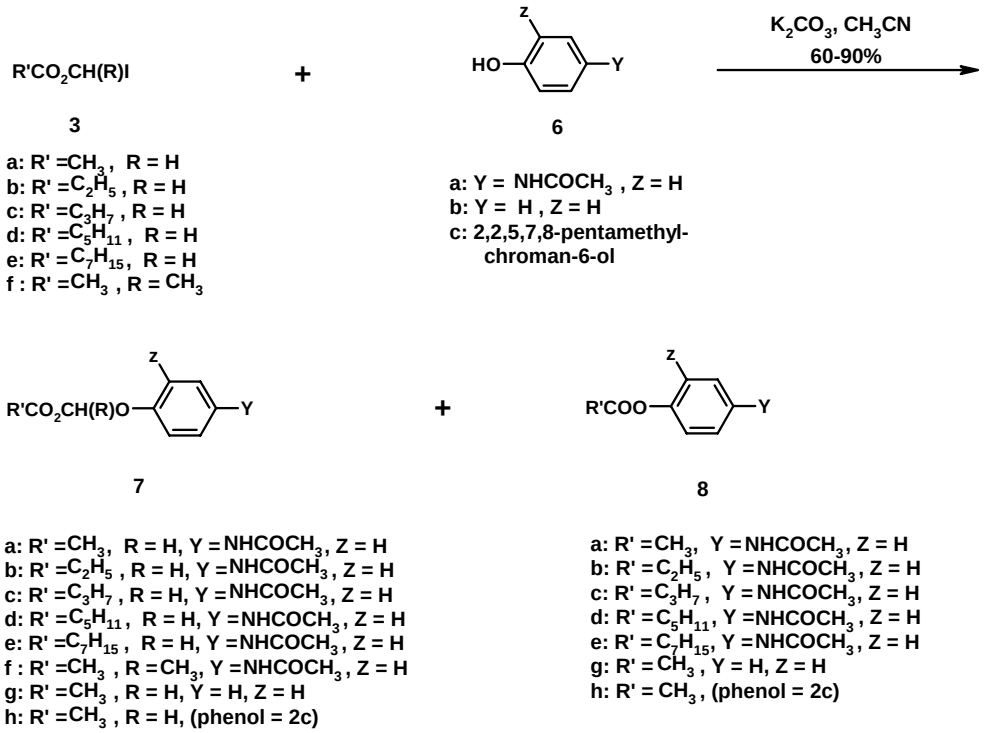

Figure 3-4: Reaction of ACOM Iodides **3a-f** with Phenols **6a-c**

As shown in Table 3-3, **7** was the *major* product in every case regardless of the steric hindrance presented by the phenol **6** or the ACOM iodide **3** (entries 1-6, 8, 9) despite the predictions of Ouyang.[91] There did seem to be a vague relationship between

product distribution and alkyl chain length, however. For alkyl chain lengths longer than propyl, the percentage of **7** remained close to 70% (entries 1-3). As the alkyl chain length decreased from propyl to methyl, there was an incremental decrease in the ratio of **7**/**8** (entries 3-5). The only instance where **8** formed in preference to **7** was when chloride was used as the leaving group X (entry 7). In addition, the reaction of the sterically hindered phenol **6c** with the relatively sterically unhindered **3a** gives credence to the idea[91] that sterically hindered phenols give higher ratios of **7**/**8** than sterically unhindered phenols (entry 9 versus entries 5 and 8). Further increases in the percentage of **7** were realized by introducing a methyl group in place of hydrogen in the methylene linker R of **3** (entry 5 versus entry 6).

Table 3-3: Product Distribution of the Reaction[a] of ACOM Halides **3** with Phenols **6**: Data from the Present Work

Entry	R'	R	X	Y	Z	Distribution (%)[b]			v[c]
						7	8	11	
1[d]	C_7H_{15}	H	I	$NHCOCH_3$	H	71 (1.7)	27 (1.7)	2 (1.2)	0.73[e]
2[f]	C_5H_{11}	H	I	$NHCOCH_3$	H	66	27	7	0.68[e]
3[f]	C_3H_7	H	I	$NHCOCH_3$	H	73	24	3	0.68[e]
4[g]	C_2H_5	H	I	$NHCOCH_3$	H	59 (7)	31 (3)	11 (9)	0.56[e]
5[d]	CH_3	H	I	$NHCOCH_3$	H	49 (2.9)	37 (4)	15 (7.5)	0.52[e]
6[f]	CH_3	CH_3	I	$NHCOCH_3$	H	60	40	0	
7[f]	CH_3	H	Cl	$NHCOCH_3$	H	0	100	0	
8[f]	CH_3	H	I	H	H	63	37	[h]	
9[f]	CH_3	H	I	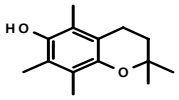		68	32	[h]	

[a] Base = K_2CO_3, solvent = acetone or acetonitrile. [b] Determined from ^1H NMR spectrum of the crude reaction mixture. [c] Charton's steric parameter for R'. [d] Average (SEM, 3 experiments). [e] Reference 94. [f] n =1. [g] Average, 2 experiments; value in parenthesis is the range. [h] Could not determine by ^1H NMR.

It is important to recognize that compounds **3a**-**3f** were not purified before they were used in the coupling reactions with **6a**-**c**. As such, they (with the exception of **3f**) contained various amounts of **4** (Table 3-1) which may or may not have influenced the

product distributions. In their initial report on the coupling reactions of **3** with **6**, Sloan and Koch observed that acylated products readily formed when X = Cl even though **4** was sterically hindered (entries 1-3, Table 3-2).[90] Although **3** is contaminated with **4** in the present study, **3** is much more reactive, and is in excess of **4** by at least 3-4 fold. Thus **6** is more likely to react with **3** than **4**. If the reaction of byproduct **4** with **6** is significant under the present conditions, then there should be a correlation between the ratio of **8**/**7** and the percentage of **4** in the crude product **3** (Table 3-1). Using entry 4 (Table 3-2) as a reference point for when **3** is pure, a plot of the ratio of **8**/**7** versus the percentage of **4** in crude **3** is shown in Figure 3-5. As shown in Figure 3-5, there does not appear to be a strong relationship between the purity of **3** and the ratio of **8**/**7**. It is therefore reasonable to assume that the product distributions observed in the present investigation result solely from the reaction of **3** with **6**.

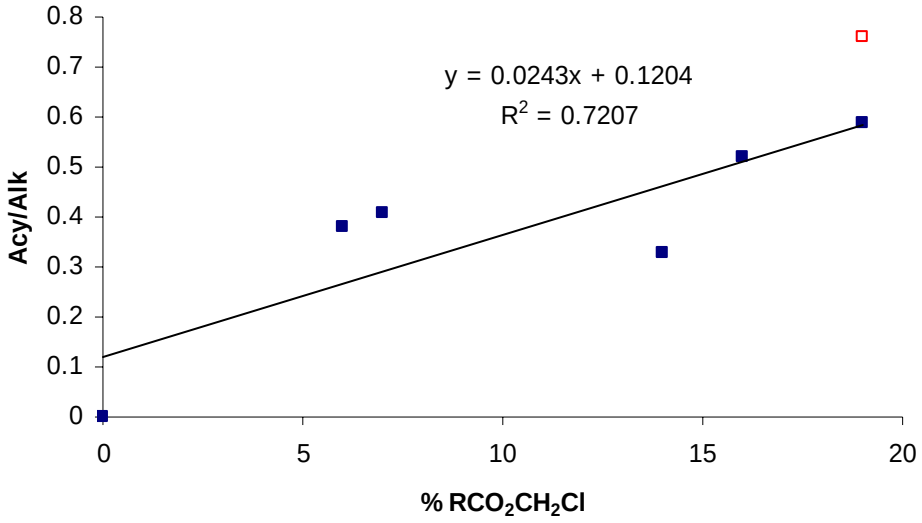

Figure 3-5: Plot of the Percentage of **4** (RCO_2CH_2Cl) in Crude **3** Versus the Ratio of **8**/**7** (Acylated/Alkylated phenol) Resulting from the Reactions of **3a-3e** with **6a** and **6b** (Taken from Entry 4, Table 3-2 and Entries 1-4, and 8, Table 3-3 ■; and Entry 5 □; Note: Entry 5 not Included in Linear Regression Analysis as it appears to be an Outlier)

When ascertaining the affect of steric hindrance on a given reaction, it is often helpful to use a quantitative measure of steric hindrance. In the present work, this was done by relating Charton's steric parameter ν[94] to the ratio of alkylated / acylated phenol (Tables 3-2 and 3-3). Since most of the derivatives of **3** shown in Tables 3-2 and 3-3 contain simple aliphatic groups in the acyl portion R', the ν values could be taken directly from the literature.[94-96] To our knowledge, ν values for the R' groups in entries 13-16 (Table 3-2) have not been reported. Since it was desirable to make all comparisons of steric effects using the same scale, the steric parameter ν for these groups were estimated by assuming that the van der Waals radius of the carbamate moiety in **9** is approximately equal to the corresponding arrangement of methylene groups in **10**.[97] Using **10** as a surrogate for **9**, ν values were then calculated[96] from $\nu = 0.497n_\alpha + 0.409n_\beta + 0.0608n_\gamma - 0.309$, where n_α, n_β, and n_γ, are the number of carbon atoms attached to the alpha, beta, and gamma carbon atoms, respectively, in **10**. Alternatively, the steric effect of R' in entries 13-16 (Table 3-2) may be evaluated by assuming that for this series, the ratio **7**/**8** is determined primarily by the steric bulk of the amino protecting group R'''. In this case, ν values may be taken from the literature since the steric parameters of R''' are known (values in parentheses, entries 13-16, Table 3-2).[94, 95]

Since neither Bundgaard[93] nor Bensel[92] mentioned product distributions in there reports, entries 7-12 (Table 3-2) offer only indirect evidence of the effect of steric hindrance on the formation of **7** and **8**. What is clear from their findings is that good yields of **7** may be obtained under essentially the same conditions used by Ouyang[91] but from a sterically *unhindered* ACOM halide (X = Br or I). For entry 4 (Table 3-2) and entries 1-5, and 8 (Table 3-3), the variation in **7**/**8** appears to be directly related to the

variation in ν. A plot of ν versus the ratio of **8/7** for these entries (Figure 3-6) gave a good correlation ($r^2 = 0.95$). If these results are representative of all reactions of acyclic **3** (where R' is aliphatic) with **6**, then the effect of R' on the product distribution is related to its ability to discourage nucleophilic attack at the carbonyl. Such a finding should not be surprising since nucleophilic substitution at a carbonyl carbon is known to be sensitive to steric hindrance.[55]

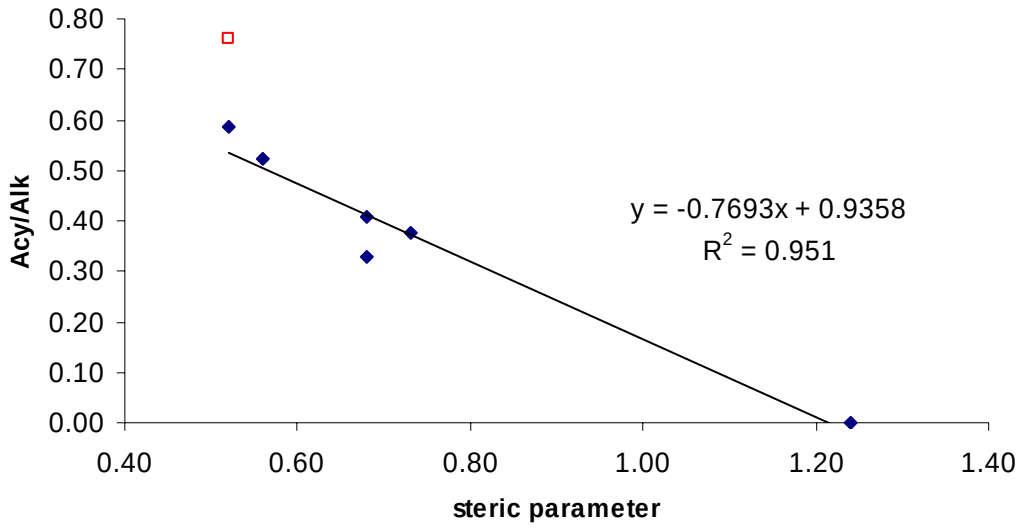

Figure 3-6: Plot of Charton's steric parameter ν for R' Versus the Ratio of **8/7** (Acylated/Alkylated Product) Resulting from the Reactions of **3a-3e** with **6a** and **6b** (Taken from Table 3-2: Entry 4, Table 3-3: Entries 1-4, and 8 ● and Entry 5 □. Note: entry 5 not included in linear regression analysis as it appears to be an outlier)

On the other hand, analysis of the steric effect in entries 13-16 (Ouyang's data, Table 3-2)) is more complicated. If one assumes that **9** (R' = protected amino acid) and **3** (R' = simple aliphatic chain) react with **6** by the same mechanism, and that the acyl group of **10** can approximate the steric effect of the acyl group in **9**, then variations in the amino

protecting group should have no effect on product distribution, contrary to the conclusions of Ouyang.[91] This follows from the work of Charton[96] that showed that for aliphatic acyl groups, substitution at the delta carbon contributes nothing to the effective van der Waals radius of the acyl group. Indeed, the fact that the ratio of **7**/**8** increases on going to bigger protecting groups (see ν values in parentheses, Table 3-2) implies that **9** reacts with **6** by a different mechanism than that prescribed[90] for simple derivatives of **1** (where R' is aliphatic). One potential mechanism for rationalizing the results of Ouyang is shown in Figure 3-7. It may be possible for compounds such as **9** to cyclize to give 5-oxazolidinone **12**. 5-Oxazolidinones are known to undergo nucleophilic addition at the carbonyl carbon to give **13**, followed by loss of formaldehyde to give **8**.[98] In this scenario, bulky protecting groups likely retard the conversion of **9** to **12** and thus permit **9** to exhibit a reactivity with phenols similar to that displayed by more conventional derivatives of **3** (i.e. where R' = aliphatic).

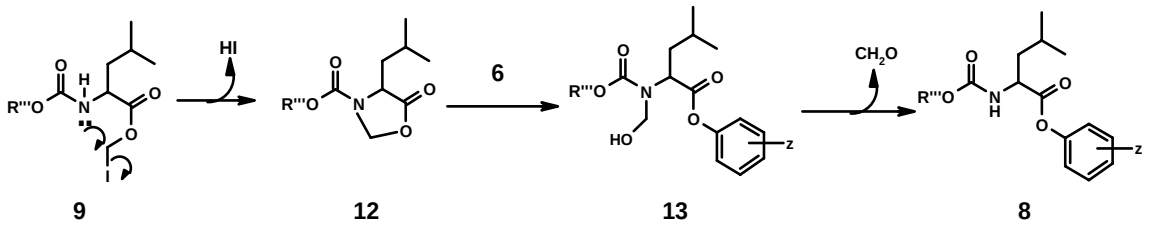

Figure 3-7: Speculative Mechanism for Reactions of Protected Amino Acid Derivatives **9** with Phenols **6**

In addition to the expected products **7** and **8**, there was also the unanticipated formation of byproduct **11** (Figure 3-3) in reactions involving APAP **6a** (entries 1-5 Table 3-2). Compound **11** was assigned the structure shown by comparison of its ^{1}H NMR to the corresponding derivatives **7** (compound **11** was also analyzed by IR, but no useful structural information could be gleaned from the spectrum). At present, it is not

clear why **11** is generated in reactions involving APAP, but fails to form when other phenols react with **3** (entries 1-16 Table 3-2 and entries 8 and 9 Table 3-3). An analysis (^{1}H NMR) of the crude reaction mixture resulting from the synthesis of **3** showed no evidence of alkylating agents such as R'$CO_2CH_2OCH_2I$ or bis(acetoxymethyl) ether[99] which might react with **6** to give **11**. Presumably, the formaldehyde generated during the acylation of **6** by **3** goes on to react with another molecule of **3** to form R'$CO_2CH_2OCH_2I$.

Several reaction conditions were employed in an effort to maximize the yield of **7**. Methods such as solid-liquid phase-transfer catalysis or the use of a non-nucleophilic organic base failed to improve the yield of **3**. Interestingly, the use of 1,8-diazabicyclo[5.4.0]undec-7-ene as a base resulted in an increase in the percentage of **7** by approximately 20% for the least sterically hindered member of the series (**3a**). However, since the conversion of **6** to **7** was lower is this case, this technique was not synthetically useful. Replacing K_2CO_3 with Cs_2CO_3 as recommended by Ouyang[91] resulted in an increase in the conversion of **6** to **7** (50% versus 40% when K_2CO_3 was used as a base) when **3a** was used but such effect was not observed with the longer alkyl chain derivatives. Likewise, the use Cs_2CO_3 resulted in a slight increase in the ratio of **7**/**8** when **3a** was used (59/32 versus 53/44), but had no effect on product distribution for a longer alkyl chain derivative such as **3e**. As it turns out, the original ACOM/phenol coupling method of Sloan and Koch[90] proved to be the most effective in the present case as well.[100]

As mentioned above and shown in Tables 3-2 and 3-3, the mixtures resulting from the coupling of **3** and **6** are frequently contaminated with a large percentage of **8**,

especially when R' offers little steric hindrance. Unfortunately, isolated yields of **7** suffer as a consequence (see Experimental). Compounds **7** and **8** could not be separated by simple crystallization, and could only be isolated in poor to low yield (1-30%) by way of a time-consuming chromatographic procedure involving multiple passes through a column of silica gel. Reverse-phase chromatography failed to improve the separation. However, other have reported that a phenolic ester can be selectively cleaved in the presence of an aliphatic ester.[101-105] Yet when these techniques were applied to mixtures of **7** and **8**, a large portion of **7** was destroyed along with **8**. Aminolysis with hydrazine[106] and *t*-butylamine[107] proved ineffective as well. Selective cleavage of **8** was finally achieved by subjecting the crude reaction mixture to a solution of imidazole in 30% aqueous acetonitrile.[108] In general, the selectivity for **8** varied with the steric hindrance in R and R'. This trend is reflected in the differences in isolated yield of **7** discussed in the Experimental Section. Even though a portion of **7** is cleaved via this procedure, it was quite practical in that it simplified the purification of **7**. For example, compound **7** is easily separated from the product of the cleavage of **8** (parent phenol **6**) via a single elution from a column of silica gel. Interestingly, byproduct **11** appeared to be unaffected by this procedure.

Conclusions

A new method has been developed for synthesizing ACOM iodides **3** in one step and in good yield starting from trioxane or paraldehyde. This reaction was found to be dependent on an unidentified catalyst that was present in older batches of NaI, but is absent in newer, purer batches. Although an optimized procedure for synthesizing the **3** using the newer brands of NaI was not developed, potential catalysts were identified. The coupling reaction of **3** with phenols **6** appears to be somewhat dependent on steric

hindrance as measured by Charton's steric parameters. In fact, the percentage of alkylated phenol **7** in the product mixture increases with increasing steric hindrance in **3** and in **6**. However, based on literature precedent[92, 93] and new data from our lab (Table 3-3), alkylated phenol is favored over acylated phenol regardless of the steric hindrance in **3** or **6**, contrary to the findings of Ouyang.[91] As Ouyang's is the only report where R' is a protected amino acid, this particular acyl group may impart a unique reactivity to **3** not found in more common derivatives (i.e. where R' = hydrocarbon).

Experimental

Batches of sodium iodide designated as "old" in the text were purchased from Aldrich (99+%, catalogue number 21763-8, lot numbers 1327 DK and 04229 CV; 99.5%, catalogue number 38311-2, lot number 11717 MG). Batches of sodium iodide designated as "new" in the text were purchased from Aldrich (99+%, catalogue number 217638, lot number 05412 BC; 99.5% catalogue number 383112, lot number 07908 CC) and from Fisher (Certified, catalogue number S324-500, lot number 037120). Thin layer chromatography (TLC) plates (Polygram Sil G/UV 254) were purchased from Brinkman. Spectra (^{1}H NMR) were recorded on a Varian Unity 400 MHz spectrometer or on a Varian EM-390 90 MHz spectrometer. Melting points were determined on a Meltemp melting point apparatus. Sodium sulfate and all solvents were purchased from Fisher. Trioxane and paraldehyde were purchased from Eastman Chemical Company. Iodine (crystalline) was purchased from Mallinckrodt. All other reagents were from Aldrich. Containers of NaI and Cs_2CO_3 were wrapped in parafilm and stored in a vacuum desiccator. Solvents listed as "dry" below were obtained as such following storage over 4-angstrom molecular sieves. Microanalyses were performed by Atlantic Microlab, Inc., Norcross, GA.

General procedure for the synthesis of 3a-e and 3g—synthesis of 3a: Sodium iodide (12 mmol, from any of the "old" batches listed above) was added to a stirred solution of **1a** (3.3 mmol) in 12 mL dichloromethane, and the suspension that resulted was cooled to 0 ^{o}C. A solution of **2a** (10 mmol) in 12 mL dichloromethane was then added, and the resulting mixture was allowed to reach room temperature. The reaction vessel was protected from light with aluminum foil while the contents were allowed to continue stirring at room temperature for 20-24 hours. The reaction mixture was filtered by vaccum followed by concentration of the filtrate at room temperature on a rotary evaporator to give an orange-colored oil. A sample of this oil was dissolved in $CDCl_3$ and analyzed by ^{1}H NMR. The yield of **3a** was then calculated on the basis of the molar ratio of the products. No further effort was made to purify **3a**, and it was used as such in subsequent reactions with phenols. Representative spectrum (^{1}H NMR, $CDCl_3$) from the reaction of **1a** with **2a** to give **3a** (R' = CH_3): δ 5.90 (s, 2 H), δ 2.10 (s, 3 H).

Reaction of 1 with 2 by modified procedure using $AlCl_3/I_2$—synthesis of 3f: Sodium iodide (15.2 mmol, 2.28 g, from Fisher) was added to a stirred solution of **1b** (R = CH_3) (4.2 mmol, 0.55 g) in 25 mL dichloromethane, and the suspension that resulted was cooled to 0 ^{o}C. A solution of **2a** (12.7 mmol, 1.00 g) in 10 mL dichloromethane was then added. Subsequent addition of aluminum chloride (0.42 mmol, 0.056 g) and iodine (0.084 mmol, 0.021 g) gave a mixture that was then allowed to warm to room temperature. The reaction vessel was protected from light with aluminum foil while the contents were allowed to continue stirring at room temperature for 20-24 hours. After such time, the reaction mixture was filtered by vacuum, diluted with 25 mL dichloromethane, then washed with 10 mL 10% aqueous $Na_2S_2O_3$ followed by 10 mL

brine. The organic phase was then dried over Na_2SO_4, filtered, and concentrated at room temperature on a rotary evaporator to give 10.2 mmol **3f** in Cl_2CH_2 (80% yield).

Reaction of 6a with 3—the reaction of 6a with 3e: To a stirred suspension of **6a** (19.9 mmol, 3.01 g) and K_2CO_3 (39.8 mmol, 5.50 g) in 50 mL dry acetonitrile was added a solution of **3e** (as indicated above, this solution is actually a mixture of 87% **3e**, 7% $C_7H_{15}CO_2CH_2Cl$, 4% $(C_7H_{15}CO_2)_2CH_2$), 1% trioxane) in 15 mL dry acetonitrile. The mixture that resulted was allowed to stir overnight at room temperature. The reaction mixture was then filtered and concentrated in vacuo to give 10.82 g oily residue. ^{1}H NMR (DMSO-d_6) analysis of the solid retained in the filter cake revealed only a trace amount of unreacted APAP. ^{1}H NMR (DMSO-d_6) analysis of the oily residue showed 89 % conversion to products and the product distribution shown in Table 3-2. Column chromatography (3 consecutive experiments) on silica gel (gradient = hexane→dichloromethane→acetone) gave 2.37 g of 4-octanoyloxymethyloxyacetanilide **7e** as an oil (39%). This oil was then triturated with pentane to give 1.89 g of **7e** as colorless crystals (31%); mp = 53-54 ^{o}C; one spot on TLC ($CHCl_3$: acetone, 97 : 3) R_f 0.13; ^{1}H NMR ($CDCl_3$) δ 7.42 (d, J = 8 Hz, 2 H), δ 7.09 (brs, 1H), δ 6.99 (d, J = 8 Hz, 2 H), δ 5.73 (s, 2 H), δ 2.35 (t, J = 7 Hz, 2 H), δ 2.16 (s, 3 H), δ 1.62 (m, 2 H), δ 1.26 (quint, J = 7 Hz, 8 H), δ 0.87 (t, J = 7, 3 H); Anal. Calcd for $C_{17}H_{25}NO_4$: C, 66.43; H, 8.20; N, 4.56. Found: C, 66.51; H, 8.19; N, 4.55.

In addition to **7e**, the chromatography procedure described above also gave 2.24 g solid material composed of a mixture of **7e** and 4-octanoyloxyacetanilide **8e** in a ratio of 1.3 : 1.0. By way of simple crystallization (EtOAc : hexane), 0.48 g of **8e** was isolated from this mixture as colorless crystals (9%); mp = 106-108 ^{o}C (lit[37] 103-105 ^{o}C); one

spot on TLC ($CHCl_3$: acetone, 97 : 3) R_f 0.10; Anal. Calcd for $C_{16}H_{23}NO_4$: C, 69.29; H, 8.36; 5.05. Found: C, 69.06; H, 8.34; N, 5.04.

The reaction of 6a with 3d was carried out and processed as described above for 3e, except that in this case, the scale was larger (52.1 mmol) and a different solvent gradient (hexane→dichloromethane→EtOAc) was used for column chromatography (3 consecutive experiments). In this way, 2.96 g of 4-hexanoyloxymethyloxyacetanilide **7d** was isolated as colorless crystals (20%); mp = 50-52 ^oC; one spot on TLC (Cl_2CH_2 : EtOAc, 85 : 15) R_f 0.20; ^1H NMR ($CDCl_3$) δ 7.42 (d, J = 8 Hz, 2 H), δ 7.10 (brs, 1H), δ 6.99 (d, J = 8 Hz, 2 H); δ 5.73 (s, 2 H), δ 2.35 (t, J = 7 Hz, 2 H), δ 2.16 (s, 3 H), δ 1.63 (quint, J = 7 Hz, 2 H), δ 1.29 (m, 4 H), δ 0.87 (t, J = 7 Hz, 3 H), Anal. Calcd for $C_{15}H_{21}NO_4$: C, 64.50; H, 7.58; N, 5.01. Found: C, 64.54; H, 7.56; N, 4.97.

In addition to **7d**, 4-hexanoyloxyacetanilide **8d** was isolated in a fashion similar to that described above for **8e**: 0.30 g of pale blue crystals (2%), mp = 105-109 ^oC (lit[37] 107-109 ^oC); one spot on TLC (Cl_2CH_2 : EtOAc, 85 : 15) R_f 0.17; Anal. Calcd. for $C_{14}H_{19}NO_4$: C, 67.45; H, 7.68; N, 5.62. Found: C, 67.17; H, 7.64; N, 5.59.

The reaction of 6a with 3c was carried out as described above for 3e, except that in this case, the scale was much larger (112 mmol). The corresponding compound **8c** was selectively destroyed as described below to give 51.24 g oil containing **7c**, **11c**, and **6a** in the ratio of 50 : 1 : 3. The oil was then subjected to column chromatography (silica gel, EtOAc : hexane, 1 : 1) to give 12.51 g of 4-butryloxymethyloxyacetanile **7c** as an oil (44%). Crystallization from diethyl ether : 2-methyl-butane gave 7.03 g of **7c** as colorless crystals (25%); mp = 56-58 ^oC; one spot on TLC (EtOAc: hexane, 1 : 1) R_f

0.16; ^{1}H NMR ($CDCl_3$) δ 7.42 (d, *J* = 8 Hz, 2 H), δ 7.13 (brs, 1H), δ 6.99 (d, *J* = 8 Hz, 2 H), δ 5.74 (s, 2 H), δ 2.34 (t, *J* = 7 Hz, 2 H), δ 2.17 (s, 3 H), δ 1.65 (m, 2 H), δ 0.94 (t, *J* = 7 Hz, 3 H); Anal. Calcd for $C_{13}H_{17}NO_4$: C, 62.14; H, 6.82; N, 5.57. Found: C, 61.92; H, 6.85; N, 5.52.

The reaction of 6a with 3b was carried out and processed as described above for 3c, except in this case, two consecutive column chromatography experiments (acetone : hexane 3 : 7) were required to separate 7b from 11b. Following crystallization from ether : pentane, 3.64 g of 4-propionyloxymethyloxyacetanilide **7b** was obtained as colorless crystals (15%); mp = 56-59 ^{o}C; one spot on TLC (acetone : hexane, 35 : 65) R_f 0.26; ^{1}H NMR ($CDCl_3$) δ 7.42 (d, *J* = 8 Hz, 2 H), δ 7.10 (brs, 1 H) δ 6.99 (d, *J* = 8 Hz, 2 H), δ 5.74 (s, 2 H), δ 2.39 (quart, *J* = 8 Hz, 2 H), δ 2.16 (s, 3 H), δ 1.15 (t, *J* = 8 Hz, 3 H); Anal. Calcd for $C_{12}H_{15}NO_4$: C, 60.75; H, 6.37; N, 5.90. Found: C, 60.85; H, 6.35; N, 5.84.

In addition to **7b**, column chromatography gave 3.14 g oil composed of a mixture of 4-propionyloxymethoxymethoxyacetanilide **11b**, solvent, and an unidentified compound. Crystallization from Cl_2CH_2 : hexane gave 1.05 g of **11b** as colorless crystals (4%); mp = 71-73 ^{o}C; one spot on TLC (acetone : hexane, 3 : 7) R_f 0.18; ^{1}H NMR ($CDCl_3$) δ 7.08 (d, *J* = 8 Hz, 2 H), δ 6.88 (d, *J* = 8 Hz, 2 H), δ 5.40 (s, 2 H), δ 5.19 (s, 2 H), δ 2.35 (quart, *J* = 8 Hz, 2 H), δ 1.91 (s, 3 H), δ 1.31 (t, *J* = 8 Hz, 3 H); Anal. Calcd for $C_{13}H_{17}NO_5$: C, 58.42; H, 6.41; N, 5.24. Found: C, 58.45; H, 6.43; N, 5.24.

The reaction of 6a with 3a was carried out and processed as described above for 3c, except that in this case, an aqueous workup was not performed on the aminolysis reaction (reaction mixture was too complex to determine ratio 7a, 8a, 11a

and 6a). Instead, the crude mixture was subjected to three consecutive column chromatography experiments (first two experiments used hexane→Cl_2CH_2→acetone; final experiment used EtOAc : hexane, 1 : 1). In this way, 4-acetyloxymethyloxyacetanilde **7a** was obtained as 1.81 g pale green crystals (6.5%, crystallized from ether : 2-methylbutane); mp = 92-95 ^oC; one spot on TLC (Cl_2CH_2 : acetone, 95 : 5) R_f 0.21; ^1H NMR ($CDCl_3$) δ 7.43 (d, J = 8 Hz, 2 H), δ 7.14 (brs, 1 H), δ 7.00 (d, J = 8 Hz, 2 H), δ 5.73 (s, 2 H), δ 2.18 (s, 3 H), δ 2.12 (s, 3 H); Anal. Calcd for $C_{11}H_{13}NO_4$: C, 59.19; H, 5.87; N, 6.27. Found: C, 58.96; H, 5.84; N, 6.22.

In addition to **7a**, column chromatography also gave 1.61 g of 4-acetyloxymethoxymethoxyacetanilide **11a** as an oil. Crystallization from diethyl ether : 2-methylbutane gave 0.40 g **11a** as colorless crystals; mp = 91-93 ^oC; one spot on TLC (acetone : hexane, 3 : 7) R_f 0.15; ^1H NMR ($CDCl_3$) δ 7.10 (d, J = 8 Hz, 2 H), δ 6.87 (d, J = 8 Hz, 2 H), δ 5.38 (s, 2 H), δ 5.18 (s, 2 H), δ 2.07 (s, 3 H), δ 1.90 (s, 3 H); Anal. Calcd for $C_{12}H_{15}NO_5$: C, 56.91; H, 5.97; N, 5.53. Found: C, 56.72; H, 5.96; N, 5.47.

The reaction 6a with 3f was carried out and processed as described above for 3c except that in this case, the scale was much smaller (8.5 mmol). Using this procedure, 1.54 g of oil containing **7f** : **6a** in the ratio of: 16 : 1 was obtained. The oil was subjected to column chromatography (silica gel, acetone : hexane, 3 : 7) to give 0.79 g 4-acetyloxyethyloxyacetanilide **7f** as a colorless solid. This solid was recrystallized from ether : 2-methylbutane to give 0.56 g **7f** as colorless crystals (28%). Upon heating, **7f** displayed an initial melting point of 82-92 ^oC. Once this material had cooled to room temperature and solidified, it was heated again. This time, **7f** displayed a sharp melting point: 81-83 ^oC; one spot on TLC (acetone : hexane, 3 : 7) R_f 0.20; ^1H NMR ($CDCl_3$) δ

7.41 (d, J = 9 Hz, 2 H), δ 7.08 (brs, 1 H), δ 6.92 (d, J = 9 Hz, 2 H), δ 6.51 (quart, J = 5 Hz, 1 H), δ 2.16 (s, 3 H), δ 2.10 (s, 3 H), δ 1.60 (d, J = 5 Hz, 3 H); Anal. Calcd for $C_{12}H_{15}NO_4$: C, 60.75; H, 6.37; N, 5.90. Found: C, 60.69; H, 6.40; N, 5.91.

General procedure for the selective aminolysis of 7 in the presence of 8. The procedure described above for the reaction of **6a** with **3** gave various mixtures of **7**, **8**, **11**, unreacted **3** and **6a** (determined by ^{1}H NMR as described above). The mixture was then triturated in dichloromethane, filtered, and concentrated in vacuo to give an oil. The oil was dissolved in 30% aqueous CH_3CN (approx. 17 mL / 1 mmol **8**), and imidazole was added (10 equiv. based on mmol **8** present in the oil, as determined by ^{1}H NMR). The resulting mixture was allowed to reflux overnight. After such time, the solvent was removed in vacuo. The residue was dissolved in dichloromethane, washed with 1 M HCl (1/6 vol. of organic phase), and water (1/6 vol. of organic phase). The organic phase was dried over Na_2SO_4, filtered, and concentrated in vacuo to give an oil containing various ratios of **7** : **8** : **11** (determined by ^{1}H NMR: specific ratios listed above).

In Vitro Determination of Flux of ACOM Prodrugs of APAP

4-Hydroxyacetanilide (APAP)

6a

4-ACOM-APAP

7a, R = CH_3
7b, R = C_2H_5
7c, R = C_3H_7
7d, R = C_5H_{11}
7e, R = C_7H_{15}

Figure 3-8. Structure of 4-Hydroxyacetanilide and Corresponding 4-ACOM Prodrugs

Materials and Methods

Melting points were determined on a Meltemp capillary melting point apparatus and are uncorrected. Ultraviolet (UV) spectra were obtained on a Shimadzu UV-265 or UV-2501 PC spectrophotometer. The vertical Franz diffusion cells (surface area 4.9 cm^2, 20 ml receptor phase volume, 15 ml donor phase volume) were purchased from Crown Glass (Somerville, NJ, USA). A Fisher (Pittsburgh, PA, USA) circulating water bath was used to maintain a constant temperature of 32 ^oC in the receptor phase. Isopropyl myristate (IPM) was purchased from Givaudan (Clifton, NJ, USA). Theophylline (Th) was purchased from Sigma Chemical Co. (St. Louis, MO, USA); all other chemicals were purchased from Fisher. The female hairless mice (SKH-hr-1) were obtained from Charles River (Boston, MA, USA). All procedures involving the care and experimental treatment of animals were performed by Professor K. B. Sloan of the department of Medicinal Chemistry in agreement with the NIH "Principles of Laboratory Animal Care."

Physicochemical properties and analysis

The molar absorptivity of each prodrug at 240 nm (ε_{240}) in acetonitrile was determined in triplicate by dissolving a known amount of prodrug in acetonitrile, and analyzing the dilute solution by UV spectrophotometry. Since the concentration C was known, ε_{240} could be calculated by way of Beer's law:

$$A_{240} = \varepsilon_{240}\, l\, C, \text{ where } l = \text{cell length} \qquad (1)$$

For each prodrug, the solubility in isopropyl myristate (IPM) was determined in triplicate by crushing a sample of the prodrug into a fine powder. Excess powder was added to a test tube containing 3 ml IPM. The test tube was then insulated and the suspension was allowed to stir at room temperature (23 ± 1 ^oC) for 24 hours on a magnetic stir plate. The

suspension was filtered through a 0.25 μm nylon syringe filter. A sample of the filtrate was diluted with acetonitrile and analyzed by UV spectrophotometry. In order to be consistent with a previous investigation of acetaminophen prodrugs,[45] the absorbance at 240 nm (A_{240}) was used to calculate the prodrug concentration C in the IPM solution using the Beer's law relationship. In this case, since C is the concentration of a saturated solution, C is the solubility in IPM (S_{IPM}):

$$C_{Saturation} = S_{IPM} = A_{240} / \varepsilon_{240} \quad (2)$$

Solubilities in water were also determined in triplicate using an identical protocol to the one described above, except that the suspensions were only stirred for one hour before filtering. This was done in order to make direct comparisons between the present investigation and previous studies.[45, 68] In each case, a sample of the filtrate was diluted with acetonitrile and analyzed by UV spectrophotometry using ε_{240} in acetonitrile (Table 3-4).

Table 3-4: Molar Absorptivities (ε) of APAP **6a** and Prodrugs **7a-e**

Compound	ε_{240} in ACN[a, b]	ε_{240} in Buffer[a, c]	ε_{280} in Buffer[a, d]
6a, APAP	1.36[e]	1.01 ± 0.053[f]	0.174 ± 0.020[f]
7a	1.48 ± 0.011		
7b	1.64 ± 0.067		
7c	1.56 ± 0.057	1.20 ± 0.025[g]	0.119 ± 0.0025[g]
7d	1.58 ± 0.050		
7e	1.46 ± 0.044		

[a] Units of 1 x 10^4 L mol^{-1}. [b] Molar absorptivities at 240 nm acetonitrile (± SD, n = 3). [c] Molar absorptivities at 240 nm in pH 7.1 phosphate buffer with 0.11% formaldehyde. [d] Molar absorptivities at 280 nm in pH 7.1 phosphate buffer with 0.11% formaldehyde. [e] Taken from Reference 45. [f] n = 5 (± SD). [g] n =6 (± SD).

Partition coefficients were also determined in triplicate for each prodrug by using the saturated IPM solutions obtained from the solubility determinations. Since solubility in pH 4.0 buffer ($S_{4.0}$) is a parameter in the Roberts-Sloan database,[20] acetate buffer (0.01 M, pH 4.0) was used as the aqueous phase in the partition coefficient experiments. In

this way, $S_{4.0}$ could be estimated as described previously[109] and the values included in the database. Thus, an aliquot of the saturated IPM solution was partitioned against pH 4.0 buffer using the following volume ratios ($V_{4.0}$ / V_{IPM}) for compounds **7a, 7b, 7c,** and **7d**: 0.5, 2, 10, and 20, respectively. The two phases were vigorously shaken for 10 seconds,[109] then allowed to separate via centrifugation. An aliquot of the IPM layer was removed, diluted with acetonitrile, and analyzed by UV spectrophotometry as described above. The partition coefficient was calculated as follows:

$$K_{IPM:4.0} = [A_a/(A_b - A_a)]V_{4.0}/V_{IPM} \quad (3)$$

where A_b and A_a are the respective absorbances before and after partitioning, and $V_{4.0}$ and V_{IPM} are the respective volumes of buffer and IPM in each phase. Due to the high solubility ratio exhibited by compound **7e**, it was not possible to accurately determine its partition coefficient using this procedure. Therefore, in this case $K_{IPM:4.0}$ was estimated from the average methylene π_K obtained for compounds **7a-d** according to the following relationship

$$\log K_{n+m} = (\pi_K)(m) + \log K_n \quad (4)$$

where n is the number of methylene units in the promoiety of one prodrug and m is the number of additional methylene units in the promoiety with which it is compared.

UV spectrophotometry was also used to determine the amount of **6a** and prodrug present in the receptor phase of the diffusion cell. Since all the prodrugs in this study were part of a homologous series, it was assumed that satisfactory results would attain for the entire series from the use of the molar absorptivity of one homolog. Thus, the molar absorptivities of compounds **7c** and **6a** were determined in pH 7.1 phosphate buffer (0.05 M, I = 0.11 M) containing 0.11% formaldehyde by first dissolving a known amount of

either compound in acetonitrile. An aliquot (0.500 mL) of the acetonitrile solution was removed, diluted with buffer, and analyzed by UV spectrophotometry to obtain the molar absorptivities shown in Table 3-4. Because there is considerable overlap between the UV spectra of APAP and its ACOM prodrugs **7a-e**, the relative concentrations of each were determined using the following approach. The differences in absorption were found to be greatest at 240 nm and at 280 nm. Therefore, considering the additive nature of absorption, the absorbance at each wavelength (assuming constant cell length) is

$$A_{240} = \varepsilon_{P240}C_P + \varepsilon_{A240}C_A \quad (5)$$

$$A_{280} = \varepsilon_{P280}C_P + \varepsilon_{A280}C_A \quad (6)$$

where A is the absorbance at the respective wavelengths, ε is the molar absorptivity of either the prodrug (P) or APAP (A) at the respective wavelengths, and C is the concentration of the respective compounds in the mixture. Solving the two simultaneous equations gives the following solution for the prodrug concentration C_P

$$C_P = (\varepsilon_{A280}A_{240} - \varepsilon_{A240}A_{280}) / (\varepsilon_{A280}\varepsilon_{P240} - \varepsilon_{A240}\varepsilon_{P280}) \quad (7)$$

Once C_P is known, it may be inserted into equation 5 to give the following solution for the concentration of APAP C_A:

$$C_A = (A_{240} - \varepsilon_{P240}C_P) / \varepsilon_{A240} \quad (8)$$

Solubility parameters. Solubility parameters were calculated by the method of Fedors[110] as demonstrated by Martin and coworkers[111] and Sloan and coworkers.[112]

Diffusion cell experiments

The flux of each prodrug was measured using skin samples from three different mice. Prior to skin removal, the mice were rendered unconscious by CO_2 then sacrificed via cervical dislocation. Skins were removed by blunt dissection and placed dermal side

down in contact with pH 7.1 phosphate buffer (0.05 M, I = 0.11 M, 32 ^{o}C) containing 0.11% formaldehyde (2.7 ml of 36% aqueous formaldehyde/liter) to inhibit microbial growth and maintain the integrity of the skins[113] throughout the experiment. A rubber O-ring was placed on top of the skin to ensure a tight seal, and the donor and receiver compartments were fastened together with a metal clamp (see Figure 3-9).

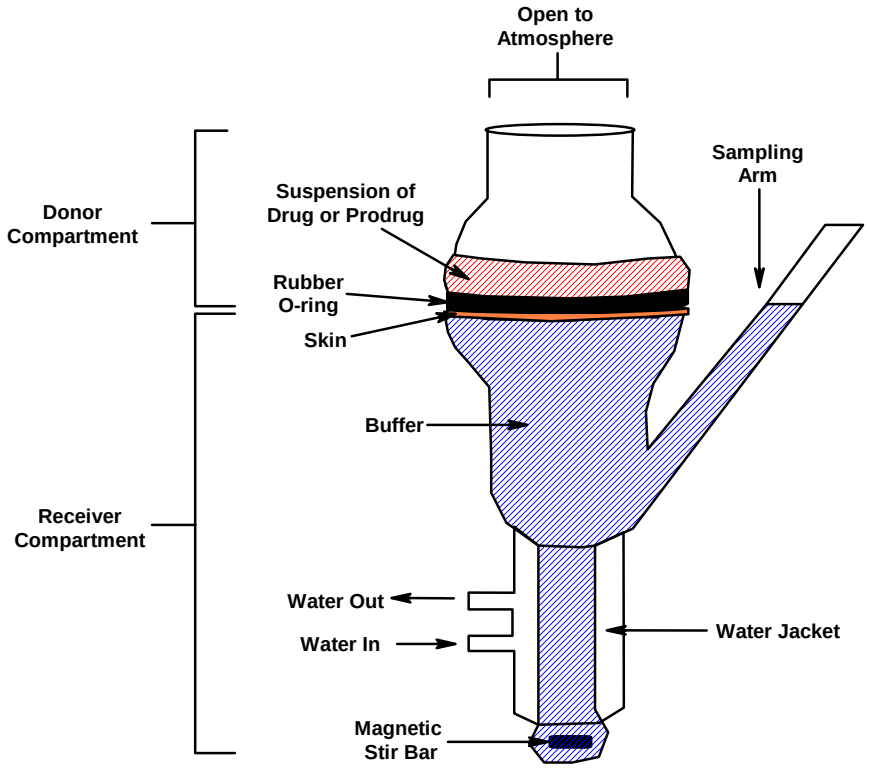

Figure 3-9. Diagram of Franz Diffusion Cell (Metal Clamp Not Shown)

Prior to the application of the prodrug, the skins were kept in contact with buffer for 48 h to allow any UV absorbing material to leach out. During this time, the receptor phase was removed and replaced with buffer 3 times in order to facilitate the leaching process. Twenty four hours before application of the prodrug, a suspension (0.09 M to 0.80 M, i.e. roughly 10 × S_{IPM}) of the prodrug in IPM was prepared and allowed to mix

until it was needed in the diffusion cell experiments. After the 48 hour leaching period, an aliquot (0.5 ml) of the prodrug suspension was added to the surface of the skin (donor phase). Samples of the receptor phase were usually taken at 8, 19, 22, 25, 28, 31, 34, and 48 h and quickly analyzed by UV spectrophotometry (Table 3-4, equations 7 and 8) to determine the amounts of permeated APAP and prodrug. At each sampling time, the entire receptor phase was replaced with fresh buffer in order to maintain sink conditions.

After the 48 h of the first application period, the donor suspension was removed and the skins were washed three times with methanol (3-5 ml) to remove any residual prodrug from the surface of the skin. The skins were kept in contact with buffer for an additional 24 h to allow all APAP species (i.e. APAP and prodrug) to leach from the skin. Following this second leaching period, the receptor phase was replaced with fresh buffer and an aliquot (0.5 ml) of a standard drug/vehicle (theophylline/propylene glycol) was applied to the skin surface: the second application period. Samples of the receptor phase were taken at 1, 2, 3, and 4 h and analyzed by UV spectrophotometry. The concentration of theophylline in the receptor phase was determined by measuring its absorbance at 270 nm (ε = 10,200 L mol^{-1}). At each sampling time, the entire receptor phase was removed and replaced with fresh buffer.

In each experiment, the flux was determined by plotting the cumulative amount of APAP species (APAP plus prodrug) against time as shown by the example in Figure 3-10. Flux could then be calculated by dividing the slope of the steady-state portion of the graph by the surface area of the skin (4.9 cm^2).

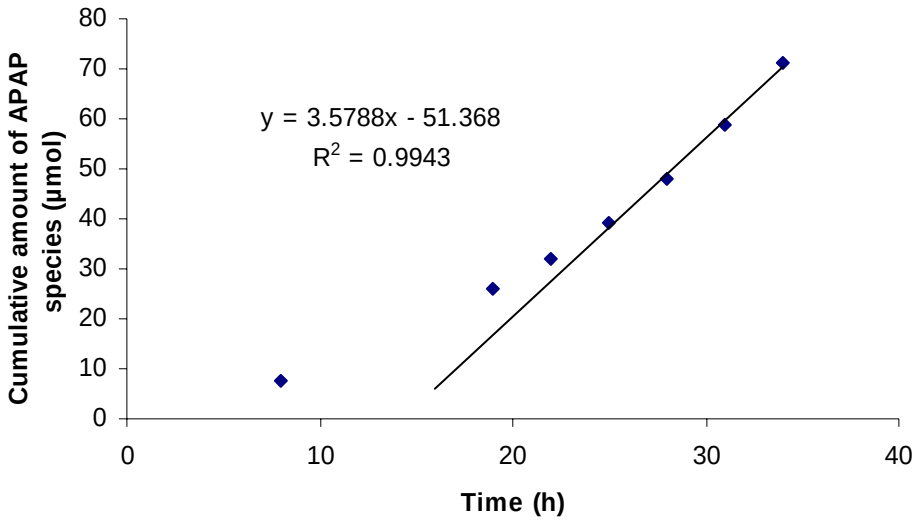

Figure 3-10: Flux of Compound **7a** through Hairless Mouse Skin

Results and Discussion

Physicochemical properties

The solubilities of compounds **7a-e** in IPM (S_{IPM}) and in water (S_{AQ}) are shown in Table 3-4. The relative standard deviations were all $\leq \pm 5\%$ except for the S_{AQ} value measured for compound **7e** ($\pm 9\%$). As expected, all the prodrugs were more soluble in IPM than APAP (Table 3-5). Although there was a thirteen fold range in S_{IPM} between the first and last member of the series, there was little variation in S_{IPM} between the second and last member of the series. The biggest increase in S_{IPM} (7 fold) occurred on going from the first (C1) to the second member (C2) of the series. Beyond C2, S_{IPM} gradually increased until the fourth member of the series (C5), but began to decrease thereafter. It is reasonable to anticipate a "point of diminishing returns" where no further increases in lipid solubility are realized by extending the length of the alkyl chain. Typically, the increase in lipid solubility exhibited by the first member of a series of prodrugs or analogues results from masking a hydrogen bond donor in the parent compound. Elimination of the offending functional group results in a compound with

lower crystal lattice energy than the parent, and is thus more easily solvated. For a homologous series in which the only difference between members is the length of an aliphatic chain, lipid solubility will increase as the chain is extended due to the incorporation of lipophilic groups. However, at a certain point van der Waals interactions between the aliphatic chains become dominant, causing an increase in melting point and a decrease in lipid solubility. In general, the trends in S_{IPM} for **7a-e** appear to follow the trends in melting point, though there was less variation in melting point among **7b** to **7e** than there was in S_{IPM}. It is important to note that the trends in S_{IPM} shown here were observed previously in other prodrug series including 1-ACOM-5-fluorouracil (1-ACOM-5U),[67] 3-ACOM-5-FU,[69] 1-AOC-5-FU,[114] and bis-6,9-ACOM-6-mercaptopurine (6,9-ACOM-6-MP).[39]

In addition to the 4-ACOM-APAP series, physicochemical data from a recently described series of alkyloxycarbonyl (AOC) derivatives of APAP (Figure 3-11) is also listed in Table 3-5. If homologs of the same alkyl chain length are compared (**7a** to **7c** versus **8i** to **8k**), the ACOM derivatives all exhibit lower melting points and, with the exception of **7a** (C1), are more soluble in IPM and water than the corresponding members of the AOC series. However, comparisons such as this do not take into account the structural differences between the promoieties in question. In order to make comparisons between homologs of approximately equal size, it is perhaps more appropriate to consider the fact that members of the ACOM series contain a CH_2O spacer between the phenoxy group of APAP and the carbonyl of the promoiety which extends the alkyl chain further from the phenyl ring of the parent. Disregarding the differences in size between a methylene unit and oxygen, the C1 member of the ACOM series should

be compared to the C2 member of the AOC series. If similar comparisons are made for the remainder of the two series, the ACOM prodrugs are 4 to 17-times more soluble in water and, with the exception of **7a**, are 3 to 5-times more soluble in IPM than the corresponding members of the AOC series.

Table 3-5: Physicochemical Properties of 4-Hydroxyacetanilide **6a**, 4-ACOM-APAP Prodrugs **7a-e** and 4-AOC-APAP[a] Prodrugs **8i-m**

Compound	MW[b]	mp °C[c]	S_{IPM}[d, e, f]	S_{AQ}[d, f, g]	$S_{4.0}$[d, h]	$K_{IPM:4.0}$[i]
6a, APAP	151	167-170	1.9[a]	100[a]		
7a, C1	223	92-95	8.41 ± 0.44	15.2 ± 0.34	16.2	0.52 ± 0.016
7b, C2	237	56-59	62.0 ± 1.91	24.7 ± 0.33	26.6	2.33 ± 0.039
7c, C3	251	56-58	73.5 ± 1.45	7.12 ± 0.0073	8.26	8.90 ± 1.00
7d, C5	279	50-52	109 ± 1.48	0.597 ± 0.018	0.90	121 ± 19.1
7e, C7	307	53-54	98.7 ± 3.77	0.0637 ± 0.0060	0.048	2077[j]
8i, C1	209	112-115	12.0	20.4	17.0	0.692
8j, C2	223	120-122	9.33	3.80	4.47	2.09
8k, C3	237	104-106	23.4	2.70	3.02	7.94
8l, C4	251	118-120	13.8	0.427	0.447	31.6
8m, C6	279	108-110	16.7	0.0479	0.0324	513

[a] Data from Reference 45. [b] Molecular weight. [c] Melting point (uncorrected). [d] Units of mM. [e] Solubility in isopropyl myristate (IPM). [f] Measured at 23 ± 1 °C. [g] Solubility in water. [h] Solubility in pH 4.0 buffer estimated from $S_{IPM}/K_{IPM:4.0}$. [i] Partition coefficient between IPM and pH 4.0 acetate buffer. [j] Extrapolated from previous $K_{IPM:4.0}$ in the series as described in the text.

Although **7a-e** were 4 to 60 times more lipid soluble than APAP, they were all much less soluble in water than APAP. In fact, the most water soluble member of the series, C2, exhibited only one-fourth the aqueous solubility of APAP (Table 3-5). S_{AQ} increased on going from C1 (**7a**) to C2 (**7b**), but dropped off quickly as the alkyl chain length increased. Interestingly, the C2 member was also the most water soluble member of the 1-ACOM-5-FU[67] and 3-ACOM-5-FU[69] prodrug series. Contrary to its effect on S_{IPM}, masking a hydrogen bond donor in the parent compound can often lead to lower S_{AQ} relative to the parent. Such was the case in the present study and in previous prodrug

series including 7-ACOM-theophylline (7-ACOM-Th),[57] 1-alkylaminocarbonyl-5-FU (1-AAC-5-FU),[115] and 4-AOC-APAP.[45]

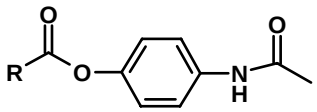

4-AOC-APAP

8 i, R = OCH_3
8 j, R = OC_2H_5
8 k, R = OC_3H_7
8 l, R = OC_4H_9
8 m, R = OC_6H_{13}

Figure 3-11: Structure of 4-alkyloxycarbonyl (AOC) derivatives of APAP

In order to incorporate the physicochemical property data for **7a-e** into the Roberts-Sloan database,[20] pH 4.0 buffer was used as the aqueous phase in determinations of partition coefficients. Partition coefficients obtained in this manner were then used to estimate the solubilities of **7a-e** in pH 4.0 buffer ($S_{4.0}$, Table 3-5). Partition coefficients between IPM and pH 4.0 buffer ($K_{IPM:4.0}$) were experimentally determined for all compounds except for **7e** (Table 3-5). The relative standard deviations in $K_{IPM:AQ}$ were all less than ± 10% except for **7c** (± 11%) and **7d** (± 16%). Although the average methylene π_K for the 4-ACOM-APAP series (0.60 ± 0.05) is somewhat higher than the 4-AOC-APAP series (0.55 ± 0.06), it is consistent with average methylene π_K values seen in other ACOM prodrug series: 1-ACOM-5-FU,[67] π_K = 0.60 ± 0.14; 3-ACOM-5-FU,[69] π_K = 0.59 ± 0.01; 7-ACOM-Th,[57] π_K = 0.58 ± 0.05). Since the partition coefficients and π_K values for **7a-d** (Table 3-6) were reasonably well-behaved, the average π_K value was used to estimate the partition coefficient for **7e** (Table 3-5). Use of the solubility ratios $SR_{IPM:AQ}$ as a surrogate for $K_{IPM:4.0}$, resulted in an average methylene π_{SR} value that was slightly higher than π_K, but exhibited a smaller standard deviation (0.62 ± 0.03). The

estimated solubilities in pH 4.0 buffer $S_{4.0}$ were somewhat higher than S_{AQ} for **7a-c** (10 ± 5%), while the calculated $S_{4.0}$ for **7e** was only 0.75 times the experimentally measured S_{AQ} for **7e**. Due to the relatively large difference between S_{IPM} and S_{AQ} of **7d** (S_{IPM}/S_{AQ} = 182), it was difficult to experimentally determine $K_{IPM:4.0}$ with reasonable precision. As a consequence, $S_{4.0}$ for **7d** was 1.5 times higher than its S_{AQ}, which is somewhat greater than the largest variation observed previously in the 4-AOC-APAP series ($S_{4.0}$ was 0.59 times the experimentally measured S_{AQ} in the case of 4-(2′-methoxyethyloxycarbonyloxy)acetanilide).[45]

Table 3-6**:** Log Solubility Ratios (log $SR_{IPM:AQ}$), Differences Between Log $SR_{IPM:AQ}$ (π_{SR}), Log Partition Coefficients (log $K_{IPM:4.0}$), Differences Between Log $K_{IPM:4.0}$ (π_K), and Solubility Parameters (δ_i) for Prodrugs **7a-e**

Prodrug	log $SR_{IPM:AQ}$[a]	π_{SR}[b]	log $K_{IPM:4.0}$[c]	π_K[d]	δ_i[e]
7a	-0.257		-0.285		12.04
7b	0.400	0.66	0.368	0.65	11.77
7c	1.01	0.61	0.949	0.58	11.54
7d	2.26	0.62	2.09	0.57	11.18
7e	3.19	0.57	3.32[f]		10.89

[a] Log of the ratio of the solubilities in IPM (S_{IPM}) and water (S_{AQ}). [b] $\pi_{SR} = (\log SR_{n+m} - \log SR_n)/m$; n is the number of methylene units in the promoiety of one prodrug and m is the number of additional methylene units in the promoiety with which it is compared. [c] Log of the partition coefficient between IPM and pH 4.0 buffer. [d] Same definition as in *b* with the exception that log $K_{IPM:4.0}$ is used in place of log $SR_{IPM:AQ}$. [e] Calculated as described in Reference 112 (units = $(\text{cal cm}^{-3})^{1/2}$. [f] Extrapolated from previous $K_{IPM:4.0}$ in the series as described in the text.

Diffusion cell experiments

To date, there has been only one report of the topical delivery of 4-hydroxyacetanilide (APAP) by a homologous series of prodrugs.[45] In order to facilitate comparisons between the results of the present investigation to those of the prior study of 4-alkyloxycarbonyloxyacetanilide derivatives (4-AOC-APAP), data from both prodrug series are listed in Table 3-7. As shown in Table 3-7, the fluxes (± SD) of the ACOM prodrugs with the exception of **7e** (± 32%) were within the typical[45] ± 30% variation of *in*

vitro experiments with hairless mice. Three of the five members of the ACOM series were more effective at delivering APAP through the skin than APAP itself. This is in contrast to the AOC series in which only one member (C1) permeated the skin better than APAP. If comparisons are made between members of the same alkyl chain length (**7a** to **7c** versus **8i** to **8k**), the ACOM derivatives are, with the exception of **7a**, 2 to 11-times more permeable than the corresponding members of the AOC series. The flux of the most permeable derivative **7b** was 3.6 times greater than that of APAP. An improvement of this magnitude is modest when compared to the results of other prodrug series. For instance, 6-ACOM derivatives of 6-mercaptopurine (6-MP)[116] and 1-ACOM derivatives of 5-fluorouracil[67] improve the flux of the parent by as much as 69 and 16 times, respectively. The apparent ineffectiveness of the ACOM promoiety in the present case may be explained by considering the differences in the physicochemical properties of the parent compounds. Compared to APAP, 5-FU and 6-MP are much less soluble in IPM and water. Thus it is not surprising to find that the flux of APAP is two fold higher than the flux of 5-FU and 134 times greater than that of 6-MP. As a consequence of its relatively high S_{IPM} and S_{AQ} values, it is more difficult to improve the flux of APAP than it is to improve the flux of polar heterocycles such as 5-FU and 6-MP. It is also worth mentioning that the 7-ACOM derivatives of theophylline (Th),[57] a polar heterocycle, exhibited only modest (2 fold) improvements in flux. Though Th is less soluble in lipid and aqueous solvents than APAP, it is 7 times more soluble in IPM than 5-FU while still exhibiting 54% of the water solubility of 5-FU. Again, the better the biphasic solubility of the parent compound, the more difficult it is to improve the flux via a prodrug approach.

When the receptor phases from the application of **7a-e** were analyzed during steady-state flux conditions, only APAP was found. The exception was compound **7b** in which the intact prodrug accounted for 9% of the total APAP species in the receptor phase (Table 3-8). Since this particular derivative was also the most permeable member of the series, the system of cutaneous esterases in this case may have been overwhelmed and unable to completely hydrolyze the prodrug on its way through the skin. A similar phenomenon was observed in the 4-AOC-APAP series[45] in which the derivative that exhibited the highest flux also delivered the highest percentage of intact prodrug through the skin (Table 3-8). Although no effort was made to determine the half-lives of **7a-e** in the receptor phase buffer, the aqueous stability may be estimated based on similar studies by others.[93, 117] For example, Bundgaard and coworkers[93] found that the 2-acetyloxymethyl and 2-butyrloxymethyl derivatives of salicylamide exhibit half-lives of 46 and 98 h, respectively at 37 ^{o}C in pH 7.4 buffer. Others have found that 4-hexanoyloxyacetanilide displays an approximate half-life of 19 hours at 37 ^{o}C in pH 7.8 buffer.[117] Given the generally higher pK_a of an aryl hemiacetal compared to its corresponding phenol, the ACOM derivatives **7a-e** should exhibit half-lives greater than 19 hours under the present experimental conditions. Thus, it is reasonable to assume that the absence of intact prodrug in the receptor phase is due to extensive enzymatic hydrolysis in the skin and is not the result of substantial chemical hydrolysis in the receptor phase.

Apparently, the fluxes of **7a-e** are not artificially high due to damage sustained by the skin over the course of the experiment. This assessment is based on control experiments in which a suspension of theophylline in propylene glycol (Th/PG) was

applied to the skin following the removal of the prodrug donor phase. This second application of Th/PG resulted in Th flux values that were not significantly different from those through skins treated with IPM alone (Table 3-7). However, it is important to recognize that IPM is a well-known penetration enhancer which can increase flux 50-fold compared to experiments where water was the vehicle.[118] Although the apparent flux values of **7a-e** are likely inflated due to IPM, this is not expected to change the rank order of flux within or between series.[118]

Table 3-7: Flux of Total APAP Species through Hairless Mouse Skin from Suspensions of 4-ACOM-APAP and 4-AOC-APAP[a] Prodrugs in IPM (J_M), Second Application Flux of Theophylline through Hairless Mouse Skin from a Suspension in Propylene Glycol (J_J), Error in Predicting Log J_M using the Roberts-Sloan Equation (Δ log $J_{predicted}$), Error in Calculating Log J_M using the Roberts-Sloan Equation (Δ log $J_{calculated}$), and Ratio of the Flux of the Prodrug to the Flux of APAP ($J_{prodrug}$ / J_{APAP}).

Compound	J_M[b]	J_J[b]	log J_M[b]	Δ log $J_{predicted}$[c]	Δ log $J_{calculated}$[d]	$J_{prodrug}$ / J_{APAP}
6a, APAP	0.51[a]	0.74[a]	-0.29[a]	-0.496[e]	-0.484	
7a, C1	0.730 ± 0.23	0.934 ± 0.136	-0.136	-0.104	-0.0911	**1.4**
7b, C2	1.86 ± 0.24	0.935 ± 0.0764	0.270	-0.213	-0.197	**3.6**
7c, C3	0.777 ± 0.20	0.780 ± 0.224	-0.109	-0.350	-0.331	**1.5**
7d, C5	0.344 ± 0.062	0.857 ± 0.148	-0.464	-0.254	-0.231	0.67
7e, C7	0.110 ± 0.028	0.687 ± 0.147	-0.957	-0.0366	-0.00703	0.22
8i, C1	1.00	1.12	0.00	-0.0953[e]	-0.0794	**2.0**
8j, C2	0.174	0.64	-0.76	-0.482[e]	-0.464	0.51
8k, C3	0.355	1.14	-0.45	-0.260[e]	-0.240	0.69
8l, C4	0.0977	0.85	-1.01	-0.264[e]	-0.241	0.20
8m, C6	0.0324	0.76	-1.49	-0.162[e]	-0.133	0.063
Control[f]		1.02 ± 0.13[g]				

[a] From Reference 45. [b] Units of µmol cm^{-2} h^{-1}. [c] Predicted from log J_M = -0.497 + 0.519 log S_{IPM} + 0.481 $S_{4.0}$ - 0.00268 MW (coefficients from n = 61 database, Reference 45, were recalculated using SAS 8.1). Error in prediction = log J_M – predicted log J_M. [d] Calculated from log J_M = -0.545 + 0.511 log S_{IPM} + 0.489 $S_{4.0}$ – 0.00253 MW (n = 61 + current data gives a new database of n = 66 compounds). Error in calculation was from log J_M – calculated log J_M. [e] Already included in the n = 61 database, so the value listed here is actually the difference between log J_M and a *calculated* value for flux, log $J_{calculated}$. [f] Skins were sequentially subjected to 48 h conditioning, 48 h contact with IPM, methanol wash, 24 h leaching. [g] From Reference 112.

If the fluxes of **7a-e** are normalized by their respective solubilities in IPM, the corresponding permeability coefficients P_M are obtained (Table 3-8). P_M has units of

distance per time (usually cm h^{-1}) and is thus a measure of how quickly a compound diffuses through the skin. Because P_M gives no indication of the amount, or dose, of the permeant that is entering the body, it is not clinically useful apart from the appropriate solubility data. Nevertheless, P_M is frequently used in the literature to quantify the permeation efficiency of a compound through skin.[5, 18] One of the most popular expressions of P_M, the Potts-Guy equation (9),[42] shows that P_M is positively dependent on the octanol-water partition coefficient ($K_{OCT:AQ}$) and negatively dependent on molecular weight (MW):

$$\log P_M = -6.3 + 0.71 \log K_{OCT:AQ} - 0.0061 \text{ MW} \quad (9)$$

Table 3-8: Percent Intact Prodrug Detected in Receptor Phase during Steady-State (% Intact), Log Permeability Coefficients (log P_M), Concentrations of APAP Species in Skin (C_S), and Dermal/Transdermal Delivery Ratios for APAP **6a**, 4-ACOM-APAP **7a-e**, and 4-AOC-APAP Prodrugs[a] **8i-m**

Compound	% Intact[b]	log P_M[c]	C_S[d]	D/T[e]
6a, APAP		-0.571	2.74 ± 0.70[f]	0.046
7a, C1	0	-1.06	2.67 ± 0.572	0.031
7b, C2	9	-1.52	13.1 ± 2.10	0.060
7c, C3	0	-1.98	5.56 ± 0.535	0.061
7d, C5	0	-2.50	3.55 ± 1.05	0.088
7e, C7	0	-2.95	2.72 ± 1.55	0.21
8i, C1	64	-1.08	5.45 ± 1.57[f]	0.046
8j, C2	14	-1.73	1.08 ± 0.13[f]	0.053
8k, C3	25	-1.82	2.84 ± 1.44[f]	0.068
8l, C4	0	-2.15	1.91 ± 0.08[f]	0.17
8m, C6	0	-2.71	1.79 ± 0.43[f]	0.47

[a] From Reference 45. [b] Percent intact prodrug detected in the 31 h receptor phase sample. [c] Calculated from log J_M – log S_{IPM}, units of cm h^{-1}. [d] Amount of total APAP species (in units of μmol) in receptor phase after 24 hours following donor phase removal to allow APAP and prodrug to leach out of skin. [e] Calculated from D/T = $[(C_S/4.9 \text{ cm}^2 \text{ 24 h})]/J_M$. [f] From Reference 119.

Such a relationship suggests that percutaneous absorption is positively dependant on lipid solubility and negatively dependant on the water solubility of a permeant. However, a plot of the log P_M values for **7a-e** versus their respective log $K_{IPM:4.0}$ values gave a negative slope (-0.519, $r^2 = 0.975$, plot not shown). Similarly, a plot of log P_M

versus the calculated solubility parameters of **7a-e** gave a positive slope (Figure 3-12), demonstrating an inverse relationship between log P_M and alkyl chain length (i.e. higher S_{IPM}, lower δ_i). These results are consistent with the findings of others[45, 69, 118] and support the idea[20] that lipophilicity alone is not a good predictor of flux.

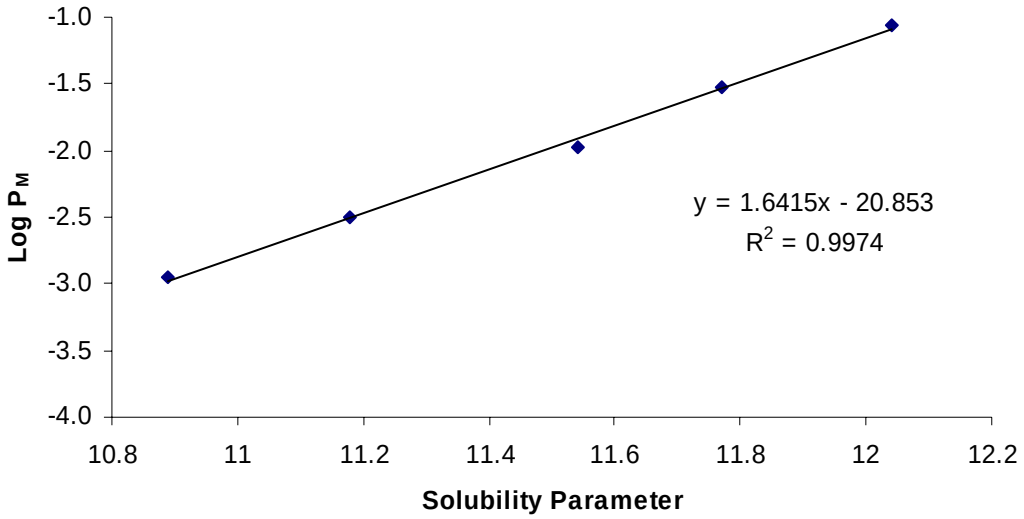

Figure 3-12: Plot of Solubility Parameter versus Log P for 4-ACOM-APAP Prodrugs **7a-e**

To further illustrate the relatively weak dependence of flux on lipid solubility, consider the S_{IPM} and S_{AQ} values for APAP prodrugs **7a-e** and **8i-m** (Table 3-5). Although compound **7c** is 6.1 times more soluble in IPM than **8i**, compound **8i** is 2.9 times more soluble in water than **7c**. This increase in water solubility on going from **7c** to **8i**, though modest, resulted in 1.3 fold greater flux for **8i** compared to **7c**. The impact of S_{AQ} on flux is more distinct when comparisons are made between individual members of a series. For instance, **7e** is 1.6 times more soluble in IPM than **7b**, but **7b** is 388 times more soluble in water. As a result, the flux of **7b** is 17 times greater than the flux of **7e**. In order to ascertain the relative impact of solubility in a lipid, solubility in water, and partition coefficient on flux, the trends in S_{IPM}, $S_{4.0}$, $K_{IPM:4.0}$, and J_M for APAP **6a** and its

prodrugs **7a-e** and **8i-m** are graphically represented in Figure 3-13 (a Wasdo plot).[119] What is clear from such a representation is that $K_{IPM:4.0}$ is of little positive predictive value in determining the rank order of flux. For each increase in alkyl chain length, there is a corresponding increase in $K_{IPM:4.0}$ regardless of the trends in J_M. It is interesting to note that while similar observations have been made by others,[118] the idea that partition coefficient is predictive of flux[120] remains an erroneous yet persistent[5] concept. A similar conclusion may be reached by examining the trends in S_{IPM}. Within the AOC series and to a lesser extent in the ACOM series, the trends in S_{IPM} are relatively flat across the series despite the fact that J_M grows progressively smaller. In contrast, the trends in $S_{4.0}$ generally mirror the trends in J_M across a series. Although such trends imply that water solubility is a better predictor of flux than lipid solubility, the reality is that flux is best predicted when *both* properties are considered.[43] This is demonstrated in the present case by the fact that the most permeable members of both series (**7b** and **8i**) exhibit the best mixture of high S_{IPM} and high $S_{4.0}$. Such behavior is no doubt related to the biphasic nature of the absorption barrier presented by the stratum corneum (see Chapter 1).

Although it is obvious that flux is positively dependent on lipid and aqueous solubility, there is currently only one mathematical model available for quantifying such a relationship (see Chapter 1):

$$\log J_M = x + y \log S_{IPM} + (1 - y) \log S_{4.0} - z\,MW \qquad (10)$$

$$\log J_M = -0.491 + 0.520 \log S_{IPM} + 0.480 \log S_{4.0} - 0.00271\,MW \qquad (11)$$

Equation 10, or the Roberts-Sloan (**RS**) model,[43] was originally based on a database (n = 42) of 7 different series of prodrugs of polar heterocycles. This database was recently updated[45] to include two new series of heterocyclic prodrugs and one new series of

phenolic prodrugs (4-AOC-APAP) resulting in a more structurally diverse database of 61 compounds. A fit of that data to equation 10 gave the form of **RS** expressed by equation 11.[45] In its present state, the model is heavily dependent on data from heterocyclic compounds: 59% 5-FU related entries, 18% 6-MP related entries, and 10% Th related entries in the database. Only 8 of the 61 entries (13%) are of a phenolic compound (i.e. APAP). Therefore, it was of interest to determine whether equation 11 could accurately predict the flux of the 4-ACOM prodrugs **7a-e** of APAP. Application of equation 11 to prodrugs **7a-e** resulted in predicted flux values ($J_{predicted}$, data not shown) that were consistently higher than the experimentally determined fluxes (J_M). The differences between log J_M and log $J_{predicted}$ (Δ log $J_{predicted}$) for **7a-e** are listed in Table 3-7. On average, the error in predicting log J_M (Δ log $J_{predicted}$) for **7a-e** was 0.192 ± 0.124 log units.

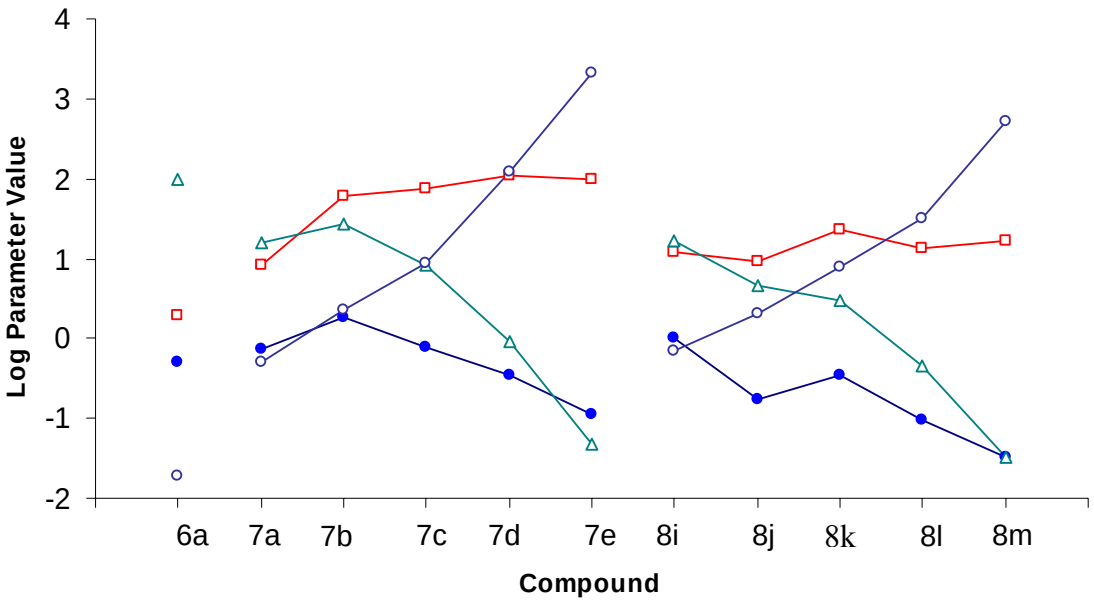

Figure 3-13: Log S_{IPM} (□), Log $S_{4.0}$ (Δ), Log $K_{IPM:4.0}$ (○), and Log J_M (●) Values for APAP **6a**, 4-ACOM-APAP Prodrugs **7a-e**, and 4-AOC-APAP Prodrugs **8i-m**.

In order to increase the diversity of the database and improve the predictive power of **RS**, prodrugs **7a-e** were incorporated into the database. A fit of the S_{IPM}, $S_{4.0}$, and MW for the resulting n = 66 entries to equation 10 gave the following estimates for x, y, and z: x = -0.545, y = 0.511, z = 0.00253, $r^2 = 0.915$. These parameter estimates were then used to calculate J_M for all 66 compounds (data not shown). A plot of J_M versus the calculated flux values is shown in Figure 3-14. The differences between the experimental and calculated fluxes ($\Delta \log J_{calculated}$) for APAP **6a** and its prodrugs **7a-e** and **8i-m** are listed in Table 3-7. As shown in Table 3-7, the $\Delta \log J_{calculated}$ for **6a**, **7a-e**, and **8i-m** decreased with the incorporation of the 4-ACOM-APAP data into the database. On average, the $\Delta \log J_{calculated}$ for **7a-e** (0.171 ± 0.126 log units) was somewhat higher than the average $\Delta \log J_{calculated}$ for the entire n = 66 database (0.155 ± 0.118 log units), but was much lower than the average $\Delta \log J_{calculated}$ for **8i-m** (0.231 ± 0.148 log units). Interestingly, APAP and its prodrugs all exhibit lower than expected fluxes based on the present form of **RS** (Figure 3-14). In addition, the average $\Delta \log J_{calculated}$ for APAP and its prodrugs (**6a** plus **7a-e**, plus **8i-m**; 0.227 ± 0.133 log units) is quite a bit higher than the average $\Delta \log J_{calculated}$ for the database as a whole.

In order to determine whether 4-ACOM-APAP prodrugs function better as dermal (delivery into the skin itself) or transdermal (delivery through the skin and into the systemic circulation) delivery agents, the skins were kept in contact with buffer for 24 hours after removing the donor phase to allow APAP and prodrugs to leach out. The amount of total APAP species leached from the skin (C_S) is shown in Table 3-8. As shown in Table 3-8, the rank order of C_S generally follows the rank order of flux. In other words, the most permeable members of the series were also the most effective at

increasing the concentration of APAP in the skin. Three out of the five ACOM derivatives were able to deliver more APAP into the skin than suspensions of topically applied APAP alone, with derivative **7b** delivering up to 5-times more APAP. Using the C_S values as an estimate for the amount of total APAP species delivered into the skin, dermal/transdermal delivery ratios (D/T, Table 3-8) were calculated from equation 12:

$$D/T = [(C_S/4.9\ cm^2\ 24\ h)]/J_M \qquad (12)$$

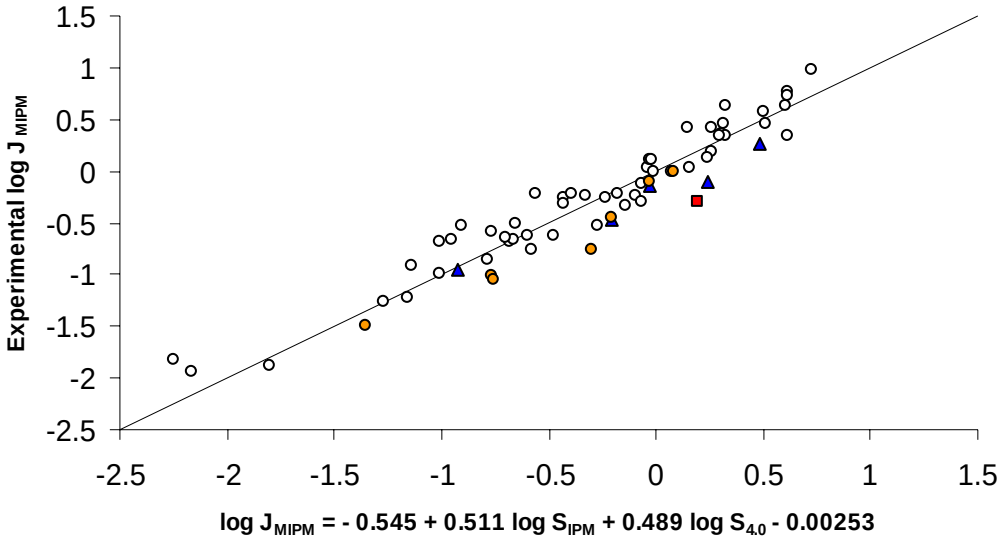

Figure 3-14: Plot of Experimental Versus Calculated Flux for 5-FU, 6-MP, and Th Prodrugs (○, n = 53), APAP (■), 4-AOC-APAP Prodrugs (●, n = 5, plus two additional compounds mentioned in Reference 1 to give n = 7), and 4-ACOM-APAP Prodrugs (▲, n = 5)

Most of the prodrugs exhibited D/T ratios that were higher than APAP. Thus, compared with topically applied APAP alone, all but one of the ACOM prodrugs (**7a**) were more effective at delivering APAP to the skin itself rather than through it. Among **7a-e**, the prodrugs that preferentially delivered more APAP into the skin itself were also the most lipophilic and least permeable members of the series. Thus, compounds such as **7d** and **7e** are best suited for a therapeutic regimen involving sustained delivery of low

levels of a drug, while the shorter chain derivatives would allow for maximum exposure of the drug to the systemic circulation.

Conclusions

Despite the success of ACOM prodrugs in improving the transdermal delivery of heterocyclic drugs, there are currently no examples of this approach being applied to a phenol. The results presented here demonstrate for the first time that ACOM derivatives are capable of improving the topical delivery of a phenol. In general, the ACOM derivatives of acetaminophen (APAP) exhibited better biphasic solubility and lower melting points than the previously studied[45] AOC derivatives. As a result, the 4-ACOM-APAP prodrugs were capable of improving the delivery of acetaminophen by 4-fold. The trends in flux were found to depend on a balance between lipid and aqueous solubility. Addition of the 4-ACOM-APAP prodrugs to the Roberts-Sloan database increased the structural diversity of the current database and resulted in a more robust **RS** model. Given that all of the 4-ACOM-APAP derivatives contained simple aliphatic groups in the acyl chain, it is likely that even greater improvements in flux will be realized by incorporating more hydrophilic functional groups into the acyl chain.[20]

CHAPTER 4
ALKYLOXYCARBONYLOXYMETHYL (AOCOM) PRODRUGS OF ACETAMINOPHEN (APAP)

Synthesis of AOCOM Prodrugs of 4-Hydroxyacetanlide (APAP)

To date, there has been only one report in the literature of the synthesis of an AOCOM derivative of a phenol.[121] In that study, Seki and coworkers arrived at the target AOCOM compound (4-ethyloxycarbonyloxymethyloxyacetanilide) by way of a four-step synthetic route starting from methyl chloroformate (Figure 4-1, R = C_2H_5). At the time of Seki's investigation, one of the key reagents, chloromethylchloroformate **16**, was commonly synthesized via the chlorination of methyl chloroformate.[84, 122] This method requires fractional distillation of the product mixture to obtain pure **16** and often provides low yields of the desired product. Currently, chloroformate **16** may be purchased from several suppliers and it is no longer synthesized in the lab on a regular basis.[123] Since the AOCOM and ACOM promoieties are structurally similar, it was of interest to determine whether the same strategy that was used to synthesize ACOM iodides (Chapter 3) could be used to eliminate the use of **16** (and **4**, R = Oalkyl) altogether (alternative routes shown in Figure 4-1 starting from **1a**). In keeping with this strategy, chloroformates were allowed to mix with trioxane and NaI at room temperature. Unfortunately, no reaction was observed at room temperature, and at higher temperatures the chloroformate apparently underwent decarboxylation as indicated by the generation of gas. Various Lewis acid / NaI mixtures also failed to result in product. If a catalytic amount of

pyridine was added, approximately 70% of the chloroformate was converted to alkyl iodide[124] even at room temperature.

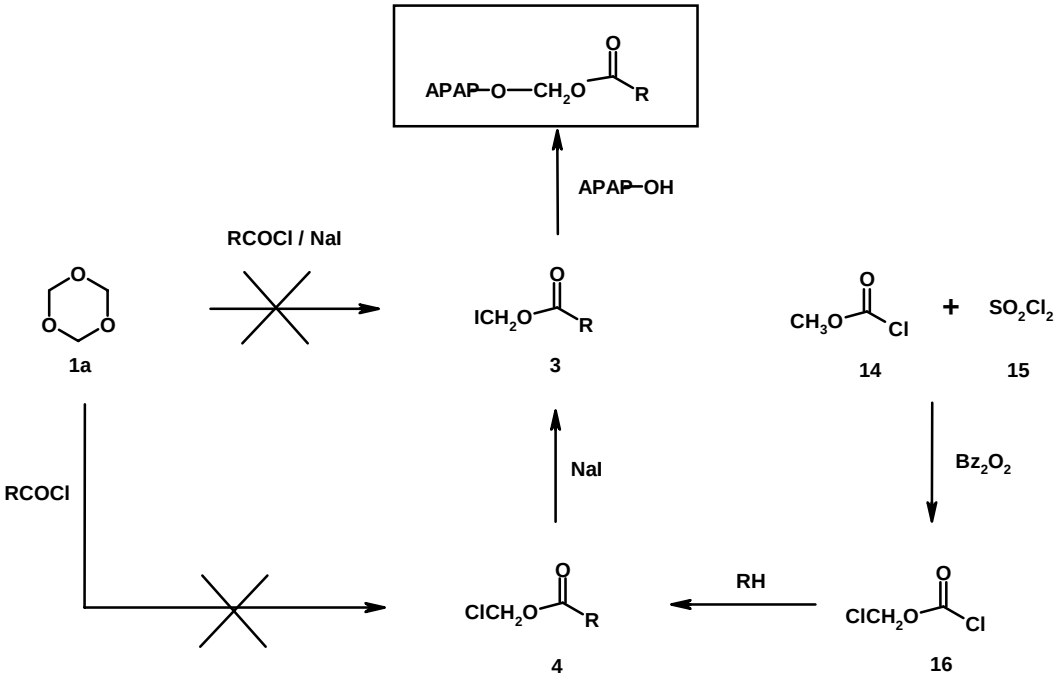

Figure 4-1: Synthetic Routes to Alkyloxycarbonyloxymethyl (AOCOM, R = Oalkyl) Prodrugs of 4-hydroxyacetanilide (APAP)

An alternative two-step route to AOCOM iodides involving an intermediate AOCOM chloride **4** (R = Oalkyl) was also attempted in order to avoid purchasing the relatively expensive **16** (Figure 4-1). There are a few reports in the literature that suggest such an approach is feasible.[81, 125] For example, ethyloxycarbonyloxyethyl chloride had been synthesized[81] previously in good yield (48%) by reacting acetaldehyde with ethyl chloroformate in the presence of a catalytic amount of $ZnCl_2$. Yet this method failed to work in the present case where the aldehyde is the formaldehyde trimer trioxane **1a**. Furthermore, although certain AOCOM alkyl halides can be synthesized from a monomeric aldehyde and chloroformate in the presence of a pyridine catalyst,[125] this method also failed in the present investigation.

As it was not possible to neither shorten the synthesis of AOCOM iodide **3** nor make the corresponding chloride **4** (R = Oalkyl) parsimoniously, **3** (R = Oalkyl) was obtained through a two-step process starting from **16** (Figure 4-1). With **3** (R = Oalkyl) in hand, the target prodrugs could be obtained by coupling **3** (R = Oalkyl) with APAP. The coupling reaction used by Seki[121] was an adaptation of the method of Sloan and Koch for the synthesis of ACOM ethers of phenols.[90] Under those conditions (K_2CO_3 as base, acetone as solvent), Seki and coworkers noted that 4-ethyloxycarbonyloxymethyloxyacetanilide was obtained in 20 % yield from the coupling of APAP with ethyloxycarbonyloxymethyl iodide following a reaction time of seven days. In an effort to improve the yield and ascertain the reaction parameters by which this reaction is governed, a series of AOCOM derivatives of phenols (with emphasis on APAP) was synthesized by the method of Seki[121] and by a more efficient method involving phase-transfer catalysis. In addition, the results were compared to those obtained from the coupling reaction of ACOM halides with phenols—an analogous system whose reaction parameters are known (see Chapter 3).[90]

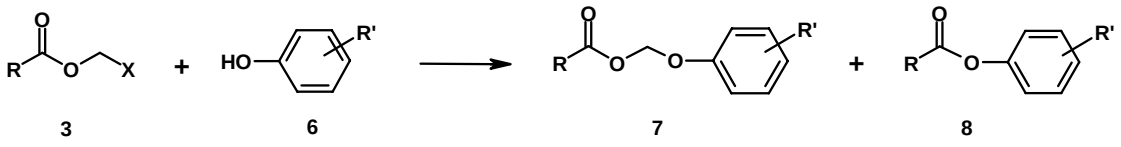

Figure 4-2: Generalized Reaction of AOCOM halides (R = Oalkyl) and ACOM halides (R = alkyl) **3** with phenols **6**

In the present investigation, 4-hydroxyacetanilide (APAP) was chosen as a model phenol in order to make a direct comparison between this work and the work of Seki.[121] In addition, if the reactivity of AOCOM halides was found to parallel that of ACOM

halides,[90] then the reaction mixtures were expected to contain various percentages of acylated phenol **8** as a byproduct (Figure 4-2). In the present case, since the carbonate derivatives of APAP had been characterized previously,[45, 126] adoption of this particular phenol as a model facilitated byproduct identification. As shown in Figure 4-3, AOCOM iodides may be obtained from the corresponding chlorides via halogen exchange in acetone, preferably in the presence of sodium bicarbonate to neutralize traces of HI formed during the reaction.[84] Subsequent reaction with phenols under the standard conditions (acetonitrile or acetone as solvent, K_2CO_3 as base)[90, 121] or in a biphasic system in the presence of tetrabutylammonium hydrogen sulfate (Figure 4-3) gave mixtures of **7** and **8**.

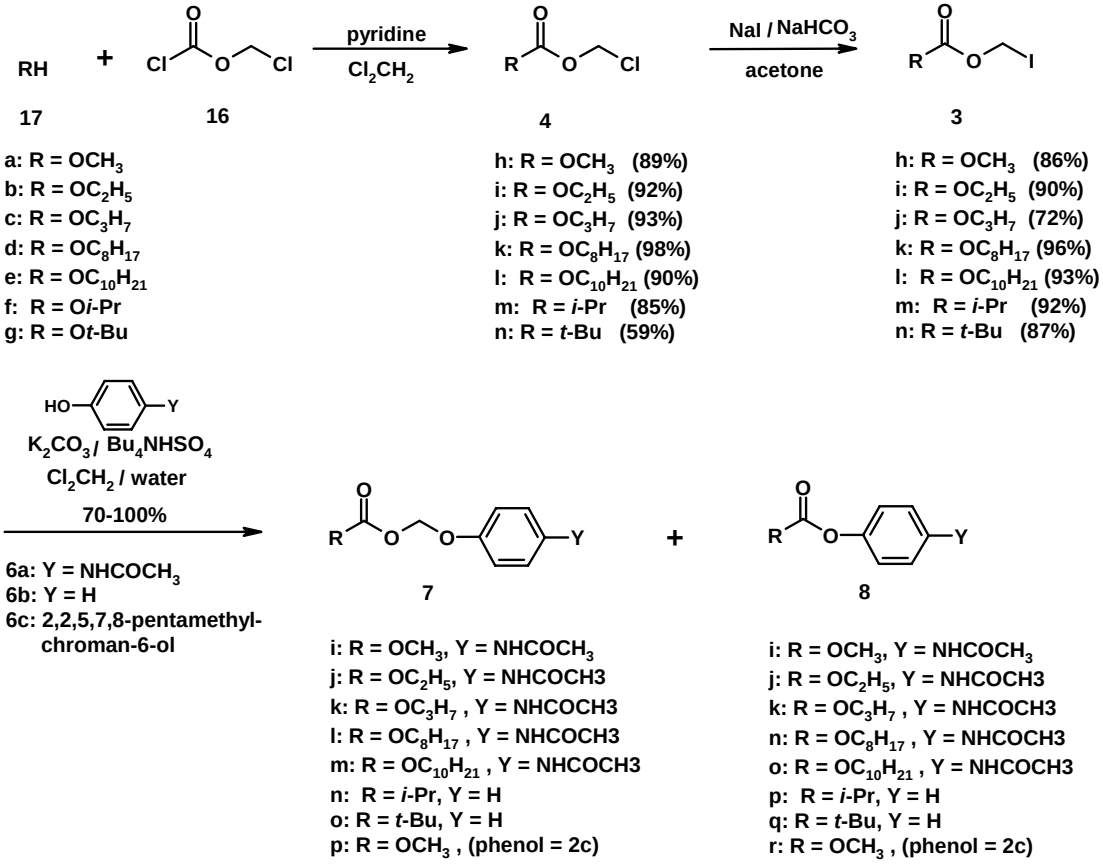

Figure 4-3: Reaction of AOCOM iodides with phenols under phase-transfer conditions

Previously, Sloan and Koch[90] had shown that the coupling of ACOM halides with phenols is sensitive to the nucleofugicity of X, with better leaving groups giving more alkylated product **7**. Recently, others[91] have suggested that the ratio **7**/**8** is also dependent on the steric hindrance of the acyl group (R group in **3**). Although the data presented in Table 4-1 is not exhaustive, it suggests that the trends observed in reactions of ACOM halides with phenols are operative in the analogous reactions of AOCOM halides. For example, if X is a poor leaving group, **8** is favored, but as the nucleofugicity of X increases, the product distribution shifts toward **7** (compare entries 1 and 2 with 4). For X = I, alkylated phenol **7** becomes the major product when the alkoxy chain length extends beyond OCH_3. Interestingly, the ratio **7**/**8** when R = OCH_3 increases by more than 3 fold when the reaction is carried out under phase-transfer conditions instead of the standard protocol (entry 3 versus entry 6). Under these conditions, there is an incremental increase in the percentage **7** with increasing steric hindrance (as measured by Charton's steric parameters[127]) in R (entries 6-8), but beyond propyloxy, the percentage of **7** remains fairly constant for the straight chain derivatives studied. However, the product distribution shifts entirely toward **7** on going to more bulky R groups (entries 11-12). On the other hand, the percentage of **7** may be increased even for sterically unhindered R if the phenol is sufficiently hindered (entry 6 versus entry 13). This particular result (entry 13) is not without precedent since others[91] have observed a similar trend in reactions of ACOM halides with phenols. Aside from its effect on product distribution, the advantages of the phase-transfer reaction include shorter reaction times (one day) and higher overall yield compared to the method of Seki.[121] Although no mention was made of product distribution, it is also worth noting that Wolff and

Hoffmann[128] have used a similar reaction system to successfully alkylate phenols with cyclic ACOM halides.

Table 4-1: Product Distribution of the Reaction of RCO_2CH_2X **3** with Phenols **6** Under Various Reaction Conditions

Entry	R	X	Phenol	Solvent	Base	Distribution (%)[a]		ν^b
						7	**8**	
1	OC_2H_5	$[MeNC_4H_8]+$	**6a**	acetonitrile	$MeNC_4H_8$	0	100 (28)[c]	0.48[d]
2	OC_2H_5	Cl	**6a**	acetonitrile	K_2CO_3	3	58	
3	OCH_3	I	**6a**	acetonitrile	K_2CO_3	36	64	0.36[d]
4	OC_2H_5	I	**6a**	acetone	K_2CO_3	57 (17)[c]	43 (13)[c]	
5	OC_4H_9	I	**6a**	acetone	K_2CO_3	58	42	0.58[d]
6[e]	OCH_3	I	**6a**	Cl_2CH_2/H_2O	K_2CO_3	66 (18)[c]	34 (6)[c]	
7[e]	OC_2H_5	I	**6a**	Cl_2CH_2/H_2O	K_2CO_3	74 (50)[c]	26 (13)[c]	
8[e]	OC_3H_7	I	**6a**	Cl_2CH_2/H_2O	K_2CO_3	84 (43)[c]	16 (6)[c]	0.56
9[e]	OC_8H_{17}	I	**6a**	Cl_2CH_2/H_2O	K_2CO_3	82 (45)[c]	18 (3)[c]	0.61
10[e]	$OC_{10}H_{21}$	I	**6a**	Cl_2CH_2/H_2O	K_2CO_3	78 (41)[c]	22 (6)[c]	0.56[f]
11[e]	O-*i*-Pr	I	**6b**	Cl_2CH_2/H_2O	K_2CO_3	100	0	0.75[d]
12[e]	O-*t*-Bu	I	**6b**	Cl_2CH_2/H_2O	K_2CO_3	100	0	1.22[d]
13[e]	OCH_3	I	**6c**	Cl_2CH_2/H_2O	K_2CO_3	90 (33)[c]	10 (0)[c]	
14[g]	CH_3	I	**6b**	acetonitrile	K_2CO_3	63	37	0.52[h]
15[g]	C_2H_5	I	**6a**	acetonitrile	K_2CO_3	59	31	0.56[h]
16[g]	C_3H_7	I	**6a**	acetonitrile	K_2CO_3	73	24	0.68[h]
17[g]	C_5H_{11}	I	**6a**	acetonitrile	K_2CO_3	66	27	0.68[h]
18[g]	C_7H_{15}	I	**6a**	acetonitrile	K_2CO_3	71	27	0.73[h]

[a] Determined from ^{1}H NMR spectrum of the crude reaction mixture. [b] Charton's steric parameter for R. [c] Isolated yield. [d] Reference 127. [e] Reaction mixture includes 1 equivalent tetrabutylammonium hydrogen sulfate. [f] Estimated from the relationship $\nu = 0.406n_\beta + 0.108n_\gamma + 0.059n_\delta - 0.00839$ in Charton, M. *J. Org. Chem.*, **1978**, *43*, 3995-4001. [g] Data taken from Chapter 3. [h] Reference 94.

As discussed previously in Chapter 3, ACOM halides react with phenols under the standard conditions to give mainly **7** as long as X is a good leaving group (≥ Br). Thus, the relatively low ratio **7**/**8** in the AOCOM series compared to the ACOM series (compare entries 3-5 with entries 14-18) was unanticipated. Moreover, since the

carbonyl of a carbonate is usually less reactive than the carbonyl of the corresponding ester,[55] one might expect less acylation when R is alkyloxy (as in AOCOM) than when it is alkyl (as in ACOM). Since the AOCOM iodides **3** (R = Oalkyl) were not purified other than to filter off NaCl and unreacted NaI (see Experimental below), it is worth considering whether any remaining AOCOM chloride in crude **3** affected the product distribution. If **4** (R = Oalkyl) was reacting with **6** to any significant extent then the percentage of acylated product **8** would have increased as the percentage of **4** increased. In the case of entries 3, 4, and 5, the percentages of unreacted AOCOM chloride **4** in crude **3** (R = Oalkyl) were 2%, 9%, and 9% respectively. Thus it does not appear that the product distribution was affected by the presence of AOCOM chloride in crude **3** (R = Oalkyl). On the other hand, analysis of the steric parameters for both series (ACOM and AOCOM) suggests that differences in **7**/**8** between the series are directly related to differences in the steric hindrance of R based on Charton's steric parameters (compare entries 3-5 to entries 14-18).[94, 127] A plot of ν versus the ratio of **8**/**7** for the entries 3-5 and entries 14-18 is shown in Figure 4-4. Although the plot of the AOCOM series consists of only three data points, the trends in the data suggest that the coupling reaction of AOCOM iodides with phenols is much more sensitive to steric effects than the analogous reactions of ACOM iodides (slope = -4.9 versus slope = -0.77). A plot of ν versus **8/7** for entries 6-11 (Figure 4-5) demonstrates a much weaker dependence of product distribution on steric effects when phase-transfer conditions are used in lieu of the standard conditions (slope = -1.3 versus slope = -4.9).

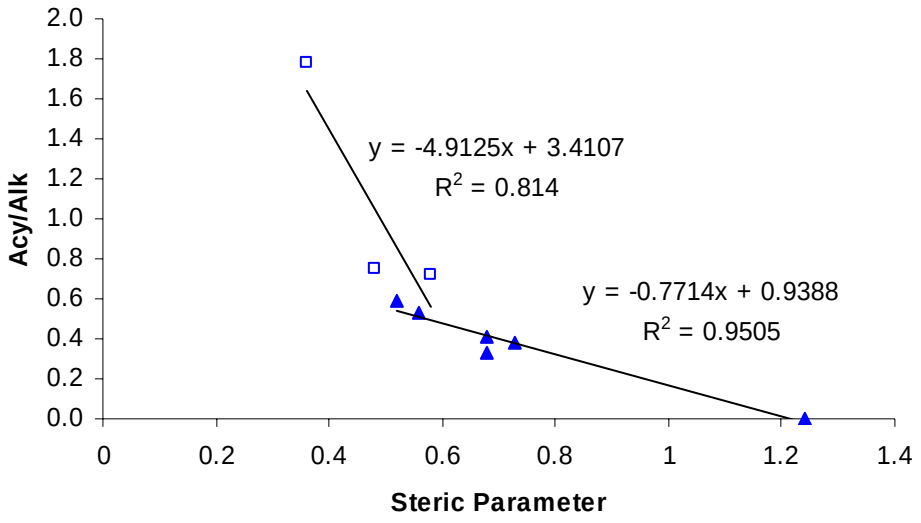

Figure 4-4: Plot of Charton's Steric Parameter ν for R Versus the Ratio of Acylated/Alkylated Product (**8**/**7**) Resulting from the Reactions of **6** with AOCOM Iodides (Entries 3-5 in Table 4-1, □) and ACOM Iodides (Entries 14-18 in Table 4-1, ▲) Under the Standard Reaction Conditions.

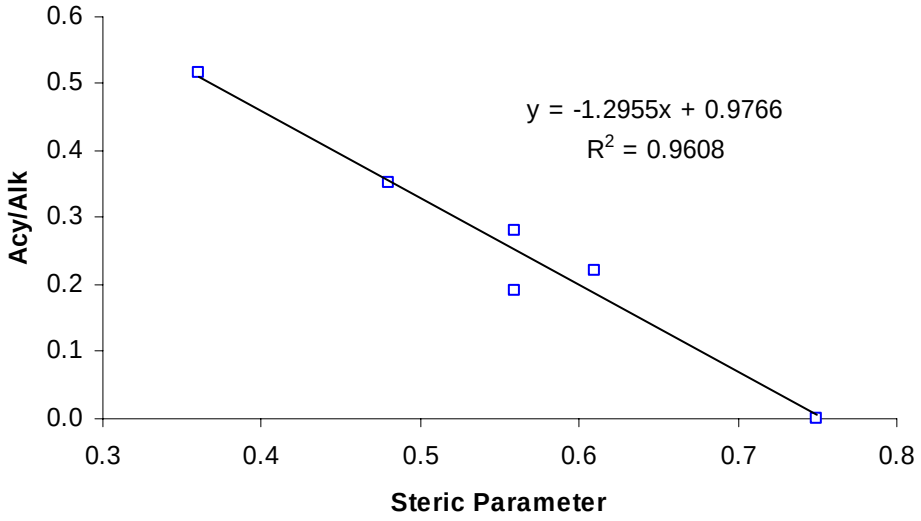

Figure 4-5: Plot of Charton's Steric Parameter ν for R Versus the Ratio of Acylated/Alkylated Product (**8**/**7**) Resulting from the Reactions of **6** with AOCOM Iodides (Entries 6-11 in Table 4-1, □) Under Phase-Transfer Conditions.

Conclusions

In conclusion, the data presented here suggests that steric hindrance plays a greater role in the coupling reactions of AOCOM halides with phenols than in the analogous

reactions of ACOM halides. However, this problem may be circumvented through the use of phase-transfer catalysis. Under these conditions, the influence of steric hindrance (as characterized by Charton's steric parameters) is minimized, reaction time is reduced, and overall yields are increased.

Experimental

Melting points were determined on a Meltemp melting point apparatus. Thin layer chromatography (TLC) plates (Polygram Sil G/UV 254) were purchased from Brinkman. Spectra (^{1}H NMR) were recorded on a Varian Unity 400 MHz spectrometer or on a Varian EM-390 90 MHz spectrometer; chemical shifts listed below are in reference to Me_4Si. Sodium iodide was from Fisher or Aldrich. *Note: there was no difference in reactivity between "old" and "new" batches of NaI (see Chapter 3) when used in the Finkelstein reactions described here*. Sodium sulfate and all solvents were purchased from Fisher. Trioxane was purchased from Eastman Chemical Company. Chloromethylchloroformate was purchased from TCI America and Lancaster Synthesis. All other reagents were from Aldrich. All bulk solvents and silica gel for chromatography were from Fisher. Containers of NaI were wrapped in parafilm and stored in a vacuum desiccator. Solvents listed as "dry" below were obtained as such following storage over 4-angstrom molecular sieves. Methanol, ethanol (absolute), propanol, and butanol were dried over 3-angstrom molecular sieves before they were used as reagents. Pyridine was dried over 4-angstrom molecular sieves before it was used. Microanalyses were performed by Atlantic Microlab, Inc., Norcross, GA.

Note: In general, the compounds described below were selected for "large scale" synthesis on the basis of whether they were solids (oils are usually more difficult to characterize and isolate than solids). With that in mind, it should be noted that 4-

butyloxycarbonyloxymethyloxyacetanilide and 4-hexyloxycarbonyloxymethyloxyacetanilide were also synthesized but since they were oils they were never isolated on a large enough scale to evaluate in diffusion cells.

General procedure for the synthesis of alkyloxycarbonyloxymethyl iodides (3, R = Oalkyl)—methyloxycarbonyloxymethyl iodide 3h (Note: it is not necessary to add $NaHCO_3$ as suggested below. However, since $NaHCO_3$ minimized the formation of 4-hydroxy-4-methyl-2-pentanone during the Finkelstein reaction, it was almost always used in this study to synthesize the AOCOM iodides): To an ice-cold solution of chloromethyl chloroformate **16** (82.8 mmol) and methanol **17a** (69 mmol) in methylene chloride (130 ml) was added pyridine (82.8 mmol) in methylene chloride drop-wise over 10 minutes. The mixture was allowed to warm to room temperature and continue stirring overnight. The reaction mixture was then washed with 1 M HCl (35 ml) and water (35 ml), dried over Na_2SO_4, filtered, and concentrated on a rotary evaporator to give **4h** as a pale yellow oil (61.1 mmol, 89% yield; by ^{1}H NMR, this oil also contained 5.8 mmol Cl_2CH_2 and 2.4 mmol H_2O; no **16** or **17a** remained); ^{1}H NMR (400 MHz, $CDCl_3$): δ 5.74 (s, 2 H) and δ 3.89 (s, 3 H). Compound **4h** was subsequently dissolved in 70 ml dry acetone and NaI (91.7 mmol) was added. This was immediately followed by the addition of $NaHCO_3$ (6.1 mmol) and the resulting mixture was allowed to react at 40 ^{o}C for 4 hours. After such time, the mixture was concentrated on a rotary evaporator and triturated in methylene chloride for approximately 30 minutes. The resulting mixture was filtered and concentrated as before to give **3h** as a dark oil (52.5 mmol, 86% yield; by ^{1}H NMR, this oil also contained 3.9 mmol $CH_3OCO_2CH_2Cl$,

29 mmol $(CH_3)_2C(OH)CH_2COCH_3$, 24 mmol Cl_2CH_2, 2.6 mmol acetone, and 3.7 mmol H_2O); ^1H NMR (400 MHz, $CDCl_3$): δ 5.96 (s, 2 H) and δ 3.87 (s, 3 H).

General procedure for the phase-transfer reactions: A mixture of phenol **6** (28.4 mmol) and K_2CO_3 (85.2 mmol) in 140 ml water was allowed to stir several minutes before adding tetrabutylammonium hydrogen sulfate (28.4 mmol) and 70 ml methylene chloride. After several minutes of stirring, a solution of **3** (R = Oalkyl, 36.8 mmol) in 70 ml methylene chloride was added in portions to the reaction mixture. The resulting biphasic system was allowed to mix overnight at the maximum stirring rate of a standard magnetic stir plate. After such time, the phases were separated and the water layer was extracted with methylene chloride. The organic phases were combined and concentrated under vacuum to give an oily residue. A sample of this residue was analyzed by ^1H NMR in order to determine the product distributions shown in Table 4-1 (Estimated % conversion of phenol to its corresponding AOCOM derivative for all reactions = 70-100 % by ^1H NMR. In all cases, with the exception of entry 6, TLC of the water phase showed no evidence of unreacted **6**). The residue was then triturated in ether and tetrabutylammonium iodide was removed by vacuum filtration. Compounds **7** and **8** were separated by column chromatography on silica gel and recrystallized from various solvents to obtain pure samples as described below.

Isolation of compounds 7 and 8 (No effort was made to purify compounds 7n and 7o and the product distributions were determined by ^1H NMR of the crude reaction mixtures.): 4-methyloxycarbonyloxymethyloxyacetanilide **(7i)** and 4-methyloxycarbonyloxyacetanilde **(8i)** (scale = 40.4 mmol **6a**) were separated by column chromatography on silica gel (gradient = 100% hexane → 70:30 hexane : acetone) to give

2.16g **7i** (22% crude yield) as a solid. Recrystallization of this solid from Cl_2CH_2 : hexane gave 1.77 g **7i** (7.41 mmol, 18% yield) as colorless crystals: mp = 104-106 ^oC; ^1H NMR (400 MHz, $CDCl_3$) δ 7.43 (d, *J* = 7 Hz, 2 H), δ 7.13 (brs, 1 H), δ 7.01 (d, *J* = 7 Hz, 2 H), δ 5.73 (s, 2 H), δ 3.83 (s, 3 H), δ 2.16 (s, 3 H); Anal. Calcd for $C_{11}H_{13}NO_5$: C, 55.23; H, 5.48; N, 5.85. Found: C, 55.23; H, 5.52; N, 5.89. Compound **8i** was obtained from the column as a solid (0.98 g, 4.7 mmol, 12 % crude yield). This solid was recrystallized from EtOAc : hexane to give 0.53 g (2.53 mmol, 6% yield) **8i** as colorless crystals: mp = 115-117 ^oC (lit. = 115.5-116.5 ^oC)[126]

4-Ethyloxycarbonyloxymethyloxyacetanilide (7j) and 4-ethyloxycarbonyloxyacetanilide (8j) (scale = 3.2 mmol 6a) were separated by column chromatography on silica gel (gradient = 100% hexane → 70:30 hexane : acetone) to give 0.58 g (2.3 mmol, 72% crude yield) 7j as a solid. This solid was recrystallized from ether : pentane to give 0.40 g (1.6 mmol, 50% yield) **7j** as colorless crystals: mp = 83-85 ^oC (lit = 74-77 ^oC);[121] ^1H NMR (400 MHz, $CDCl_3$) δ 7.42 (d, *J* = 9 Hz, 2 H), δ 7.18 (brs, 1 H), δ 7.02 (d, *J* = 9 Hz, 2 H), δ 5.73 (s, 2 H), δ 4.24 (quart, *J* = 7 Hz, 2 H), δ 2.16 (s, 3 H), δ 1.32 (t, *J* = 7 Hz, 3 H); Anal. Calcd for $C_{12}H_{15}NO_5$: C, 56.91; H, 5.97; N, 5.53. Found: C, 56.91; H, 6.05; N, 5.54. Compound **8j** was also obtained from the column as a solid (0.20 g, 0.90 mmol, 28% crude yield). Recrystallization of this solid from EtOAc : hexane gave 0.08 g (0.4 mmol, 13% yield) **8j** as colorless crystals; mp = 119-120 ^oC (lit = 121-122 ^oC).[126]

4-Propyloxycarbonyloxymethyloxyacetanilide (7k) and 4-propyloxycarbonyloxyacetanilide (8k) (scale = 24.8 mmol 6a) were separated by column chromatography on silica gel (gradient = 100% hexane → 75:25 hexane :

acetone) to give 4.38 g 7k (16.4 mmol, 66% crude yield) as an oil. This oil was crystallized from ether : pentane to give 2.83 g (10.6 mmol, 43% yield) **7k** as colorless crystals: mp = 68-69 ^{o}C; ^{1}H NMR (400 MHz, $CDCl_3$) δ 7.42 (d, *J* = 9 Hz, 2 H), δ 7.16 (brs, 1 H), δ 7.02 (d, *J* = 9 Hz, 2 H), δ 5.73 (s, 2 H), δ 4.14 (t, *J* = 7 Hz, 2 H), δ 2.16 (s, 3 H), δ 1.71 (m, 2 H), δ 0.96 (t, *J* = 7 Hz, 3 H); Anal. Calcd for $C_{13}H_{17}NO_5$: C, 58.42; H, 6.41; N, 5.24. Found: C, 58.46; H, 6.42; N, 5.25. Compound **8k** was isolated from the column as a solid (0.80 g, 3.4 mmol, 14% crude yield). Recrystallization of this solid from EtOAc : hexane produced 0.39 g (1.6 mmol, 6% yield) **8k** as colorless crystals: mp = 107-110 ^{o}C (lit = 105-108).[129]

4-Octyloxycarbonyloxymethyloxyacetanilide (7l) and 4-octyloxycarbonyloxyacetanilide (8n) (scale = 28.4 mmol 6a) were separated by column chromatography on silica gel (gradient = 100% hexane → 80:20 hexane : acetone) to give 4.10 g 7l (12.2 43% crude yield) as a white solid. A second fraction from the column contained a mixture of **7l** and **8n**. Both fractions were recrystallized from ether : pentane and combined to give 4.36 g (12.9 mmol, 45% yield) **7l** as colorless crystals: mp = 64-65 ^{o}C; ^{1}H NMR (400 MHz, $CDCl_3$) δ 7.42 (d, *J* = 9 Hz, 2 H), δ 7.23 (brs, 1 H), δ 7.02 (d, *J* = 9 Hz, 2 H), δ 5.73 (s, 2 H), δ 4.17 (t, *J* = 7 Hz, 2 H), δ 2.16 (s, 3 H), δ 1.67 (m, 2 H), δ 1.40-1.20 (m, 10 H), δ 0.87 (t, *J* = 7 Hz, 3 H); Anal. Calcd for $C_{18}H_{27}NO_5$: C, 64.07; H, 8.07; N, 4.15. Found: C, 64.04; H, 8.12; N, 4.10. Compound **8n** was also isolated from the column as a solid. This solid was recrystallized from EtOAc : hexane to produce 0.29 g (0.94 mmol, 3% yield) **8n** as colorless crystals: mp = 80-82 ^{o}C (lit = 82.5-83 ^{o}C).[126]

4-Decyloxycarbonyloxymethyloxyacetanilide (7m) and 4-decyloxycarbonyloxyacetanilide (8o) (scale = 23.2 mmol 6a) were separated by column chromatography on silica gel (gradient = 90:10 hexane : acetone → 80:20 hexane : acetone) to give 4.45 g 7m as a white solid. Recrystallization of this solid produced 3.55 g (9.73 mmol, 42% yield) **7m** as a white powder: mp = 54-56 ^{o}C; ^{1}H NMR (400 MHz, $CDCl_3$) δ 7.42 (d, *J* = 9 Hz, 2 H), δ 7.08 (brs, 1 H), δ 7.03 (d, *J* = 9 Hz, 2 H), δ 5.73 (s, 2 H), δ 4.17 (t, 7 Hz, 2 H), δ 2.17 (s, 3 H), δ 1.67 (m, 2 H), δ 1.40-1.20 (m, 14 H), δ 0.88 (t, *J* = 7 Hz, 3 H); Anal. Calcd for $C_{20}H_{31}NO_5$: C, 65.73; H, 8.55; N, 3.83. Found: C, 65.90; H, 8.62; N, 3.82. Compound **8o** was also isolated from the column as a solid (1.19 g, 3.36 mmol, 14% crude yield). This solid was recrystallized from EtOAc : hexane to give 0.42 g (1.3 mmol, 6% yield) **8o** as colorless crystals: mp = 85-88 ^{o}C. Although **8o** had not been previously synthesized, the chemical shifts for $CH_2CH_2O_2C$ (δ 4.24, t, 2 H) and the AB quartet (δ 7.50, d, 2 H; δ 7.13, d, 2 H) in **8o** were consistent with those exhibited by other members in the series.

6-Methyloxycarbonyloxymethyloxy-2,2,5,7,8-pentamethylchroman (7p) and 6-methyloxycarbonyloxy-2,2,5,7,8-pentamethylchroman (8r) (scale = 8.6 mmol 6c) were separated by column chromatography on silica gel (gradient = 100% hexane → 97:3 hexane : acetone) to obtain 1.56 g 7p (5.06 mmol, 59% crude yield) as a yellow oil. The oil was crystallized from ether : pentane to get 0.86 g (2.8 mmol, 33% yield) **7p** as pale yellow crystals: mp = 94-95 ^{o}C; ^{1}H NMR (400 MHz, $CDCl_3$) δ 5.51 (s, 2 H), δ 3.82 (s, 3 H), δ 2.59 (t, *J* = 7 Hz, 2 H), δ 2.15 (s, 3 H), δ 2.11 (s, 3 H), δ 2.08 (s, 3 H), δ 1.79 (t, *J* = 7 Hz, 2 H), δ 1.29 (s, 6 H); Anal. Calcd for $C_{17}H_{24}O_5$: C, 66.21; H, 7.84. Found: C, 66.16; H, 7.86. Compound **8r** eluted from the column as a mixture of **7p** and

8r in a ratio of 85:15. Compound **8r** could not be separated from this mixture by crystallization, and no further effort was made to isolate **8r**.

In Vitro Determination of Flux of AOCOM APAP Prodrugs

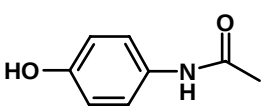

4-Hydroxyacetanilide (APAP)

6a

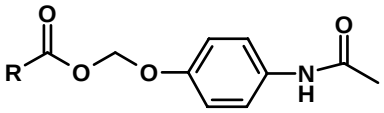

4-AOCOM-APAP

7i, R = OCH_3
7j, R = OC_2H_5
7k, R = OC_3H_7
7l, R = OC_8H_{17}
7m, R = $OC_{10}H_{21}$

Figure 4-6: Structure of 4-Hydroxyacetanilide (APAP) and Corresponding 4-AOCOM-APAP Prodrugs

Methods and Materials

Melting points were determined on a Meltemp capillary melting point apparatus and are uncorrected. Ultraviolet (UV) spectra were obtained on a Shimadzu UV- 2501 PC spectrophotometer. The vertical Franz diffusion cells (surface area 4.9 cm^2, 20 ml receptor phase volume, 15 ml donor phase volume) were purchased from Crown Glass (Somerville, NJ, USA). A Fisher (Pittsburgh, PA, USA) circulating water bath was used to maintain a constant temperature of 32 ^oC in the receptor phase. Isopropyl myristate (IPM) was purchased from Givaudan (Clifton, NJ, USA). Theophylline (Th) was purchased from Sigma Chemical Co. (St. Louis, MO, USA); all other chemicals were purchased from Fisher. The female hairless mice (SKH-hr-1) were obtained from Charles River (Boston, MA, USA). All procedures involving the care and experimental

treatment of animals were performed by Professor K. B. Sloan of the department of Medicinal Chemistry in agreement with the NIH "Principles of Laboratory Animal Care."

Physicochemical properties and analysis

The molar absorptivity of each prodrug at 240 nm (ε_{240}) in acetonitrile (Table 4-2) was determined in triplicate by dissolving a known amount of prodrug in acetonitrile, and analyzing the dilute solution by UV spectrophotometry. Since the concentration C was known, ε_{240} could be calculated by way of Beer's law:

$$A_{240} = \varepsilon_{240}\, l\, C, \text{ where } l = \text{cell length} \quad (1)$$

For each prodrug, the solubility in isopropyl myristate (IPM) was determined in triplicate by crushing a sample of the prodrug into a fine powder. Excess powder was added to a test tube containing 3 ml IPM. The test tube was then insulated and the suspension was allowed to stir at room temperature (23 ± 1 ^{o}C) for 24 hours on a magnetic stir plate. The suspension was filtered through a 0.25 μm nylon syringe filter. A sample of the filtrate was diluted with acetonitrile and analyzed by UV spectrophotometry. In order to be consistent with a previous investigation of acetaminophen prodrugs,[45] the absorbance at 240 nm (A_{240}) was used to calculate the prodrug concentration C in the IPM solution using the Beer's law relationship. In this case, since C is the concentration of a saturated solution, C is the solubility in IPM (S_{IPM}):

$$C_{Saturation} = S_{IPM} = A_{240} / \varepsilon_{240} \quad (2)$$

Solubilities in water were also determined in triplicate using an identical protocol to the one described above, except that the suspensions were only stirred for one hour before filtering. This was done in order to make direct comparisons between the present investigation and previous studies.[45, 68] In each case, a sample of the filtrate was diluted

with acetonitrile and analyzed by UV spectrophotometry using ε_{240} in acetonitrile (Table 4-2).

Table 4-2: Molar Absorptivities (ε) of APAP **6a** and Prodrugs **7i-m**

Compound	ε_{240} in ACN[a, b]	ε_{240} in Buffer[a, c]	ε_{280} in Buffer[a, d]
6a, APAP	1.36[e]	1.01 ± 0.053	0.174 ± 0.020
7i	1.44 ± 0.023		
7j	1.53 ± 0.041	1.11 ± 0.036	0.101 ± 0.014
7k	1.46 ± 0.056		
7l	1.52 ± 0.048		
7m	1.54 ± 0.0027		

[a] Units of 1 x 10^4 L mol^{-1}. [b] Molar absorptivities at 240 nm acetonitrile (± SD, n = 3). [c] Molar absorptivities at 240 nm in pH 7.1 phosphate buffer with 0.11% formaldehyde (± SD, n = 5). [d] Molar absorptivities at 280 nm in pH 7.1 phosphate buffer with 0.11% formaldehyde (± SD, n = 5). [e] Taken from Reference 45.

Partition coefficients were also determined in triplicate for each prodrug by using the saturated IPM solutions obtained from the solubility determinations. Since solubility in pH 4.0 buffer ($S_{4.0}$) is a parameter in the Roberts-Sloan database,[20] acetate buffer (0.01 M, pH 4.0) was used as the aqueous phase in the partition coefficient experiments. In this way, $S_{4.0}$ could be estimated as described previously[109] and the values included in the database. Thus, an aliquot of the saturated IPM solution was partitioned against pH 4.0 buffer using the following volume ratios ($V_{4.0}$ / V_{IPM}) for compounds **7i, 7j,** and **7k**: 0.7, 2.5, and 10, respectively. The two phases were vigorously shaken for 10 seconds,[109] then allowed to separate via centrifugation. An aliquot of the IPM layer was removed, diluted with acetonitrile, and analyzed by UV spectrophotometry as described above. Using the previously measured absorbance at 240 nm for the saturated solution, the partition coefficient was calculated as follows:

$$K_{IPM:4.0} = [A_a/(A_b - A_a)]V_{4.0}/V_{IPM} \quad (3)$$

where A_b and A_a are the respective absorbances before and after partitioning, and $V_{4.0}$ and V_{IPM} are the respective volumes of buffer and IPM in each phase. It was not possible to experimentally determine partition coefficients for compounds **7l** and **7m** since their respective solubility ratios (S_{IPM}/S_{AQ}) were much too high. Therefore, in these cases $K_{IPM:4.0}$ was estimated from the average methylene π_K obtained for compounds **7i-k** according to the following relationship

$$\log K_{n+m} = (\pi_K)(m) + \log K_n \quad (4)$$

where n is the number of methylene units in the promoiety of one prodrug and m is the number of additional methylene units in the promoiety with which it is compared.

UV spectrophotometry was also used to determine the amount of **6a** and prodrug present in the receptor phase of the diffusion cell. Since all the prodrugs in this study were part of a homologous series, it was assumed that satisfactory results would attain for the entire series from the use of the molar absorptivity of one homolog. Thus, the molar absorptivities of compounds **7j** and **6a** were determined in pH 7.1 phosphate buffer (0.05 M, I = 0.11 M) containing 0.11% formaldehyde by first dissolving a known amount of either compound in acetonitrile (n = 5). An aliquot (1 ml) of the acetonitrile solution was removed, diluted with buffer, and analyzed by UV spectrophotometry to obtain the molar absorptivities shown in Table 4-2. Because there is considerable overlap between the UV spectra of APAP and its AOCOM prodrugs **7i-m**, the relative concentrations of each were determined using the following approach. The differences in absorption were found to be greatest at 240 nm and at 280 nm. Therefore, considering the additive nature of absorption, the absorbance at each wavelength (assuming constant cell length) is

$$A_{240} = \varepsilon_{P240}C_P + \varepsilon_{A240}C_A \quad (5)$$

$$A_{280} = \varepsilon_{P280}C_P + \varepsilon_{A280}C_A \quad (6)$$

where A is the absorbance at the respective wavelengths, ε is the molar absorptivity of either the prodrug (P) or APAP (A) at the respective wavelengths, and C is the concentration of the respective compounds in the mixture. Solving the two simultaneous equations gives the following solution for the prodrug concentration C_P

$$C_P = (\varepsilon_{A280}A_{240} - \varepsilon_{A240}A_{280}) / (\varepsilon_{A280}\varepsilon_{P240} - \varepsilon_{A240}\varepsilon_{P280}) \quad (7)$$

Once C_P is known, it may be inserted into equation 5 to give the following solution for the concentration of APAP C_A:

$$C_A = (A_{240} - \varepsilon_{P240}C_P) / \varepsilon_{A240} \quad (8)$$

Solubility parameters. Solubility parameters were calculated by the method of Fedors[110] as demonstrated by Martin and coworkers[111] and Sloan and coworkers.[112]

Diffusion cell experiments

The flux of each prodrug was measured using skin samples from three different mice. Prior to skin removal, the mice were rendered unconscious by CO2 then sacrificed via cervical dislocation. Skins were removed by blunt dissection and placed dermal side down in contact with pH 7.1 phosphate buffer (0.05 M, I = 0.11 M, 32 ^{o}C) containing 0.11% formaldehyde (2.7 ml of 36% aqueous formaldehyde/liter) to inhibit microbial growth and maintain the integrity of the skins[113] throughout the experiment. A rubber O-ring was placed on top of the skin to ensure a tight seal, and the donor and receiver compartments were fastened together with a metal clamp (see Chapter 3, Figure 3-9).

Prior to the application of the prodrug, the skins were kept in contact with buffer for 48 to allow any UV absorbing material to leach out. During this time, the receptor phase was removed and replaced with buffer 3 times in order to facilitate the leaching

process. Twenty four hours before application of the prodrug, a suspension (0.095 M to 0.664 M, i.e. generally 10 × SIPM) of the prodrug in IPM was prepared and allowed to mix until it was needed in the diffusion cell experiments. After the 48 hour leaching period, an aliquot (0.5 ml) of the prodrug suspension was added to the surface of the skin (donor phase). Samples of the receptor phase were usually taken at 8, 19, 22, 25, 28, 31, 34, and 48 h and quickly analyzed by UV spectrophotometry (Table 4-2; equations 7 and 8) to determine the amounts of permeated APAP and prodrug. At each sampling time, the entire receptor phase was replaced with fresh buffer in order to maintain sink conditions.

After the 48 h of the first application period, the donor suspension was removed and the skins were washed three times with methanol (3-5 ml) to remove any residual prodrug from the surface of the skin. The skins were kept in contact with buffer for an additional 24 h to allow all APAP species (i.e. APAP and prodrug) to leach from the skin. Following this second leaching period, the receptor phase was replaced with fresh buffer and an aliquot (0.5 ml) of a standard drug/vehicle (theophylline/propylene glycol) was applied to the skin surface: the second application period. Samples of the receptor phase were taken at 1, 2, 3, and 4 h and analyzed by UV spectrophotometry. The concentration of theophylline in the receptor phase was determined by measuring its absorbance at 270 nm (ε = 10,200 L mol-1). At each sampling time, the entire receptor phase was removed and replaced with fresh buffer.

In each experiment, the flux was determined by plotting the cumulative amount of APAP species (APAP plus prodrug) against time as shown by the example in Figure 4-7.

Flux could then be calculated by dividing the slope of the steady-state portion of the graph by the surface area of the skin (4.9 cm2).

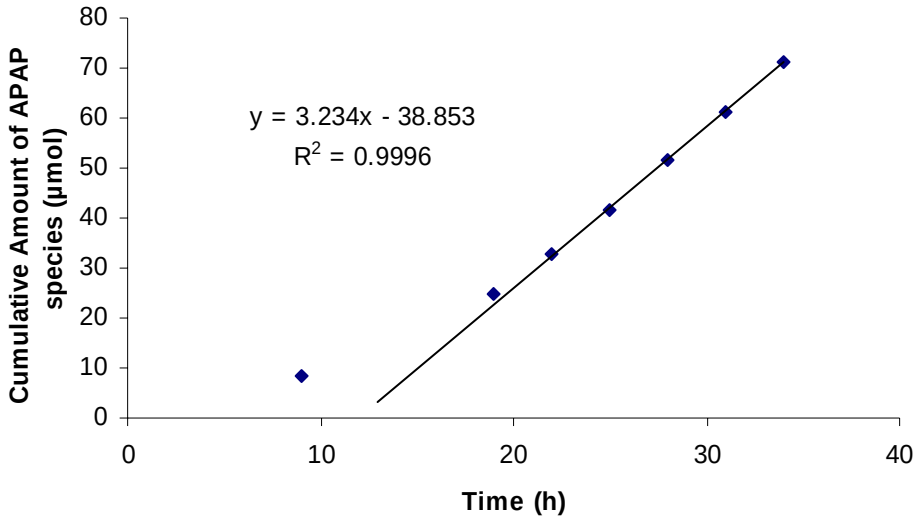

Figure 4-7: Flux of Compound **7j** through Hairless Mouse Skin

Results and Discussion

Physicochemical properties

The solubilities in IPM (S_{IPM}) and in water (S_{AQ}) for prodrugs **7i-m** are listed in Table 4-3. The relative standard deviations of the S_{IPM} and S_{AQ} values were all $\leq \pm 5\%$ except for the S_{AQ} value for **7l** which was ± 11%. As expected, all of the AOCOM prodrugs exhibited lower melting points than APAP and were more soluble in IPM than APAP. There was a steady increase in S_{IPM} on going from the first to the last member of the series, with the last member of the series (C10) exhibiting the greatest increase (68-fold) in S_{IPM} over APAP. As seen in the alkyloxycarbonyloxy (AOC)[45] and alkylcarbonyloxymethyl (ACOM, Chapter 3) prodrugs of APAP, all of the AOCOM derivatives were much less soluble in water than APAP. In fact, the most water soluble member of this series, **7j**, exhibited only 0.08-times the S_{AQ} of APAP. In general, the S_{AQ} values decreased along the series except for a slight increase in S_{AQ} on going from

C1 to C2. Interestingly, the present S_{AQ} value for **7j** (C2) is twice as high as the value previously reported by Seki (Table 4-3).[121] Although the reason for this discrepancy is unclear, it must be noted that the S_{AQ} value of 4-ethyloxycarbonyloxyacetanilide **8j** measured by Seki[121] (S_{AQ} = 2.15 mM, 25 °C, 0.01 M phosphate buffer, pH 7.0) is also about one-half the S_{AQ} value measured by others[45] under similar conditions.

Table 4-3**:** Physicochemical Properties of 4-Hydroxyacetanilide **6a**, 4-ACOM-APAP Prodrugs **7a-e**,[a] 4-AOC-APAP Prodrugs **8i-m**,[b] and 4-AOCOM APAP Prodrugs **7i-m**

Compound[c]	**MW**[d]	**mp °C**[e]	$\mathbf{S_{IPM}}^{f, g, h}$	$\mathbf{S_{AQ}}^{f, h, i}$	$\mathbf{S_{4.0}}^{f, j}$	$\mathbf{K_{IPM:4.0}}^{k}$
6a, APAP	151	167-170	1.9[b]	100[b]		
7a, C1	223	95-95	8.41	15.2	16.2	0.519
7b, C2	237	56-59	62.0	24.7	26.6	2.33
7c, C3	251	56-58	73.5	7.12	8.26	8.90
7d, C5	279	50-52	109	0.597	0.90	121
7e, C7	307	53-54	98.7	0.0637	0.048	2077[l]
8i, C1	209	112-115	12.0	20.4	17.0	0.692
8j, C2	223	120-122	9.33	3.80	4.47	2.09
8k, C3	237	104-106	23.4	2.70	3.02	7.94
8l, C4	251	118-120	13.8	0.427	0.447	31.6
8m, C6	279	108-110	16.7	0.0479	0.0324	513
7i, C1	239	104-106	7.93 ± 0.14	7.20 ± 0.14	8.39	0.946 ± 0.022
7j, C2	253	83-85 (74-77)[m]	20.7 ± 1.0	7.76 ± 0.41 (3.72)[n]	7.51	2.76 ± 0.22
7k, C3	267	68-69	45.8 ± 1.5	2.00 ± 0.091	4.97	9.21 ± 0.51
7l, C8	337	64-65	66.4 ± 1.9	0.00440 ± 0.00047	0.029	2720[l]
7m, C10	365	54-56	130 ± 2.4	[o]	0.0062	26500[l]

[a] Data from Chapter 3. [b] Data from reference 45. [c] C1, C2... refer to the length of the alkyl chain. [d] Molecular weight. [e] Melting point (uncorrected). [f] Units of mM. [g] Solubility in isopropyl myristate (IPM). [h] Measured at 23 ± 1 °C. [i] Solubility in water. [j] Solubility in pH 4.0 buffer estimated from $S_{IPM}/K_{IPM:4.0}$. [k] Partition coefficient between IPM and pH 4.0 acetate buffer. [l] Extrapolated from previous $K_{IPM:4.0}$ in the series as described in the text. [m] Previously reported value from reference 121. [n] Value measured at 25 °C in 0.01 M phosphate buffer, pH 7.0 from reference 121. [o] Could not be determined

In order to incorporate the physicochemical property data for **12** to **16** into the Roberts-Sloan database,[20] pH 4.0 buffer was used as the aqueous phase in partition coefficient determinations ($K_{IPM:4.0}$). Partition coefficients obtained in this manner were then used to estimate the solubilities of **7i-m** in pH 4.0 buffer ($S_{4.0}$, Table 4-3). Partition coefficients between IPM and buffer could be determined for all but the last two members of the series. These last two homologs, C8 and C10, exhibited such low solubilities in water that the present method for measuring partition coefficient was not useful. Relative standard deviations for the $K_{IPM:4.0}$ values were all $\leq \pm$ 8%. The average methylene π_K for this series (0.49 ± 0.04) was much lower than the average π_K for the 4-ACOM-APAP series (π_K = 0.60 ± 0.05), but was within the standard deviation of the average π_K for the 4-AOC-APAP series (π_K = 0.55 ± 0.06).[45] While an average π_K of 0.49 is certainly lower than the values typically seen in prodrug series, an even lower value (π_K = 0.44) has been reported[45] for a series of methoxyethyleneoxycarbonyl derivatives of APAP. Thus it seems that the experimental $K_{IPM:4.0}$ values of the present series are reasonably well-behaved. Since the $K_{IPM:4.0}$ values obtained for the first three homologs were reasonable, the average π_K value was used to calculate $K_{IPM:4.0}$ for the last two members of the series (C8 and C10). Use of the solubility ratios $S_{IPM:AQ}$ as a surrogate for partition coefficient resulted in a slightly higher value for the average π_{SR} (0.54 ± 0.14). The estimated solubility in pH 4.0 buffer was somewhat higher than the experimentally determined S_{AQ} in the case of **7i** and somewhat lower in the case of **7j**. For **7k** and **7l**, the values for $S_{4.0}$ were all much higher (2.5 and 5.5-times higher, respectively) than the corresponding values for S_{AQ}.

Table 4-4**:** Log Solubility Ratios (log $SR_{IPM:AQ}$), Differences between Log $SR_{IPM:AQ}$ (π_{SR}), Log Partition Coefficients (log $K_{IPM:4.0}$), Differences between Log $K_{IPM:4.0}$ (π_K), and Solubility Parameters (δ_i) for Prodrugs **7i-m**

Prodrug	log $SR_{IPM:AQ}$[a]	π_{SR}[b]	log $K_{IPM:4.0}$[c]	π_K[d]	δ_i[e]
7i, C1	0.0424		-0.0242		11.87
7j, C2	0.427	0.38	0.441	0.47	11.62
7k, C3	1.36	0.66	0.964	0.52	11.41
7l, C8	4.18	0.56	3.43[f]		10.68
7m, C10			4.42[f]		10.48

[a] Log of the ratio of the solubilities in IPM (S_{IPM}) and water (S_{AQ}). [b] π_{SR} = (log SR_{n+m} - log SR_n)/m; n is the number of methylene units in the promoiety of one prodrug and m is the number of additional methylene units in the promoiety with which it is compared. [c] Log of the partition coefficient between IPM and pH 4.0 buffer. [d] Same definition as in *b* with the exception that log $K_{IPM:4.0}$ is used in place of log $SR_{IPM:AQ}$. [e] Calculated as described in Reference 112 (units = $(cal\ cm^{-3})^{1/2}$. [f] Extrapolated from previous $K_{IPM:4.0}$ in the series as described in the text.

In order to facilitate comparisons between the AOCOM APAP series and other APAP derivatives (Figure 4-8), the relevant physicochemical property data of the 4-AOC-APAP[45] and 4-ACOM APAP series (Chapter 3) has been included in Table 4-3. If comparisons are made between members of the same alkyl chain length (C1 to C3), the AOCOM series is generally more soluble in IPM and less soluble in water than the AOC series. For instance, C2 and C3 AOCOM are 2.2 and 2.0-times, respectively, more soluble in IPM than the corresponding members of the AOC series, while C1 and C3 AOC are 2.8 and 1.4-times, respectively, more soluble in water than the corresponding members of the AOCOM series. If similar comparisons are made between the AOCOM and ACOM series, the C1 to C3 ACOM derivatives exhibit higher solubilities in both water and IPM than the corresponding members of the AOCOM series.

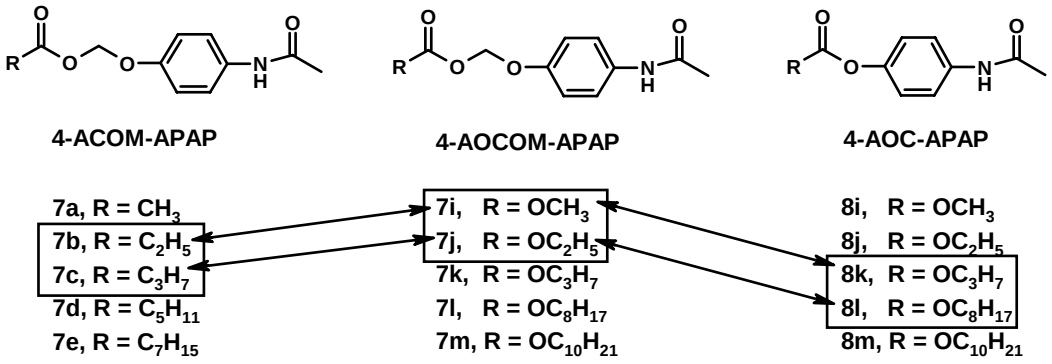

Figure 4-8: Structures of Alkylcarbonyloxymethyl (ACOM) and Alkyloxycarbonyl (AOC) Derivatives of APAP and Comparisons between Homologs of Approximately Equal Size.

If the structural differences between the promoieties are taken into account, slightly different conclusions are reached. Since the AOCOM derivatives contain a CH_2O linker between the phenoxy group of APAP and the carbonyl of the prodrug, the alkyl chain in this series is extended two atoms farther from APAP than members of the same alkyl chain length in the AOC series. Therefore, rather than simply counting the number of methylene units in the alkyl chain, it may be more appropriate to include this two-atom unit in the total chain length when making comparisons between homologs of approximately equal size. Using this rationale, C1 and C2 AOCOM are 2.7 and 18-times, respectively, more soluble in water than the corresponding members of the AOC series (C3 and C4). The differences in S_{IPM} are not as one-sided. In one case the AOC member (C3) is more soluble in IPM (compared to C1 AOCOM), while in the other case the AOCOM member (C2) is more soluble (compared to C4 AOC). This approach may also be used to compare the AOCOM derivatives with the corresponding ACOM derivatives. In this case, C2 and C3 ACOM are 7.8 and 3.6-times more soluble in IPM than the corresponding members of the AOCOM series (C1 and C2). In addition, C2 ACOM is 3.4-times more soluble in water than C1 AOCOM. Based on these results, it appears that

substitution of oxygen for a methylene unit for in the carbonyl group of the prodrug (ACOM → AOCOM) results in a decrease in lipid solubility with little to no improvement in water solubility.

Diffusion cell experiments

Results from the diffusion cell experiments for the 4-AOCOM-APAP prodrugs are listed in Table 4-5. For most of the prodrugs, samples of the receptor phase were taken every 3 h once steady-state flux was established. The exception was compound **7m** in which samples only were taken every 12 h. Unfortunately, only two of the four samples were concentrated enough to be detected using the UV spectrophotometric method described above. As a consequence, the flux value for **7m** listed in Table 4-5 is an estimate of J_M based on the samples taken at 31 and 43 h. Also included in this table are the diffusion cell results from the 4-AOC-APAP[45] and 4-ACOM-APAP (Chapter 3) series. With the exception of **7j** (± 47%) and **7k** (± 32%), the fluxes of **7i-m** were all within the ± 30% variation typically observed[45] in diffusion cell experiments with hairless mice. As a whole, the AOCOM derivatives were not very effective at increasing the transdermal delivery of APAP. In the one case (**7j**) where the flux of the prodrug was greater than that of APAP, the improvement was only marginal (1.3-fold). If the fluxes of members of the same alkyl chain length are compared, the first three homologs of the AOCOM series (C1 to C3) performed worse on average than the corresponding members of the ACOM series (average ratio of fluxes $J_{AOCOM} / J_{ACOM} = 0.44$) but performed better on average than the corresponding members of the AOC series (average ratio of fluxes $J_{AOCOM} / J_{AOC} = 1.7$). If structural differences between the promoieties are taken into account (as in Figure 4-8), the AOCOM series is even more effective at delivering APAP

than the AOC series (average ratio of fluxes $J_{AOCOM} / J_{AOC} = 4.0$), but still less effective than the ACOM series (average ratio of fluxes $J_{AOCOM} / J_{ACOM} = 0.55$).

When the receptor phases from the application of **7i-m** were analyzed during steady-state flux conditions, various percentages of intact prodrug and APAP were found (Table 4-6). The entries in Table 4-6 are from samples taken at 31 h and are representative of percentages of intact prodrug observed at other times during steady-state. Although no effort was made to determine the half-times of **7i-m** in the receptor phase buffer, aqueous stability may be estimated based on the work of others. For example, Seki and coworkers[121] found that **7j** exhibited a half-life of 200 h in pH 7.0 phosphate buffer (0.01 M) at 25 ^{o}C. Thus, under the present experimental conditions it is reasonable to assume that presence of APAP in the receptor phase is due to enzymatic hydrolysis of the prodrugs in the skin and is not the result of chemical hydrolysis in the receptor phase. In that regard, it is important to recognize that the skins were kept in contact with buffer for 48 h prior to application of the prodrugs. During this preapplication period, the enzymatic activity of the skin decreases as hydrolytic enzymes are leached from the skin.[116] Therefore, the extent to which **7i-m** are hydrolyzed in the skin should be greater *in vivo*. In general, the percent of intact prodrug decreased as the alkyl chain length increased. A similar trend was previously observed[45] in the 4-AOC-APAP series (Table 4-6) and in fact should not be surprising based on literature precedent.[130] Given that **7j** is the most permeable member of the series, the relatively high percentage of intact prodrug in this case is likely due to saturation of the esterase system in the skin.

Table 4-5: Flux of Total APAP Species through Hairless Mouse Skin from Suspensions of 4-ACOM-APAP,[a] 4-AOC-APAP,[b] and 4-AOCOM-APAP Prodrugs in IPM (log J_M), Second Application Flux of Theophylline through Hairless Mouse Skin from a Suspension in Propylene Glycol (J_J), Error in Predicting Log J_M using the Roberts-Sloan Equation (Δ log $J_{predicted}$), Error in Calculating Log J_M using the Roberts-Sloan Equation (Δ log $J_{calculated}$) and Ratio of the Flux of the Prodrug to the Flux of APAP ($J_{prodrug}$ / J_{APAP})

Compound	J_M[c]	J_J[c]	log J_M[c]	Δ log $J_{predicted}$[d]	Δ log $J_{predicted}$[e]	Δ log $J_{calculated}$[f]	$J_{prodrug}$ / J_{APAP}
6a, APAP[g]	0.51	0.74	-0.29	-0.496[h]	-0.484[h]	-0.492	
7a, C1	0.730 ± 0.23	0.934 ± 0.14	-0.136	-0.104	-0.091[h]	-0.088	**1.4**
7b, C2	1.86 ± 0.24	0.935 ± 0.076	0.270	-0.213	-0.197[h]	-0.188	**3.6**
7c, C3	0.777 ± 0.20	0.780 ± 0.22	-0.109	-0.350	-0.331[h]	-0.317	**1.5**
7d, C5	0.344 ± 0.062	0.857 ± 0.15	-0.464	-0.254	-0.231[h]	-0.207	0.67
7e, C7	0.110 ± 0.028	0.687 ± 0.15	-0.957	-0.037	-0.0070[h]	0.028	0.22
8i, C1	1.00	1.12	0.00	-0.095[h]	-0.079[h]	-0.074	**2.0**
8j, C2	0.174	0.64	-0.76	-0.482[h]	-0.464[h]	-0.455	0.51
8k, C3	0.355	1.14	-0.45	-0.260[h]	-0.240[h]	-0.226	0.69
8l, C4	0.0977	0.85	-1.01	-0.264[h]	-0.241[h]	-0.221	0.20
8m, C6	0.0324	0.76	-1.49	-0.162[h]	-0.133[h]	-0.103	0.063
7i, C1[i]	0.443 ± 0.051	0.884 ± 0.087	-0.353	-0.096	-0.083	-0.077	0.87
7j, C2[i]	0.660 ± 0.31	1.12 ± 0.43	-0.181	-0.117	-0.103	-0.094	**1.3**
7k, C3[i]	0.283 ± 0.091	1.12 ± 0.26	-0.549	-0.342	-0.323	-0.305	0.55
7l, C8[i]	0.0211 ± 0.0018	1.03 ± 0.0056	-1.67	-0.088	-0.056	-0.014	0.041
7m, C10[i]	0.00739 ± 0.00018	0.713 ± 0.059	-2.13	-0.313	-0.277	-0.227	0.014
Control[j]		1.02 ± 0.13[k]					

[a] From Chapter 3. [b] From Reference 45. [c] Units of µmol cm^{-2} h^{-1}. [d] Predicted from equation 10 (coefficients from n = 61 database, Reference 45, were recalculated using SAS 8.1). Error in prediction = log J_M – log $J_{predicted}$. [e] Predicted from equation 11 (n = 61 + 4-ACOM-APAP (Chapter 3, n = 5) to give a database of n = 66 compounds). Error in prediction = log J_M – log $J_{predicted}$. [f] Calculated from equation 12 (n = 61 + 4-ACOM-APAP (n = 5) + present data (n = 5) to give a new database of n = 71 compounds). [g] From Reference 45. [h] Already included in the database, so the value listed here is actually the difference between log J_M and a *calculated* value for flux. [i] Directly measured S_{AQ} values were used in all equations to calculate flux. In the case of **7m**, S_{AQ} was calculated from the average π_{SR} for the series. [j] Skins were sequentially subjected to 48 h conditioning, 48 h contact with IPM, methanol wash, 24 h leaching. [k] From Reference 112.

Apparently, the fluxes of **7i-m** are not artificially high due to damage sustained by the skin over the course of the first application or the leaching periods. This assessment is based on control experiments in which a suspension of theophylline in propylene glycol (Th/PG) was applied to the skin following the removal of the prodrug donor phase. This second application of Th/PG resulted in Th flux values that were not significantly different from those through skins treated with IPM alone (Table 4-5). However, it is important to recognize that IPM is a well-known penetration enhancer which can increase flux 50-fold compared to experiments where water was the vehicle.[118] Although the apparent flux values of **7i-m** are likely inflated due to IPM, this is not expected to change the rank order of flux within or between series.[118]

If skin damage did not influence the rank order of flux, then the rank order of the observed flux is directly related to the rank order of the solubility of the prodrug in the skin (S_{MEM})—a property which must be determined indirectly.[41] Since the stratum corneum is a highly lipophilic membrane,[3] it is commonly believed that percutaneous absorption is directly dependant on lipid solubility (octanol, S_{OCT}, is a typical model)[131] or its surrogate, partition coefficient $K_{OCT:AQ}$.[5, 18, 120] Given the emphasis in the literature on the importance of lipid solubility in governing flux, it was of interest to determine the effect of lipid solubility on the fluxes of **7i-m**. If the fluxes of **7i-m** are normalized by their respective solubilities in IPM, the corresponding permeability coefficients P_M are obtained (Table 4-6). Permeability coefficients P_M will be used in this section instead of J_M since P_M is frequently used in the literature to quantify the permeation efficiency of compounds through skin.[5, 18] For the sake of comparison, P_M of the ACOM and AOC prodrugs of APAP have also been included in Table 4-6. A plot of the log P_M values for

7i-m versus their respective log $K_{IPM:4.0}$ values gave a negative slope (-0.654, $r^2 = 0.987$, plot not shown). These results are consistent with the findings of others[45, 69, 118] and support the idea[20] that lipophilicity alone as defined by $K_{IPM:4.0}$ is not a good predictor of flux. Similarly, a plot of log P_M versus the calculated solubility parameters of **7i-m** gave a positive slope (Figure 4-9), demonstrating an inverse relationship between log P_M and alkyl chain length (i.e. higher S_{IPM}, lower δ_i).

Table 4-6: Percent Intact Prodrug Detected in Receptor Phase during Steady-State (% Intact), Log Permeability Coefficients (log P_M), Concentrations of APAP Species in Skin (C_S), and Dermal/Transdermal Delivery Ratios for 4-ACOM-APAP,[a] 4-AOC-APAP,[b] and 4-AOCOM APAP Prodrugs

Compound	% Intact[c]	log P_M[d]	C_S[e]	D/T[f]
6a, APAP		-0.57	2.74 ± 0.70[g]	0.046
7a, C1	0	-1.06	2.67 ± 0.57	0.031
7b, C2	9	-1.52	13.1 ± 2.1	0.060
7c, C3	0	-1.98	5.56 ± 0.54	0.061
7d, C5	0	-2.50	3.55 ± 1.05	0.088
7e, C7	0	-2.95	2.72 ± 1.55	0.21
8i, C1	64	-1.08	5.45 ± 1.57[g]	0.046
8j, C2	14	-1.73	1.08 ± 0.13[g]	0.053
8k, C3	25	-1.82	2.84 ± 1.44[g]	0.068
8l, C4	0	-2.15	1.91 ± 0.08[g]	0.17
8m, C6	0	-2.71	1.79 ± 0.43[g]	0.47
7i, C1	32	-1.25	2.83 ± 0.62	0.054
7j, C2	46	-1.50	3.03 ± 2.17	0.039
7k, C3	25	-2.21	4.53 ± 1.38	0.14
7l, C8	0	-3.50	1.57 ± 0.37	0.63
7m, C10	0	-4.25	0.825 ± 0.118	0.95

[a] From Chapter 3. [b] From Reference 45. [c] Percent intact prodrug detected in the 31 h receptor phase sample. [d] Calculated from log J_M – log S_{IPM}, units of cm h^{-1}. [e] Amount of total APAP species (in units of μmol) in receptor phase after 24 hours following donor phase removal to allow APAP and prodrug to leach out of skin. [f] Calculated from $D/T = [(C_S/4.9\ cm^2\ 24\ h)]/J_M$. [g] From Reference 119.

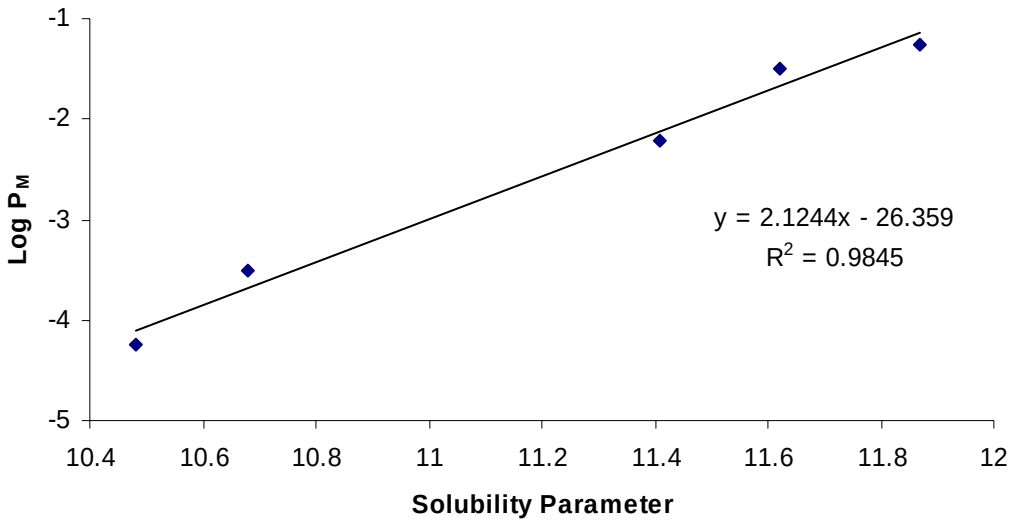

Figure 4-9: Plot of Solubility Parameters versus Log P_M for 4-AOCOM-APAP Prodrugs **7i-m**

If lipid solubility as defined by $K_{IPM:4.0}$ is poorly correlated with skin permeability, then on which physicochemical properties is flux dependant? In order to ascertain the relative impact of solubility in a lipid, solubility in water, and partition coefficient on flux, the trends in S_{IPM}, $S_{4.0}$, $K_{IPM:4.0}$, and J_M for APAP **6a** and its prodrugs (**7a-e**, **8i-m**, and **7i-m**) are graphically represented in Figure 4-10 (a Wasdo plot).[119] The most consistent trend between the series is the steady increase in $K_{IPM:4.0}$ with increasing alkyl chain length. This is spite of the fact the J_M generally decreases along a series. Thus it is clear from the present results that $K_{IPM:4.0}$ is of little positive predictive value in determining the rank order of flux. Similarly, there is no obvious relationship between S_{IPM} and flux as S_{IPM} grows larger along the AOCOM series (**7i-m**), but remains relatively constant along the ACOM (**7a-e**) and AOC (**8i-m**) series. On the other hand, the trends in $S_{4.0}$ generally mirror the trends in flux. Such a relationship should not be surprising as the literature is replete with similar examples.[57, 67, 68, 114-116] Although the

dependence of flux on water solubility is most apparent in homologous series of compounds, such dependence has recently been demonstrated for a large number of unrelated compounds through human skin *in vitro*[46] and for a small set of nonsteroidal anti-inflammatory drugs through human skin *in vivo*.[132] Though water solubility is clearly important, flux is not governed by this property alone. In fact, most quantitative treatments of skin permeation data indicate that lipid solubility is either more important than[42, 46, 132] or is equal in importance[43] to water solubility. This is demonstrated in the present case by the fact that the most permeable compounds in each series (**7b**, **8i**, and **7j**) are those that exhibit the best mixture of high S_{IPM} and high $S_{4.0}$.

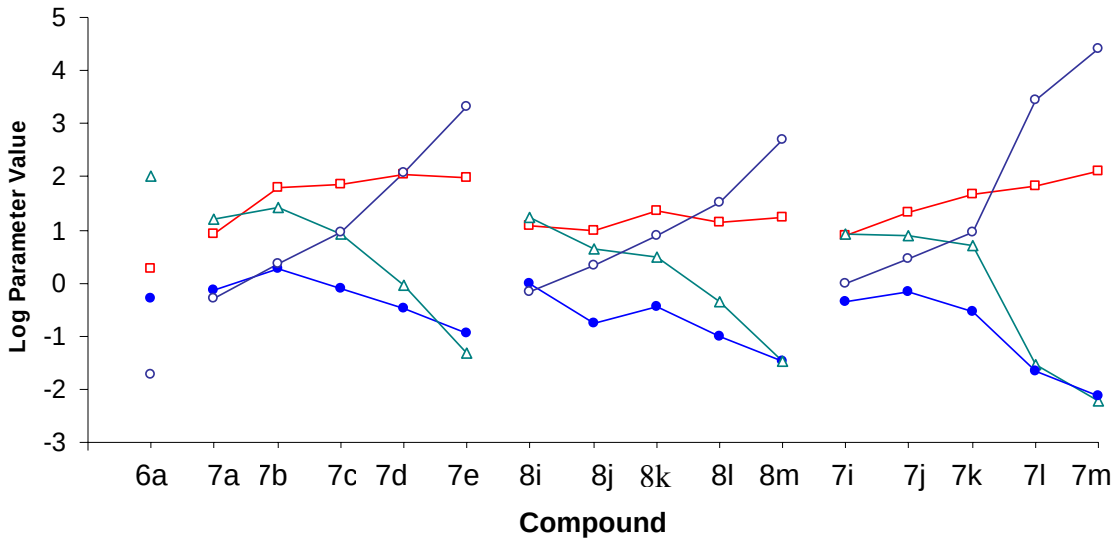

Figure 4-10: Log S_{IPM} (□), Log $S_{4.0}$ (Δ), Log $K_{IPM:4.0}$ (○), and Log J_M (●) Values for APAP **6a**, 4-ACOM-APAP Prodrugs **7a-e**, 4-AOC-APAP Prodrugs **8i-m,** and 4-AOCOM-APAP Prodrugs **7i-m**.

Although it is obvious that flux is positively dependent on lipid and aqueous solubility, the Roberts-Sloan equation (RS, equation 9) is currently the only mathematical model available for quantifying such a relationship (see Chapter 1):

$$\log J_M = x + y \log S_{IPM} + (1 - y) \log S_{4.0} - z\,MW \qquad (9)$$

$$\log J_M = -0.491 + 0.520 \log S_{IPM} + 0.480 \log S_{4.0} - 0.00271\ MW \quad (10)$$

Since it was first introduced in 1999,[43] the database upon which **RS** (originally referred to as the Transformed Potts-Guy model) is based has been modified only once by the addition of 19 new entries to give an extended database of 61 compounds.[45] A fit of that data to the **RS** model gave the form of **RS** expressed by equation 10.[45] Use of equation 10 to predict the fluxes of **7i-m** resulted in flux values ($J_{predicted}$, not shown) that were higher than the experimentally determined values. In particular, the $J_{predicted}$ values for **7k** to **7m** were unusually high. A plot of log J_M versus log $J_{predicted}$ using equation 10 is shown in Figure 4-11. The error in predicting log J_M (Δ log $J_{predicted}$) for **7i**, **7j**, **7k**, **7l**, and **7m** using equation 10 was 0.128, 0.110, 0.532, 0.481, and 0.692 respectively. The average Δ log $J_{predicted}$ for **7i** to **7m** (0.388 ± 0.258 log units) was much higher than the average Δ log $J_{predicted}$ for the entire database (n = 61, 0.154 ± 0.117 log units). In addition, the average Δ log $J_{predicted}$ for **7i** to **7m** was also substantially higher than the average Δ log $J_{predicted}$ obtained for the 4-ACOM-APAP prodrugs **7a** to **7e** (0.192 ± 0.124 log units) using equation 10 (Chapter 3). However, when the measured S_{AQ} values for **7i** to **7m** [S_{AQ} for **7m** (0.00101 mM) was calculated from the average methylene π_{SR} (0.54) for the series] were used in equation 10 instead of their respective estimated $S_{4.0}$ values (Table 4-3), the $J_{predicted}$ values were much closer to the experimental flux values (i.e. lower Δ log $J_{predicted}$, Table 4-5). This improvement in accuracy is apparent in a comparison of Figure 4-11 with a new plot of log J_M versus log $J_{predicted}$ using equation 10 (Figure 4-12). Use of the measured S_{AQ} values for **7i** to **7m** also resulted in an average Δ log $J_{predicted}$ for **7i** to **7m** (0.191 ± 0.125 log units) that was much closer to the average Δ log $J_{predicted}$ for the database as a whole (n = 61). Since **RS** predicts the flux of the

AOCOM compounds (**7i** to **7m**) with greater accuracy when their respective S_{AQ} values are used instead of their $S_{4.0}$ values, the S_{AQ} values for **7i** to **7m** will be used in all subsequent flux equations presented in this thesis.

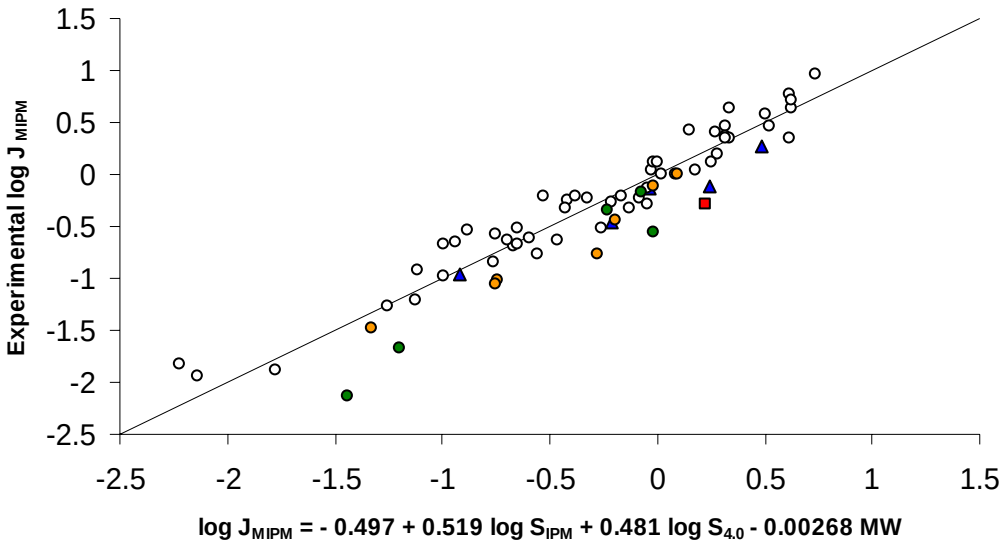

Figure 4-11: Plot of Experimental Versus Calculated Flux for 5-FU, 6-MP, and Th Prodrugs (○, n = 53), APAP (■), 4-AOC-APAP Prodrugs (●, n = 5, plus two additional compounds mentioned in Reference 1 to give n = 7), 4-ACOM-APAP Prodrugs (▲, n = 5), and 4-AOCOM-APAP Prodrugs (●, n = 5)

As discussed in Chapter 3, equation 10 is heavily dependent on data from heterocyclic prodrugs, and therefore lacks a certain structural diversity. It was for this reason that the 4-ACOM-APAP **7a-e** prodrugs were added to the database in Chapter 3. A fit of this new database (now n = 66) to the model gave the form of **RS** expressed by equation 11.

$$\log J_M = -0.545 + 0.511 \log S_{IPM} + 0.489 \log S_{4.0} - 0.00253\ MW \qquad (11)$$

With the incorporation of the 4-ACOM-APAP prodrugs into the database, equation 11 should be able to predict the fluxes of non-heterocyclic compounds with somewhat greater accuracy. This hypothesis was tested by using equation 11 to predict the fluxes of

7i-m. The individual Δ log $J_{predicted}$ values for **6a**, **7a-e**, **8i-m**, and **7i-m** using equation 11 are shown in Table 4-4. Although the experimental fluxes of **7i-m** were all lower than predicted based on equation 11, the average Δ log $J_{predicted}$ for **7i-m** (0.168 ± 0.122 log units) decreased compared to when equation 10 was used.

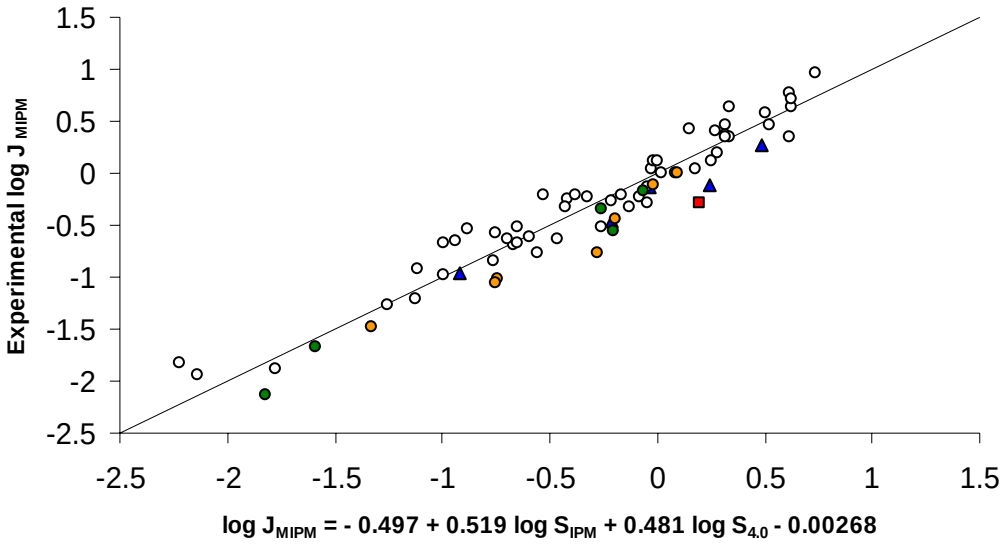

Figure 4-12: Plot of Experimental Versus Calculated Flux for 5-FU, 6-MP, and Th Prodrugs (○, n = 53), APAP (■), 4-AOC-APAP Prodrugs (●, n = 5, plus two additional compounds mentioned in Reference 1 to give n = 7), 4-ACOM-APAP Prodrugs (▲, n = 5), and 4-AOCOM-APAP Prodrugs (●, n = 5). Note: In the 4-AOCOM-APAP series, S_{AQ} has been substituted for $S_{4.0}$

In order to further diversify the database and improve the predictive power of **RS**, the 4-AOCOM-APAP prodrugs **7i-m** were incorporated into the database. A fit of the S_{IPM}, $S_{4.0}$ (again, S_{AQ} is used for **7i-m** instead of $S_{4.0}$), MW, and J_M for the resulting n = 71 entries to equation 9 gave the following estimates for x, y, and z: x = -0.562, y = 0.501, z = 0.00248, r^2 = 0.923:

$$\log J_M = -0.562 + 0.501 \log S_{IPM} + 0.499 \log S_{4.0} - 0.00248\ MW \qquad (12)$$

Equation 12 was then used to calculate J_M for all 71 compounds (data not shown). A plot of J_M versus the calculated flux values is shown in Figure 4-13. The differences between

the experimental and calculated fluxes (Δ log $J_{calculated}$) for APAP **6a** and its prodrugs (**7a-e**, **8i-m**, and **7i-m**) are listed in Table 4-5. As shown in Table 4-5, the Δ log $J_{calculated}$ for **7a-d**, **8i-m**, and **7i-m** decreased with the inclusion of the 4-AOCOM-APAP data. However, the average Δ log $J_{calculated}$ for APAP and its prodrugs (**6a**, **7a-e**, **8i-m**, and **7i-m**; 0.195 ± 0.143 log units) is still higher than the average Δ log $J_{calculated}$ for the database as a whole (0.156 ± 0.117 log units). Although equation 12 was able to predict the fluxes of APAP and its prodrugs with greater accuracy than equations 10 and 11, there was no advantage in using equation 12 to predict the rank order to flux since all three equations predicted the same rank order within each series. Interestingly, although the rank order of flux within the 4-AOC and 4-ACOM-APAP series was predicted with complete accuracy, the rank order of only three of the five 4-AOCOM-APAP compounds was accurately predicted.

In order to determine whether AOCOM prodrugs of phenols would be more effective at delivering the parent compound to the skin (dermal delivery) or through the skin and into the systemic circulation (transdermal delivery), the skins were left in contact with buffer for 24 hours after removing the donor phase to allow APAP and prodrug to leach out. The amount of total APAP species leached from the skin (C_S) is shown in Table 4-6. If the homologs of equal alkyl chain length are compared (C1 to C3), the AOCOM prodrugs are generally more effective than the AOC prodrugs (average $C_{S\ AOCOM} / C_{S\ AOC} = 4.9$), but less effective than the ACOM prodrugs (average $C_{S\ AOCOM} / C_{S\ ACOM} = 0.71$) at increasing the concentration of APAP in the skin. In addition, all but the most lipophilic AOCOM derivatives **7l** and **7m** delivered more APAP to the skin than APAP itself. Using the C_S values as an estimate of the amount of total APAP species

delivered to the skin, dermal/transdermal delivery ratios (Table 4-6) were calculated from equation 13:

$$D/T = [(C_S/4.9\ cm^2\ 24\ h)]/J_M \qquad (13)$$

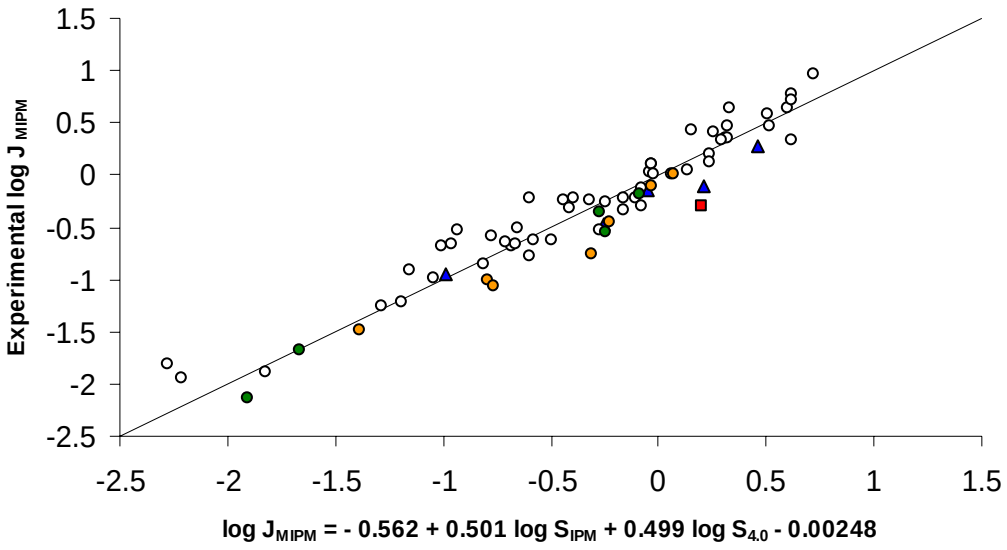

Figure 4-13: Plot of Experimental Versus Calculated Flux for 5-FU, 6-MP, and Th Prodrugs (○, n = 53), APAP (■), 4-AOC-APAP Prodrugs (●, n = 5, plus two additional compounds mentioned in Reference 1 to give n = 7), 4-ACOM-APAP Prodrugs (▲, n = 5), and 4-AOCOM-APAP prodrugs (●, n = 5). Note: In the 4-AOCOM-APAP series, S_{AQ} has been substituted for $S_{4.0}$

Within each series, the derivatives that preferentially delivered more APAP into the skin than through the skin are also the least permeable members of the series. Based on the D/T ratios, the AOCOM C1 to C3 derivatives are on average more effective dermal delivery agents than the corresponding members of the AOC (average $[D/T_{AOCOM}]/[D/T_{AOC}] = 1.3$) and ACOM (average $[D/T_{AOCOM}]/[D/T_{ACOM}] = 1.6$) series. Regardless of the differences between the series, all but two of the derivatives (**7j** and **7a)** delivered more APAP to the skin than topically applied APAP itself.

Conclusions

Although there are numerous reports of the use of prodrugs to improve the topical delivery of phenols,[45, 60-63] all have made exclusive use of the acyl promoiety in which the prodrug is directly attached to the parent phenol through an ester-type bond. Such derivatives frequently exhibit higher melting points and poorer biphasic solubility than the corresponding soft alkyl derivatives. Moreover, the only reported example of an AOCOM derivative of a phenol (compound **7j**) was not evaluated in topical delivery experiments. Thus, the results presented here are significant in that they demonstrate for the first time that AOCOM derivatives of a phenol are capable of improving the topical delivery of the parent compound. While the improvement in flux was marginal (1.3-fold), three out of the five prodrugs tested were more effective at increasing the concentration of APAP in the skin than topically applied APAP itself. Furthermore, all but one of the compounds tested were more effective than APAP at selectively delivering APAP to the skin rather than through it. The AOCOM derivatives of APAP are generally more effective dermal delivery agents than the previously described ACOM derivatives (Chapter 3). Based on these results, AOCOM prodrugs of phenols appear to be best suited for targeted delivery to the skin itself as opposed to the systemic circulation.

CHAPTER 5
CONCLUSIONS AND FUTURE WORK

The main advantages of topical drug delivery over other routes of administration are avoidance of first-pass metabolism, minimal side effects, high incidence of patient compliance, and targeted delivery to the skin for treating local conditions. In order for topical delivery to be effective, the barrier properties of the skin must be overcome in such a way that the skin does not become irreversibly damaged or that local irritation does not limit patient compliance. The rate-limiting barrier to percutaneous absorption is the stratum corneum, and more specifically, it is the intercellular matrix of the stratum corneum that is responsible for limiting diffusion. Electron microscopic analysis of the stratum corneum indicates that the intercellular matrix consists of alternating polar and nonpolar regions. These findings are indirectly supported by numerous skin permeability experiments which show that flux through skin is positively dependant on the aqueous and lipid solubilities of the permeant. In that respect, the Roberts-Sloan model (**RS**) for flux is particularly useful since it allows flux to be predicted based on molecular weight and solubilities in aqueous and lipid solvents.

Prodrug modification has been identified as a useful approach to overcome the skin barrier by transiently improving the biphasic solubility of the active drug. In this thesis, alkylcarbonyloxymethyl (ACOM) and alkyloxycarbonyloxymethyl (AOCOM) promoieties were selected as novel derivatives for improving the topical delivery of phenol-containing drugs based on their successful use in the oral delivery of a wide range of drugs and (in the case of ACOM) the topical delivery of heterocyclic drugs.

Acetaminophen (4-hydroxyacetanilide, APAP) was chosen as a model phenol in order to justify further work on more pharmaceutically interesting phenols.

The first objective of this work was to synthesize a homologous series of ACOM and AOCOM prodrugs of APAP. In the ACOM series, ACOM iodides were synthesized in good yield via a new one-step route. Subsequent reactions between the ACOM iodides and various phenols gave mainly alkylated phenol regardless of the steric hindrance in the ACOM iodide—a finding that contradicted previous assertions that the ACOM iodide must be sterically hindered in order to shift the product distribution in favor of alkylated phenol.[91] A slightly different situation was found in the AOCOM series. Compared to the ACOM series, steric hindrance (as measured by Charton's steric parameters) in the AOCOM iodide was more influential in determining the product distribution—especially when the length of the alkoxy chain was short. However, under phase-transfer conditions the influence of steric hindrance was minimized, reaction time was reduced, and yields of the alkylated product were improved.

Although a potentially useful reaction for synthesizing ACOM iodides was identified, it is currently of little value since its success was dependant upon an unidentified catalyst that was present in older batches of NaI but is absent from newer, purer batches of NaI. A new catalyst system involving $AlCl_3$ and I_2 was identified but was not optimized due to time constraints. In order to make this reaction available for future work, the new catalyst system must be optimized (i.e. determine optimum molar ratios of $AlCl_3$ and I_2). Whether this catalyst system is optimized or not, this does not preclude future work with ACOM derivatives of phenols since the method of Adams[79] is still available for synthesizing the requisite ACOM iodides.

The second objective of this work was to determine whether the ACOM and AOCOM derivatives were capable of improving the topical delivery of APAP. The diffusion cell experiments demonstrate that both types of prodrug are capable of improving the flux of APAP. If comparisons are made between the two series, the ACOM prodrugs are more soluble in water and isopropyl myristate (IPM) than the AOCOM prodrugs. As a consequence, the greatest improvement in flux (4-fold) was by a member of the ACOM series (4-propionyloxymethyloxyacetanilide). Three out of the five members of the ACOM series exhibited higher fluxes than APAP as compared to only one member from the AOCOM series. Although both types of prodrug delivered mainly APAP through the skin, the ACOM series delivered a somewhat greater percentage of APAP (90-100% of total APAP species in receptor phase as APAP) than the AOCOM series (50-100% of total APAP species in receptor phase as APAP). In general, both series delivered more APAP to the skin than topically applied APAP itself.

Although the ACOM and AOCOM prodrugs were capable of improving the topical delivery of APAP, the maximum increase in flux was only 4-fold. Such a modest increase in flux is due to the substantial loss in water solubility that occurs on conversion of APAP to its prodrugs. In order to experience further increases in flux, water solubility must be increased without significantly decreasing lipid solubility.[20] Simple ACOM and AOCOM derivatives are able to improve the lipid (and often aqueous) solubility of a parent compound by eliminating a hydrogen bond donor in the parent, thereby lowering the crystal lattice energy. Lipid solubility may be further increased by extending the alkyl chain, but this only decreases water solubility. Therefore, in order to increase water solubility by an ACOM or AOCOM approach, hydrophilic groups must be incorporated

into the acyl chain. Though there are many ways to proceed with such a strategy, some of the most successful methods for simultaneously improving water and lipid solubility involve incorporating a basic amine into the promoiety.[19, 20]

An interesting series of articles with particular relevance to the present situation was recently published by Rautio and coworkers on alkylcarbonyloxyalkyl derivatives of naproxen (2-(6-methoxy-2-naphthyl)propionic acid, Figure 5-1).[133-135] In the first paper,[133] an acetyloxy group was attached by way of an alkyl linkage to the carboxylic acid portion of naproxen. Though none of the alkylcarbonyloxyalkyl derivatives were as soluble in octanol (S_{OCT}) and pH 7.4 buffer (S_{AQ}) as naproxen, the prodrug that exhibited the best biphasic solubility (the acetyloxyethyl ester, Figure 5-1) also exhibited the highest flux. However, since there was no improvement in aqueous and lipid solubilities when naproxen was converted to its prodrugs, the increase in flux was only 1.9-times higher than the flux of naproxen. In the next two articles,[134, 135] Rautio et. al. incorporated various amino groups into acyl portion of the promoiety in an attempt to improve biphasic solubility. The best results were finally obtained by incorporating methylpiperazine into the acyl chain as shown in Figure 5-1. With this promoiety, S_{OCT} of the derivative (methylpiperazinylacetyloxyethyl ester) was 120-times higher than naproxen, but S_{AQ} was still only 0.49-times the S_{AQ} of naproxen. Even though the S_{AQ} of the methylpiperazinylacetyloxyethyl ester was less than the parent, the S_{AQ} of this derivative was still 830-times higher than the S_{AQ} of the best performing member of the previous series of acetyloxyethyl prodrugs (Figure 5-1). As a consequence, the flux of the methylpiperazinylacetyloxyethyl prodrug was 50-times higher than the flux of naproxen.

Based on the success of Rautio et al. with alkylcarbonyloxyalkyl derivatives of naproxen,[133-135] similar derivatives may be proposed for ACOM and AOCOM prodrugs of phenols as shown in Figure 5-1 (APAP is used as a model). Such derivatives would likely exhibit higher solubilities in water and lipids than the corresponding simple ACOM and AOCOM prodrugs investigated in the present work. In the AOCOM case, an additional methylene unit would likely be required in the alkyl spacer between the methylpiperazine and carbonyl moieties in order to prevent unintentional chemical hydrolysis (see Figure 5-1).[19]

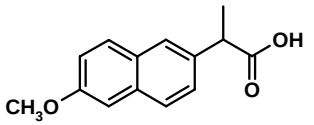

Naproxen

S_{OCT} = 200 mM
S_{AQ} = 100 mM
J_{MAQ} = 0.23 nmol cm^{-2} h^{-1}

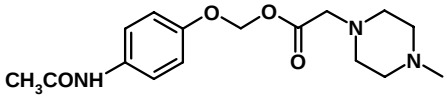

APAP Methylpiperzinylacetyloxymethyl Ether

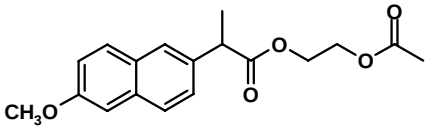

Naproxen Acetyloxyethyl Ester

S_{OCT} = 190 mM
S_{AQ} = 0.06 mM
J_{MAQ} = 0.44 nmol cm^{-2} h^{-1}

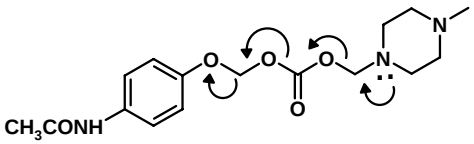

APAP Methylpiperzinylmethyloxycarbonyloxymethyl Ether

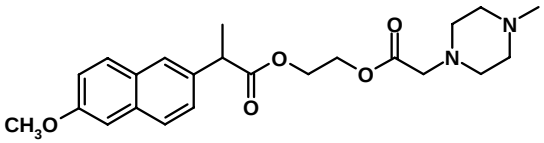

Naproxen Methylpiperazinylacetyloxyethyl Ester

S_{OCT} = 2.5 x 10^{4} mM
S_{AQ} = 50 mM
J_{MAQ} = 13 nmol cm^{-2} h^{-1}

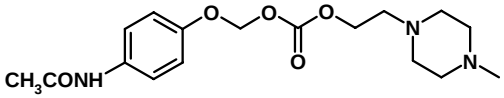

APAP Methylpiperzinylethyloxycarbonyloxymethyl Ether

Figure 5-1: Structures of Naproxen, Naproxen Prodrugs,[133, 135] Proposed Methylpiperazinyl ACOM and AOCOM Prodrugs of APAP, and Potential Mechanism for Hydrolysis of Methylpiperzinylmethyloxycarbonyloxymethyl Ether of APAP

The results from the coupling reactions of ACOM and AOCOM iodides with 2,3,5,7,8-pentamethyl-chroman-6-ol indicate that the corresponding reactions with Vitamin E should favor alkylated phenol. Vitamin E is so lipophilic that it is unlikely that masking its phenolic OH with a simple ACOM or AOCOM promoiety will increase its water solubility and ultimately its flux. On the other hand, an ACOM or AOCOM derivative of Vitamin E should be much more labile than the acetate and succinate esters of Vitamin E that are currently on the market. Therefore, even if the flux of Vitamin E is not improved by a ACOM/AOCOM derivative, the application of such a soft alkyl approach is justified if the *in vivo* conversion of the soft alkyl derivative is higher than the currently available derivatives of Vitamin E. Future work should focus on determining the half-lives of ACOM and AOCOM derivatives of Vitamin E in the skin.

The third objective of this work was to improve the accuracy of the Roberts-Sloan (**RS**) equation for predicting flux through hairless mouse skin. This objective was met by incorporating the physicochemical data and flux values for the ACOM and AOCOM prodrugs into the prodrug database (n = 61) to obtain a new database of 71 compounds. A fit of the solubility, molecular weight, and flux (J_M) values to **RS** gave the following estimates for x, y, and z: x = -0.562, y = 0.501, z = 0.00248, $r^2 = 0.923$:

$$\log J_M = -0.562 + 0.501 \log S_{IPM} + 0.499 \log S_{4.0} - 0.00248\ MW \qquad (1)$$

The previously published **RS** equation[45] based on the n = 61 database is shown below:

$$\log J_M = -0.491 + 0.520 \log S_{IPM} + 0.480 \log S_{4.0} - 0.00271\ MW \qquad (2)$$

The average error in calculating the fluxes ($\Delta \log J_M$) of all 71 compounds using equation 1 (0.15 ± 0.12 log units) was somewhat less than the $\Delta \log J_M$ associated with using equation 2 to calculate the fluxes of all 71 compounds (0.16 ± 0.12 log units). In other

words, the model is only slightly more accurate for the database as a whole when equation 1 is used instead of equation 2. On the other hand, with the incorporation of the ACOM and AOCOM data into the prodrug database, the new model (equation 1) should be able to predict the flux of a wider range of compounds (e.g., nonheterocyclic compounds) with greater accuracy. This is demonstrated by the lower $\Delta \log J_M$ obtained for APAP and its prodrugs (AOC, ACOM, and AOCOM) when equation 1 is used instead of equation 2 (0.19 ± 0.14 log units versus 0.23 ± 0.14 log units). In order to further extend the applicability of **RS** to a wider range of drugs, more nonheterocyclic compounds need to be added to the database.

LIST OF REFERENCES

1. Waterbeemd, H.; Smith, D.; Beaumont, K.; Walker, D., Property-Based Design: Optimization of Drug Absorption and Pharmacokinetics. *J. Med. Chem.* **2001,** 44, (9), 1313-1333.

2. Beaumont, K.; Webster, R.; Gardner, I.; Dack, K., Design of Ester Prodrugs to Enhance Oral Absorption of Poorly Permeable Compounds: Challenges to the Drug Discovery Scientist. *Curr. Drug Metab.* **2003,** 4, 461-485.

3. Schaefer, H.; Redelmeier, T., *Skin Barrier: Principles of Percutaneous Absorption*. S. Karger: Basel, 1996.

4. Swanson, H., Cytochrome P450 Expression in Human Keratinocytes: an Aryl Hydrocarbon Receptor Perspective. *Chem-Biol. Interact.* **2004,** 149, 69-79.

5. Williams, A., *Transdermal and Topical Drug Delivery*. Pharmaceutical Press: London, 2003.

6. Pham, M.; Magdalou, J.; Totis, M.; Fournel-Gigleux, S.; Siest, G.; Hammock, B., Characterization of Distinct Forms of Cytochromes P-450, Epoxide Metabolizing Enzymes, and UDP-Glucuronosyltransferases in Rat Skin. *Biochem. Pharmacol.* **1989,** 38, (13), 2187-2194.

7. Bashir, S.; Maibach, H., Cutaneous Metabolism of Xenobiotics. In *Percutaneous Absorption: Drugs--Cosmetics--Mechanisms--Methodology*, 4th ed.; Bronaugh, R.; Maibach, H., Eds. Taylor and Francis: Boca Raton, 2005; pp 51-63.

8. Madison, K., Barrier Function of the Skin: "La Raison d'Etre" of the Epidermis. *J. Invest. Dermatol.* **2003,** 121, (2), 231-241.

9. Prausnitz, M.; Mitragotri, S.; Langer, R., Current Status and Future Potential of Transdermal Drug Delivery. *Nat. Rev. Drug Discovery* **2004,** 3, 115-124.

10. O'Sullivan, A.; Crampton, L.; Freund, J.; Ho, K., The Route of Estrogen Replacement Therapy Confers Divergent Effects on Substrate Oxidation and Body Composition in Postmenopausal Women. *J. Clin. Invest.* **1998,** 102, 1035-1040.

11. Vongpatanasin, W.; Tuncel, M.; Wang, Z.; Arbique, D.; Mehrad, B.; Jialal, I., Differential Effects of Oral versus Transdermal Estrogen Replacement Therapy on C-Reactive Protein in Postmenopausal Women. *J. Am. Coll. Cardiol.* **2003,** 41, (8), 1358-1363.

13. Eilertsen, A.; Hoibraaten, E.; Os, I.; Anderson, T.; Sandvik, L.; Sandset, P., The Effects of Oral and Transdermal Hormone Replacement Therapy on C-reactive Protein Levels and other Inflammatory Markers in Women with High Risk of Thrombosis. *Maturitas* **2005,** 52, 111-118.

14. Ridker, P.; Hennekens, C.; Buring, J.; Rifai, N., C-Reactive Protein and other Markers of Inflammation in the Prediction of Cardiovascular Disease in Women. *N. Engl. J. Med.* **2000,** 342, 836-843.

15. Helton, D.; Osborne, D.; Pierson, S.; Buonarati, M.; Bethem, R., Pharmacokinetic Profiles in Rats After Intravenous, Oral, or Dermal Administration of Dapsone. *Drug Metab. Dispos.* **2000,** 28, (8), 925-929.

16. Carter, E.; Elewski, B.; Sharata, H.; Rafal, E., Dapsone Gel 5 % is an Effective, Safe, and Novel Topical Treatment of Acne Vulgaris: First of 2 Controlled, Parallel-Design Studies (DAP0203). *J. Am. Acad. Dermatol.* **2006,** 54, (3), AB26-AB26 Suppl. S.

17. Pieters, F.; J., Z., The Absolute Oral Bioavailability of Dapsone in Dogs and Humans. *Int. J. Clin. Pharmacol. Ther. Toxicol.* **1987,** 25, 396-400.

18. Hadgraft, J.; Guy, R., Feasibility Assesment in Topical and Transdermal Delivery: Mathematical Models and In Vitro Studies. In *Transdermal Drug Delivery*, 2 ed.; Hadgraft, J.; Guy, R., Eds. Marcel Dekker: New York, 2003; pp 1-23.

19. Sloan, K. B., Functional Group Considerations in the Development of Prodrug Approaches to Solving Topical Delivery Problems. In *Prodrugs: Topical and Ocular Drug Delivery*, Sloan, K. B., Ed. Marcel Dekker: New York, 1992; pp 17-116.

20. Sloan, K. B.; Wasdo, S., Designing for Topical Delivery: Prodrugs Can Make the Difference. *Med. Res. Rev.* **2003,** 23, 763-793.

21. Skin and the Integumentary System. In *Hole's Human Anatomy and Physiology*, Shier, D.; Butler, J.; Lewis, R., Eds. McGraw-Hill: Boston, 1999; pp 160-183.

22. Menon, G. K., New Insights Into Skin Structure: Scratching the Surface. *Adv. Drug Delivery Rev.* **2002,** 54, (Suppl. 1), S3-S17.

23. Wertz, P.; Downing, D., Glycolipids in Mammalian Epidermis: Structure and Function in the Water Barrier. *Science* **1982,** 217, 1261-1262.

24. Madison, K. C.; Swartzendruber, D. C.; Wertz, P. W.; Downing, D. T., Presence of Intact Intercellular Lipid Lamellae in the Upper Layers of the Stratum Corneum. *J. Invest. Dermatol.* **1987,** 88, (6), 714-718.

25. Potts, R. O.; Francoeur, M., The Influence of Stratum Corneum Morphology on Water Permeability. *J. Invest. Dermatol.* **1991,** 96, (4), 495-499.

26. Hou, S. Y. E.; Mitra, A.; White, S.; Menon, G. K.; Ghadially, R.; Elias, P. M., Membrane Structures in Normal and Essential Fatty Acid-Deficient Stratum Corneum: Characterization by Ruthenium Tetroxide Staining and X-Ray Diffraction. *J. Invest. Dermatol.* **1991,** 96, (2), 215-223.

27. Martin, R.; Denyer, S.; Hadgraft, J., Skin Metabolism of Topically Applied Compounds. *Int. J. Pharm.* **1987,** 39, 23-32.

28. Kao, J.; Carver, M., Cutaneous Metabolism of Xenobiotics. *Drug Metab. Rev.* **1990,** 22, (4), 363-410.

29. Thiebaut, F.; Tsuruo, T.; Hamada, H.; Gottesman, M.; Pastan, I.; Willingham, M., Cellular Localization of the Multidrug-Resistance Gene Product P-Glycoprotein in Normal Human Tissues. *Proc. Natl. Acad. Sci. U S A* **1987,** 84, 7735-7738.

30. Baron, J. M.; Holler, D.; Schiffer, R.; Frankenberg, S.; Neis, M.; Merk, H. F.; Jugert, F. K., Expression of multiple cytochrome p450 enzymes and multidrug resistance-associated transport proteins in human skin keratinocytes. *J Invest Dermatol* **2001,** 116, (4), 541-8.

31. Merk, H. F.; Abel, J.; Baron, J. M.; Krutmann, J., Molecular Pathways in Dermatotoxicology. *Toxicol. Appl. Pharmacol.* **2004,** 195, 267-277.

32. Randolph, G. J.; Beaulieu, S.; Pope, M.; Sugawara, I.; Hoffman, L.; Steinman, R. M.; Muller, W. A., A physiologic function for p-glycoprotein (MDR-1) during the migration of dendritic cells from skin via afferent lymphatic vessels. *Proc Natl Acad Sci U S A* **1998,** 95, (12), 6924-9.

33. Li, Q.; Kato, Y.; Sai, Y.; Imai, T.; Tsuji, A., Multidrug Resistance-Associated Protein 1 Functions as an Efflux Pump of Xenobiotics in the Skin. *Pharm. Res.* **2005,** 22, (6), 842-846.

34. Bronaugh, R.; Maibach, H., *Percutaneous Absorption: Drugs--Cosmetics--Mechanisms--Methodology*. 4th ed.; Taylor and Francis: Boca Raton, 2005.

35. Banga, A.; Bose, S.; Ghosh, T., Iontophoresis and Electroporation: Comparisons and Contrasts. *Int. J. Pharm.* **1999,** 179, 1-19.

36. Williams, A.; Barry, B., Penetration Enhancers. *Adv. Drug Delivery Rev.* **2004,** 56, 603-618.

37. Prausnitz, M., Microneedles for Transdermal Drug Delivery. *Adv. Drug Delivery Rev.* **2004,** 56, 581-587.

38. Sloan, K. B.; Wasdo, S., The Role of Prodrugs in Penetration Enhancement. In *Percutaneous Penetration Enhancers*, 2nd ed.; Smith, E.; Maibach, H., Eds. Taylor and Francis: Boca Raton, 2006; pp 51-64.

39. Waranis, R. P.; Sloan, K. B., Effects of Vehicles and Prodrug Properties on the Delivery of 6-Mercaptopurine Through Skin: Bisacyloxymethyl-6-mercaptopurine Prodrugs. *J. Pharm. Sci.* **1987,** 76, 587-595.

40. Flynn, G. L., Physicochemical Determinants of Skin Absorption. In *Principles of Route-to-Route Extrapolation for Risk Assessment*, Gerrity, T.; Henry, C., Eds. Elsevier: New York, 1990; pp 93-127.

41. Kasting, G. B.; Smith, R. L.; Cooper, E. R., Effect of Lipid Solubility and Molecular Size on Percutaneous Absorption. In *Skin Pharmokinetics*, Shroot, B.; Schaefer, H., Eds. Karger: Basel, 1987; Vol. 1, pp 138-153.

42. Potts, R.; Guy, R., Predicting Skin Permeability. *Pharm. Res.* **1992,** 9, (5), 663-669.

43. Roberts, W.; Sloan, K. B., Correlation of Aqueous and Lipid Solubilities with Flux for Prodrugs of 5-Fluorouracil, Theophylline and 6-Mercaptopurine: A Potts-Guy Approach. *J. Pharm. Sci.* **1999,** 88, 515-532.

44. van Hal, D. A.; Jeremiasse, E.; Junginger, H. E.; Spies, F.; Bouwstra, J., Structure of Fully Hydrated Human Stratum Corneum: A Freeze-Fracture Electron Microscopy Study. *J. Invest. Dermatol.* **1996,** 106, (1), 89-95.

45. Wasdo, S. C.; Sloan, K. B., Topical Delivery of a Model Phenolic Drug: Alkyloxycarbonyl Prodrugs of Acetaminophen. *Pharm. Res.* **2004,** 21, (6).

46. Majumdar, S.; Thomas, J.; Wasdo, S.; Sloan, K. B., The Effect of Water Solubility of Solutes on their Flux through Human Skin: the Extended and Edited Flynn Database. *AAPS J.* **2004,** 6, (S1), W4250.

47. Billich, A.; Vyplel, H.; Grassberger, M.; Schmook, F.; Steck, A.; Stuetz, A., Novel Cyclosporin Derivatives Featuring Enhanced Skin Penetration Despite Increased Molecular Weight. *Bioorg. Med. Chem.* **2005,** 13, 3157-3167.

48. Ettmayer, P.; Amidon, G.; Clement, B.; Testa, B., Lessons Learned from Marketed and Investigational Prodrugs. *J. Med. Chem.* **2004,** 47, (10), 2393-2404.

49. Anderson, R.; Kudlacek, P.; Clemens, D., Sulfation of Minoxidil by Multiple Human Cytosolic Sulfotransferases. *Chem. Biol. Interact.* **1998,** 109, 53-67.

50. Messenger, A.; Rundegren, J., Minoxidil: Mechanisms of Action on Hair Growth. *Br. J. Dermatol.* **2004,** 150, 186-194.

51. Buhl, A.; Baker, C.; Dietz, A., Minoxidil Sulfotransferase Activity Influences the Efficacy of Rogaine Topical Solution (TS): Enzyme Studies using Scalp and Platelets. *J. Invest. Dermatol.* **1994,** 102, 534.

52. Testa, B., Prodrug Research: Futile or Fertile. *Biochem. Pharmacol.* **2004,** 68, 2097-2106.

53. Moss, G.; Gullick, D.; Cox, P.; Alexander, C.; Ingram, M.; Smart, J.; Pugh, W., Design, Synthesis, and Characterization of Captopril Prodrugs for Enhanced Percutaneous Absorption. *J. Pharm. Phamacol.* **2006,** 58, 167-177.

54. Milosovich, S.; Hussain, A.; Dittert, L.; Aungst, B.; Hussain, M., Testosteronyl-4-dimethylaminobutyrate HCl: A Prodrug with Improved Skin Penetration Rate. *J. Pharm. Sci.* **1993,** 82, (2), 227-228.

55. Smith, M.; March, J., Aliphatic Nucleophilic Substitution. In *March's Advanced Organic Chemistry: Reactions, Mechanisms, and Structure*, 5th ed.; Smith, M.; March, J., Eds. John Wiley and Sons: New York, 2001; pp 389-675.

56. Sloan, K. B.; Hashida, M.; Alexander, J.; Bodor, N.; Higuchi, T., Prodrugs of 6-Thiopurines: Enhanced Delivery Through the Skin. *J. Pharm. Sci.* **1983,** 72, (4), 372-377.

57. Kerr, D.; Roberts, W.; Tebbett, I.; Sloan, K. B., 7-Alkylcarbonyloxymethyl Prodrugs of Theophylline: Topical Delivery of Theophylline. *Int. J. Pharm.* **1998,** 167, 37-48.

58. Sloan, K. B.; Bodor, N., Hydroxymethyl and Acyloxymethyl Prodrugs of Theophylline: Enhanced Delivery of Polar Drugs Through Skin. *Int. J. Pharm.* **1982,** 12, 299-313.

59. Ehrnebo, M.; Nilsson, S.; Boreus, L., Pharmacokinetics of Ampicillin and its Prodrugs Bacampicillin and Pivampicillin in Man. *J. Pharmacokinet. Biopharm.* **1979,** 7, (5), 429-451.

60. Drustrup, J.; Fullerton, A.; Christrup, L.; Bundgaard, H., Utilization of Prodrugs to Enhance the Transdermal Absorption of Morphine. *Int. J. Pharm.* **1991,** 71, 105-116.

61. Hansen, L. B.; Fullerton, A.; Christrup, L.; Bundgaard, H., Enhanced Transdermal Delivery of Ketobemidone with Prodrugs. *Int. J. Pharm.* **1992,** 84, 253-260.

62. Stinchcomb, A. L.; Paliwal, A.; Dua, R.; Imoto, H.; Woodard, R. W.; Flynn, G. L., Permeation of Buprenorphine and Its 3-Alkyl-Ester Prodrugs through Human Skin. *Pharm. Res.* **1996,** 13, (10), 1519-1523.

63. Sung, K. C.; Fang, J.; Hu, O. Y., Delivery of Nalbuphine and its Prodrugs Across Skin by Passive Diffusion and Iontophoresis. *J. Control. Rel.* **2000,** 67, 1-8.

64. Stinchcomb, A. L.; Swaan, P.; Ekabo, O.; Harris, K.; Browe, J.; Hammell, D.; Cooperman, T.; Pearsall, M., Straight-Chain Naltrexone Ester Prodrugs: Diffusion and Concurrent Esterase Biotransformation in Human Skin. *J. Pharm. Sci.* **2002,** 91, (12), 2571-2578.

65. Pillai, O.; Hamad, M.; Crooks, P.; Stinchcomb, A. L., Physicochemical Evaluation, *in Vitro* Human Skin Diffusion, and Concurrent Biotransformation of 3-O-Alkyl Carbonate Prodrugs of Naltrexone. *Pharm Res* **2004,** 21, (7), 1146-1152.

66. Beall, H. D.; Sloan, K. B., Transdermal Delivery of 5-fluorouracil (5-FU) through Hairless Mouse Skin by 1-Alkylcarbonyl-5-FU Prodrugs. *Int. J. Pharm.* **1996,** 129, 203-210.

67. Taylor, H. E.; Sloan, K. B., 1-Alkylcarbonyloxymethyl Prodrugs of 5-Fluorouracil (5-FU): Synthesis, Physicochemical Properties, and Topical Delivery. *J. Pharm. Sci.* **1998,** 87, (1), 15-20.

68. Beall, H. D.; Sloan, K. B., Topical Delivery of 5-Fluorouracil (5-FU) by 3-Alkylcarbonyl-5-FU Prodrugs. *Int. J. Pharm.* **2001,** 217, 127-137.

69. Roberts, W.; Sloan, K. B., Topical Delivery of 5-Fluorouracil (5-FU) by 3-Alkylcarbonyloxymethyl-5-FU Prodrugs. *J. Pharm. Sci.* **2003,** 92, 1028-1036.

70. Pinnell, S., Cutaneous Photodamage, Oxidative Stress, and Topical Antioxidant Protection. *J. Am. Acad. Dermatol.* **2003,** 48, (1), 1-19.

71. Fuchs, J.; Kern, H., Modulation of UV-Light-Induced Skin Inflammation by alpha-Tocopherol and L-Ascorbic Acid: A Clinical Study Using Solar Simulated Radiation. *Free Radical Bio. Med.* **1998,** 25, (9), 1006-1012.

72. Mireles-Rocha, H.; Galindo, I.; Huerta, M.; Trujillo-Hernadez, B.; Elizalde, A.; Cortes-Franco, R., UVB Photoprotection with Antioxidants: Effects of Oral Therapy with d-alpha-Tocopherol and Ascorbic Acid on the Minimal Erythema Dose. *Acta Derm-Venereol.* **2002,** 82, (1), 21-24.

73. Alade, S.; Brown, R.; Paquet, A., Polysorbate-80 and E-Ferol Toxicity. *Pediatrics* **1986,** 77, (4), 593-597.

74. Windholz, M., *The Merck Index: An Encyclopedia of Chemicals, Drugs, and Biologicals*. 10th ed.; Merck & CO.: Rahway, 1983.

75. Pedraz, J.; Calvo, B.; Bortolotti, A.; Celardo, A.; Bonati, M., Bioavailability of Intramuscular Vitamin-E Acetate in Rabbits. *J. Pharm. Phamacol.* **1989,** 41, (6), 415-417.

76. Jansen, A. B. A.; Russell, T. J., Some Novel Penicillin Derivatives. *J. Chem. Soc.* **1965**, 2127-2131.

77. Binderup, E.; Hansen, E. T., Chlorosulfates as Reagents in the Synthesis of Carboxylic Acid Esters Under Phase-Transfer Conditions. *Synth. Commun.* **1984,** 14, (9), 857-864.

78. Harada, N.; Hongu, M.; Tanaka, T.; Kawaguchi, T.; Hashiyama, T.; Tsujihara, K., A Simple Preparation of Chloromethyl Esters of the Blocked Amino Acids. *Synth. Commun.* **1994,** 24, (6), 767-772.

79. Adams, R.; Vollweiler, E. H., The Reaction Between Acid Halides and Aldehydes. I. *J. Am. Chem. Soc.* **1918,** 40, 1732-1746.

80. Ulich, L. H.; Adams, R., The Reaction Between Acid Halides and Aldehydes. III. *J. Am. Chem. Soc.* **1921,** 43, 660-667.

81. Iyer, R.; Yu, D.; Ho, N.; Agrawal, S., Synthesis of Iodoalkylacylates and their use in the Preparation of *S*-Alkyl Phosphorothiolates. *Synth. Commun.* **1995,** 25, (18), 2739-2749.

82. Fleischmann, K.; Adam, F.; Durckheimer, W.; Hertzsch, W.; Horlein, R.; Jendralla, H.; Lefebvre, C.; Mackiewicz, P.; Roul, J.; Wollmann, T., Synthesis of HR 916 B: The First Technically Feasible Route to the 1-(pivaloyloxy)ethyl Esters of Cephalosporins. *Liebigs Ann.* **1996,** 11, 1735-1741.

83. Taylor, H. E. Bioreversible Derivatives of 5-Fluorouracil: The Synthesis and Evaluation of a Series of 1-Alkylcarbonyloxymethyl-5-fluorouracil Derivatives. University of Florida, Gainesville, 1997.

84. Folkmann, M.; Lund, F., Acyloxymethyl Carbonochloridates. New Intermediates in Prodrug Synthesis. *Synthesis* **1990,** 12, 1159-1166.

85. Burness, D. M.; Wright, C. J.; Perkins, W. C., Bis(methylsulfonoxymethyl) Ether. *J. Org. Chem.* **1977,** 42, (17), 2910-2913.

86. French, H. E.; Adams, R., The Reaction Bewteen Acid Halides and Aldehydes. II. *J. Am. Chem. Soc.* **1921,** 43, 651-659.

87. Bhar, S.; Ranu, B. C., Zinc-Promoted Selective Cleavage of Ethers in Presence of Acyl Chloride. *J. Org. Chem.* **1995,** 60, 745-747.

88. Balme, G.; Gore, J., Conversion of Acetals and Ketals to Carbonyl Compounds Promoted by Titanium Tetrachloride. *J. Org. Chem.* **1983,** 48, 3336-3338.

89. Sloan, K. B.; Koch, S., Effect of Nucleophilicity and Leaving Group Ability on the S_N2 Reactions of Amines with (Acyloxy)alkyl alpha-Halides: A Product Distribution Study *J. Org. Chem.* **1983,** 48, 635-640.

90. Sloan, K. B.; Koch, S., Reaction of (Acyloxy)alkyl alpha-Halides with Phenols: Effects of Nucleofugicity and Nucleophilicity on Product Distribution *J. Org. Chem.* **1983,** 48, (21), 3777-3783.

91. Ouyang, H.; Borchardt, R.; Siahaan, T., Steric Hindrance is a Key Factor in the Coupling Reaction of (Acyloxy)Alkyl-alpha-Halides with Phenols to Make a New Promoiety for Prodrugs. *Tet. Lett.* **2002,** 43, 577-579.

92. Bensel, N.; Reymond, M.; Reymond, J., Pivalase Catalytic Antibodies: Towards Abzymatic Activation of Prodrugs. *Chem. Eur. J.* **2001,** 7, (21), 4604-4612.

93. Bundgaard, H.; Klixbull, U.; Falch, E., Prodrugs as Drug Delivery Systems. 44: O-Acyloxymethyl, O-acyl, and N-acyl Salicylamide Derivatives as Possible Prodrugs for Salicylamide. *Int. J. Pharm.* **1986,** 30, 111-121.

94. Charton, M., Steric Effects. I. Esterification and Acid-Catalyzed Hydrolysis of Esters. *J. Am. Chem. Soc.* **1975,** 97, (6), 1552-1556.

95. Charton, M., Steric Effects.7. Additional Steric Constants. *J. Org. Chem.* **1976,** 41, (12), 2217-2220.

96. Charton, M., Steric Effects.13. Composition of the Steric Parameter as a Function of Alkyl Branching. *J. Org. Chem.* **1978,** 43, (21), 3995-4001.

97. Obviously, this is a rough estimation. Since nitrogen and oxygen are smaller than a methylene unit, the v value obtained by this method likely overestimates the true steric parameter for 9.

98. Bundgaard, H.; Rasmussen, G., Prodrugs of Peptides. 9. Bioreversible *N*-alpha-Hydroxalkylation of the Peptide Bond to Effect Protection Against Carboxypeptidase or Other Proteolytic Enzymes. *Pharm. Res.* **1991,** 8, (3), 313-322.

99. Wadsworth, D.; Vinal, R., Reactions of Bis(acetoxymethyl) Ether and Several of Its Aryloxy Analogues. *J. Org. Chem.* **1982,** 47, 1623-1626.

100. Although Sloan and Koch recommend using acetone as a solvent, under those conditions the product mixtures were frequently contaiminated with a substantial amount of 3-hydroxy,3-methyl,2-butanone formed from the aldol condensation of acetone in the presence of base. This problem could be circumvented by using acetonitrile instead. The ratio of 7:8 did not change on going from acetone to acetonitrile.

101. Ramesh, C.; Mahender, G.; Ravindranath, N.; Das, B., A Mild, Highly Selective and Remarkably Easy Procedure for Deprotection of Aromatic Acetates Using Ammonium Acetate as a Neutral Catalyst in Aqueous Medium. *Tetrahedron* **2003,** 59, 1049-1054.

102. Blay, G.; Cardona, M.; Garcia, M.; Pedro, J., A Selective Hydrolysis of Aryl Acetates. *Synthesis* **1989**, 438-439.

103. Kunesch, N.; Miet, C.; Poisson, J., Mild, Rapid, and Selective Deprotection of Acetylated Carbohydrates and Phenols with Guanidine. *Tet. Lett.* **1987,** 28, (31), 3569-3572.

104. Bell, K., Facile Selective Aminolysis of Phenolic Benzoates with 1-Butamine in Benzene. *Tet. Lett.* **1986,** 27, (20), 2263-2264.

105. Chakraborti, A.; Sharma, L.; Sharma, U., A Mild and Chemoselective Method for Deprotection of Acryl Acetates and Benzoates Under Non-hydrolytic Condition. *Tetrahedron* **2001,** 57, 9343-9346.

106. Datta, A.; Hepperle, M.; Georg, G., Selective Deesterification Studies on Taxanes: Simple and Efficient Hydrazinolysis of C-10 and C-13 Ester Functionalities. *J. Org. Chem.* **1995,** 60, 761-763.

107. Roberts, W.; Sloan, K. B., Synthesis of 3-Alkylcarbonyloxymethyl Derivatives of 5-Fluorouracil. *J. Heterocyclic Chem.* **2002,** 39, 905-910.

108. Nagase and Cowokers have used similar procedure for deprotecting 1-Benzyloxycarbonyloxymethyl-5-fluorouracil as described in Chem. Lett., 1988, 1381-1384.

109. Beall, H. D.; Getz, J. J.; Sloan, K. B., The Estimation of Relative Water Solubility for Prodrugs that are Unstable in Water. *Int. J. Pharm.* **1993,** 93, 37-47.

110. Fedors, R. F., A Method for Estimating Both the Solubility Parameters and Molar Volumes of Liquids. *Polym. Eng. Sci.* **1974,** 14, (2), 147-154.

111. Martin, A.; Wu, P. L.; Velasquez, T., Extended Hildebrand Solubility Approach: Sulfonamides in Binary and Ternary Solvents. *J. Pharm. Sci.* **1985,** 74, 277-282.

112. Sloan, K. B.; Koch, S.; Siver, K.; Flowers, F., The Use of Solubility Parameters of Drug and Vehicle to Predict Flux. *J. Invest. Dermatol.* **1986,** 87, 244-252.

113. Sloan, K. B.; Beall, H. D.; Weimar, W. R.; Villaneuva, R., The Effect of Receptor Phase Composition on the Permeability of Hairless Mouse Skin in Diffusion Cell Experiments. *Int. J. Pharm.* **1991,** 73, 97-104.

114. Beall, H. D.; Prankerd, R. J.; Sloan, K. B., Transdermal Delivery of 5-Fluorouracil (5-FU) Through Hairless Mouse Skin by 1-Alkyloxycarbonyl-5-FU Prodrugs: Physicochemical Characterization of Prodrugs and Correlations with Transdermal Delivery. *Int. J. Pharm.* **1994,** 111, 223-233.

115. Sloan, K. B.; Getz, J. J.; Beall, H. D.; Prankerd, R. J., Transdermal Delivery of 5-Fluorouracil (5-FU) Through Hairless Mouse Skin by 1-Alkylaminocarbonyl-5-FU Prodrugs: Physicochemical Characterization of Prodrugs and Correlations with Transdermal Delivery. *Int. J. Pharm.* **1993,** 93, 27-36.

116. Waranis, R. P.; Sloan, K. B., Effects of Vehicles and Prodrug Properties on the Delivery of 6-Mercaptopurine through Skin: S^6-Acyloxymethyl-6-mercaptopurine Prodrugs. *J. Pharm. Sci.* **1988,** 77, 210-215.

117. Bauguess, C. T.; Sadik, F.; Fincher, J. H.; Hartman, C. W., Hydrolysis of Fatty Acid Esters of Acetaminophen in Buffered Pancreatic Lipase Systems I. *J. Pharm. Sci.* **1975,** 64, (1), 117-120.

118. Sloan, K. B.; Wasdo, S.; Ezike-Mkparu, U.; Murray, T.; Nickels, D.; Singh, S.; Shanks, T.; Tovar, J.; Ulmer, K.; Waranis, R. P., Topical Delivery of 5-Fluorouracil and 6-Mercaptopurine by Their Alkylcarbonyloxymethyl Prodrugs from Water: Vehicle Effects on Design of Prodrugs. *Pharm. Res.* **2003,** 20, (4), 639-645.

119. Wasdo, S. Topical Delivery of a Model Phenolic Compound: Alkyloxycarbonyl Prodrugs of Acetaminophen. Ph.D. Dissertation, University of Florida, Gainesville, 2006.

120. Flynn, G. L.; Yalkowsky, S. H., Correlation and prediction of mass transport across membranes. I. Influence of alkyl chain length on flux-determining properties of barrier and diffusant. *J Pharm Sci* **1972,** 61, (6), 838-52.

121. Seki, H.; Kawaguchi, T.; Higuchi, T., Specificity of Esterases and Structure of Prodrug Esters: Reactivity of Various Acylated Acetaminophen Compounds and Acetylaminobenzoated Compounds. *J. Pharm. Sci.* **1988,** 77, (10), 855-860.

122. Alexander, J.; Fromtling, R.; Bland, J.; Pelak, B.; Gilfillan, E., (Acyloxy)alkyl Carbamate Prodrugs of Norfloxacin. *J. Med. Chem.* **1991,** 34, 78-81.

123. Ichikawa, T.; Kitazaki, T.; Matsushita, Y.; Yamada, M.; Hayashi, R.; Yamaguchi, M.; Kiyota, Y.; Okonogi, K.; Itoh, K., Optically Active Antifungal Azoles. XII. Synthesis and Antifungal Activity of the Water-Soluble Prodrugs of 1-[(1*R*,2*R*)-2-(2,4-Difluorophenyl)-2-hydroxy-1-methyl-3-(1*H*-1,2,4-triazol-1-yl)propyl]-3-[4-(1*H*-1-tetrazoyl)phenyl]-2-imidazolidinone. *Chem. Pharm. Bull.* **2001,** 49, (9), 1102-1109.

124. Hoffmann, H. M. R.; Iranshahi, L., Synthesis and CuCN-Promoted Cyanation of Iodoformic Esters. *J. Org. Chem.* **1984,** 49, 1174-1176.

125. Senet, J.; Sennyey, G.; Wooden, G., A Convenient New Route to 1-Haloalkyl Carbonates. *Synthesis* **1988**, (5), 407-410.

126. Dittert, L.; Caldwell, H.; Adams, H.; Irwin, G.; Swintosky, Acetaminophen Prodrugs I: Synthesis, Physicochemical Properties, and Analgesic Activity. *J. Pharm. Sci.* **1968,** 57, (5), 774-780.

127. Charton, M., Steric Effects.9. Substituents at Oxygen in Carbonyl Compounds. *J. Org. Chem.* **1977,** 42, (22), 3531-3535.

128. Wolff, S.; Hoffmann, H., Aflatoxins Revisited:Convergent Synthesis of the ABC-Moiety. *Synthesis* **1988,** 10, 760-763.

129. Merck, E., Zur Kenntnis der Einwirkung von Phosgen bxw Chlorkohlensaure Ester auf p-Aacetylaminophenole und p-Oxyphenylurethane. *Chem. Zentralbl.* **1897,** I, 468-469.

130. Milstien, J. B.; Fife, T. H., Steric Effects in the Acylation of alpha-Chymotrypsin. *Biochemistry* **1969,** 8, (2), 623-627.

131. Kasting, G. B.; Smith, R. L.; Anderson, B. D., Prodrugs for Dermal Delivery: Solubility, Molecular Size, and Functional Group Effects. In *Prodrugs: Topical and Ocular Drug Delivery*, Sloan, K. B., Ed. Marcel Dekker: New York, 1992; pp 142-158.

132. Roberts, W. J.; Sloan, K. B., Application of the Transformed Potts-Guy Equation to In vivo Human Skin Data. *J. Pharm. Sci.* **2001,** 90, (9), 1318-1323.

133. Rautio, J.; Taipale, H.; Gynther, J.; Vepsalainen, J.; Nevalainen, T.; Jarvinen, T., In Vitro Evaluation of Acyloxyalkyl Esters as Dermal Prodrugs of Ketoprofen and Naproxen. *J. Pharm. Sci.* **1998,** 87, (12), 1622-1628.

134. Rautio, J.; Nevalainen, T.; Taipale, H.; Vepsalainen, J.; Gynther, J.; Pedersen, T.; Jarvinen, T., Synthesis and In Vitro Evaluation of Aminoacyloxyalkyl Esters of 2-(6-methoxy-2-naphthyl)propionic Acid as Novel Naproxen Prodrugs for Dermal Drug Delivery. *Pharm Res* **1999,** 16, (8), 1172-1178.

135. Rautio, J.; Nevalainen, T.; Taipale, H.; Vepsalainen, J.; Gynther, J.; Laine, K.; Jarvinen, T., Synthesis and In Vitro Evaluation of Novel Morpholinyl- and Methylpiperazinylacyloxyalkyl Prodrugs of 2-(6-Methoxy-2-naphthyl)propionic Acid (Naproxen) for Topical Drug Delivery *J. Med. Chem.* **2000,** 43, 1489-1494.

BIOGRAPHICAL SKETCH

Joshua D. Thomas was born in Peachland, North Carolina, on January 5, 1978, where he lived until graduating from Anson County High School in June, 1996. In the fall of that year, he enrolled in Wingate University where he met his wife Amber. After graduating from Wingate University in May 2001, he and Amber married. Later that year they moved to Gainesville, where Joshua began his studies in the graduate program in medicinal chemistry at the University of Florida. He and Amber are the parents of Miriam Faith Thomas, born July 19, 2005.